

**SYNTHESIS OF A WASTE-DERIVED HETEROGENEOUS BIFUNCTIONAL
CATALYST TERNARY BLEND FROM BANANA PEEL ASH, ZEOLITE, AND
CALCINED PERIWINKLE SHELL FOR BIODIESEL PRODUCTION FROM NEEM OIL
AND WASTE COOKING OIL**

BY

CHUKWUEMEKA IFEOMA BRIDGET

ENG2002038

DEPARTMENT OF CHEMICAL ENGINEERING

FACULTY OF ENGINEERING

UNIVERSITY OF BENIN

EDO STATE, NIGERIA

OCTOBER, 2025

**SYNTHESIS OF A WASTE-DERIVED HETEROGENEOUS
BIFUNCTIONAL CATALYST TERNARY BLEND FROM BANANA PEEL
ASH, ZEOLITE, AND CALCINED PERIWINKLE SHELL FOR BIODIESEL
PRODUCTION FROM NEEM OIL AND WASTE COOKING OIL**

BY

CHUKWUEMEKA IFEOMA BRIDGET

ENG2002038

**A PROJECT SUBMITTED TO THE DEPARTMENT OF CHEMICAL
ENGINEERING, UNIVERSITY OF BENIN, BENIN CITY, NIGERIA
IN PARTIAL FULFILLMENT OF THE REQUIREMENTS FOR THE
AWARD OF BACHELOR DEGREE IN CHEMICAL ENGINEERING**

(B ENG)

OCTOBER, 2025

CERTIFICATION

This is to certify that this research project, submitted to the Department of Chemical Engineering, was carried out by, CHUKWUEMEKA IFEOMA BRIDGET from the University of Benin, Benin City, Edo State, Nigeria.

.....

Engr. Prof. E.O. Aluyor

Project Supervisor

.....

Date

.....

Engr. Prof. S.E. Uwadiae

Project Coordinator

.....

Date

.....

Engr. Prof. (Mrs) E. A. Oyedoh

Head of Department

.....

Date

.....

External Examiner

.....

Date

DEDICATION

This research work is dedicated to God Almighty, the source of all wisdom and strength, whose divine grace enabled the successful completion of this study, and to my beloved parents, Mr and Mrs Chukwuemeka Nwabunike, whose unwavering encouragement, sacrificial support, and enduring faith in my abilities have been the cornerstone of my academic journey and an invaluable source of inspiration throughout this endeavor.

ACKNOWLEDGEMENT

I give thanks to Almighty God for His grace, wisdom, and strength throughout the duration of this project. Without His divine guidance and sustenance, the completion of this work would not have been possible. Also, I am deeply grateful to my parents, Mr and Mrs Chukwuemeka Nwabunike, for their unwavering support, encouragement, and sacrifices throughout my academic journey. Their love and belief in me have been a constant source of motivation.

My sincere appreciation goes to my Project supervisor, Engr. Prof. E.O. Aluyor, for accepting to supervise this project and providing valuable guidance and direction.

Profound gratitude is extended to Engr. Prof. (Mrs) E. A. Oyedoh, Head of Department of Chemical Engineering, for her leadership and for providing the conducive academic environment that made this research possible.

Special thanks go to Engr. Dr. Fred Oshomogbo who stood in place of my supervisor and patiently guided me throughout this research. His expertise, constructive feedback, and willingness to share his wealth of knowledge in chemical engineering have greatly enriched my understanding and contributed immensely to the success of this project.

Additionally, I extend my sincere appreciation to all the lecturers of the Department of Chemical Engineering for their dedication to academic excellence and for imparting the knowledge and skills that formed the foundation of this work.

Finally, my appreciation goes to my friends and colleagues, especially Hilda, David, and Chinedu, for their support and encouragement throughout the course of this project. Their presence made the challenges more bearable and the journey more memorable.

ABSTRACT

This study addresses the growing demand for renewable energy and sustainable chemical processes by investigating the production of a novel, bifunctional heterogeneous catalyst derived from readily available waste banana peels, zeolite, and periwinkle shells for biodiesel synthesis.

The methodology involved systematic catalyst synthesis from the three precursor materials through calcination at 800°C for 3 hours, followed by characterization using X-ray diffraction (XRD) and Fourier-transform infrared (FTIR) spectroscopy to confirm Ca–Si–Ti oxide phase formation and identify crystalline structures contributing to catalytic activity. Feedstock physicochemical properties including acid value, iodine value, saponification value, density, and viscosity were determined. Simplex lattice mixture design optimized the neem oil-waste cooking oil blending ratio for maximum free fatty acid reduction. The transesterification process employed response surface methodology (RSM) with 29 experimental runs to optimize reaction parameters: time (30–150 minutes), temperature (40–80°C), catalyst loading (1–10 wt%), and methanol-to-oil ratio (3:1–10:1). Kinetic studies determined reaction order and activation energy, while gas chromatography-mass spectrometry (GC-MS) analyzed the fatty acid methyl ester (FAME) composition of the produced biodiesel.

The results demonstrated the effectiveness of the developed catalyst. XRD and FTIR analyses confirmed active catalyst phases including Portlandite (77%), Muscovite (15%), Titanite (4.6%), and Calcite (2.7%), correlating with the strong basicity essential for transesterification. The optimal feedstock blend ratio of 1:3 (neem oil to waste cooking oil) achieved 86.62% free fatty acid reduction. Optimal transesterification conditions—90 minutes, 60°C, 5.5 wt% catalyst loading, and 6.5:1 methanol-to-oil ratio—produced 92.27% biodiesel yield with acid value of 0.28 mg KOH/g, density of 0.8896 g/cm³, and viscosity of 3.75 mm²/s at 40°C, all meeting ASTM D6751 and EN 14214

standards. Kinetic studies revealed pseudo-first-order reaction behavior with activation energy of 37.68 kJ/mol, consistent with heterogeneous catalysis literature. GC-MS analysis confirmed 92.24% total FAME conversion, with methyl decanoate (30.87%) and methyl oleate (26.07%) as major components, indicating excellent fuel quality. This research successfully developed a viable heterogeneous catalyst made from banana peel ash, calcined periwinkle shell and zeolite for high-quality biodiesel production from mixed non-edible oil feedstocks.

TABLE OF CONTENT

CERTIFICATION	i
DEDICATION	ii
ACKNOWLEDGEMENT	iii
ABSTRACT	iv
TABLE OF CONTENT	vi
LIST OF FIGURES	xii
LIST OF PLATES	xiv
LIST OF TABLES	xv
LIST OF EQUATIONS	xvi
NOMENCLATURE	xvii
CHAPTER 1	1
INTRODUCTION	1
1.1: BACKGROUND OF STUDY	1
1.2 PROBLEM STATEMENT	5
1.3 AIM AND OBJECTIVES	6
1.4 SCOPE OF STUDY	7
1.5 SIGNIFICANCE OF STUDY	8
CHAPTER 2	11
LITERATURE REVIEW	11
2.1 ENERGY	11
2.2 BIOFUELS	12
2.2.2 Biogas	15
2.3 BIODIESEL	16

2.3.1 Factors Affecting Biodiesel Yield	18
2.3.1.1 Effect of free fatty acid and moisture	18
2.3.1.2 The effect of molar ratio and type of alcohol	19
2.3.1.3 Catalyst effect	19
2.3.1.4 The effect of temperature and time.....	19
2.3.2 Properties and Qualities of Biodiesel	20
2.3.2.1 Viscosity	21
2.3.2.2 Fuel density and relative density	21
2.3.2.3 Cetane number	21
2.3.2.4 Flash point	22
2.3.2.5 Titre	22
2.3.2.6 Cloud point, pour point, and cold filter plugging point (cfpp).....	22
2.3.2.7 Oxidation stability of fuel.....	23
2.3.2.8 Lubrication properties of fuel.....	23
2.3.2.9 Acid value of fuel.....	23
2.3.2.10 Free glycerin	24
2.3.2.11 Available water and sediment in fuel.....	24
2.3.2.12 Ash or sulfate content	25
2.3.2.13 Total glycerol	25
2.3.2.14 Carbon residue	25
2.3.2.15 Corrosion of copper strip	25
2.3.2.16 Cold soak filtration	26
2.3.2.17 Presence of phosphorus, calcium and magnesium	26
2.3.3 Advantages of Biodiesel.....	26
2.4 BIODIESEL PRODUCTION TECHNOLOGIES	28

2.5 BIODIESEL PRODUCTION METHODS	29
2.5.1 Pyrolysis	29
2.5.2 Microemulsification	30
2.5.3 Direct Use and Blending	30
2.5.4 Transesterification	31
2.5.5 Catalytic Transesterification	32
2.5.6 Alkali Catalytic Transesterification	33
2.5.7 Acid-Catalyzed Transesterification	34
2.5.8 Enzymatic Transesterification	34
2.5.9 Non-Catalytic Supercritical Methanol Transesterification	35
2.6 BIODIESEL FEEDSTOCKS	35
2.6.1 First-Generation Biodiesel	36
2.6.1.1 Palm Oil	37
2.6.1.2 Coconut	38
2.6.2 Second-Generation Biodiesel	38
2.6.2.1 Jatropha curcas.....	40
2.6.2.2 Neem (Azadirachta Indica).....	41
2.6.3 Third-Generation Biodiesel	42
2.6.3.1 Microalgae	42
2.6.3.2 Animal fat	43
2.6.3.3 Waste oil	44
2.6.4 Fourth Generation Biofuels	44
2.7 CATALYSTS IN BIODIESEL PRODUCTION	47
2.7.1 Homogeneous Catalysts	48
2.7.1.1 Homogeneous alkaline catalysts.....	48

2.7.1.2 Homogeneous acidic catalysts	49
2.7.2 Heterogeneous Catalysts	49
2.7.2.1 Heterogeneous alkaline catalysts	50
2.7.2.2 Heterogeneous acidic catalysts	51
2.7.2.3 Heterogeneous nano-catalysts.....	52
2.7.3 Biocatalysts (Enzymatic)	53
2.8 OPTIMIZATION TECHNIQUES IN BIODIESEL PRODUCTION.....	55
2.8.1 Design of Experiments (Doe)	56
2.8.1.1 Prominent Doe Designs	58
2.8.2 Response Surface Methodology (RSM)	60
2.8.2.1 Applications of RSM.....	61
2.8.2.2 Advantages of RSM	62
2.8.2.3 Disadvantages of RSM.....	63
2.9 KINETIC STUDY OF THE BIODIESEL PROCESS.....	63
2.10 RESEARCH GAPS.....	66
CHAPTER 3	71
MATERIALS AND METHODS	71
3.1 RAW MATERIALS AND REAGENTS	71
3.1.2 APPARATUS AND EQUIPMENT.....	73
3.2 METHODOLOGY	75
3.2.1 PREPARATION OF RAW MATERIALS	75
3.2.1.1 Banana Peel Pre-Treatment.....	75
3.2.1.2 Periwinkle Shell Pre-treatment	77
3.2.1.3 Zeolite Pre-treatment.....	77
3.2.2 CATALYST SYNTHESIS	77

3.2.2.1 Physical Mixing and Homogenization	77
3.2.2.2 Calcination Process	78
3.2.3 CATALYST CHARACTERIZATION	78
3.2.3.1 X-ray diffraction (XRD) Analysis	78
3.2.3.2 Fourier-Transform Infrared Spectroscopy (FTIR)	79
3.2.4 Feedstock Preparation	79
3.2.4.1 Waste cooking oil pre-treatment	79
3.2.4.1 Neem oil pre-treatment	80
3.2.5 Feedstock Characterization	80
3.2.5.1 Acid value or Acid number (Canesin et al., 2014.) ASTM D 664	80
3.2.5.2 Peroxide value (Canesin et al., 2014.)	81
3.2.5.3 Iodine value (Canesin et al., 2014.)	82
3.2.5.4 Density and specific gravity (Canesin et al., 2014.)	83
3.2.5.5 Saponification value (Canesin et al., 2014.)	83
3.2.5.6 Viscosity value (Canesin et al., 2014.)	84
3.2.6 Experimental Design And Optimization	85
3.2.6.1 Esterification reaction	85
3.2.6.2 Simplex lattice mixture design for feedstock blending	85
3.2.6.3 Response surface methodology for process optimization	86
3.2.7 Transesterification Procedure	87
3.2.7.1 Feedstock preparation and pre-treatment	87
3.2.7.2 Transesterification reaction	87
3.2.7.3 Product separation and purification	88
3.2.8 Biodiesel Yield Calculation	90
3.2.9 Biodiesel Characterization	90

3.2.9.1 Physicochemical properties	90
3.2.9.2 Gas chromatography-mass spectrometry (GC-MS) analysis	90
3.2.10 Statistical Analysis And Data Processing	91
CHAPTER 4	92
RESULTS AND DISCUSSION	92
4.1 OIL CHARACTERIZATION	92
4.2 CATALYST CHARACTERIZATION	95
4.3 MIXTURE DESIGN AND FEEDSTOCK OPTIMIZATION	100
4.4 PROCESS OPTIMIZATION USING RESPONSE SURFACE METHODOLOGY	109
4.5 RESPONSE SURFACE ANALYSIS OF BIODIESEL YIELD	113
4.6 KINETIC BEHAVIOR OF TRANSESTERIFICATION REACTION ..	122
4.7 OPTIMUM REACTION CONDITIONS AND MODEL VALIDATION FOR BIODIESEL	125
4.8 BIODIESEL CHARACTERIZATION	126
4.9 GAS CHROMATOGRAPHY–MASS SPECTROMETRY ANALYSIS OF FATTY ACID METHYL ESTER COMPOSITION	128
CHAPTER 5	131
CONCLUSION AND RECOMMENDATION	131
5.1 CONCLUSION	131
5.2 RECOMMENDATIONS	133
REFERENCES	136
APPENDIX	176

LIST OF FIGURES

Figure 4.1: X-ray Diffraction phase composition of the synthesized catalyst	95
Figure 4.2: Fourier-Transform Infrared Spectroscopy (FTIR) spectrum of banana peel–zeolite–periwinkle shell catalyst	97
Figure 4.3: Optima Components Mixture	102
Figure 4.4: Response surface plot showing FFA reduction vs. Neem/WCO ratio	105
Figure 4.5: Parity plot of Predicted vs Actual biodiesel yield	112
Figure. 4.6: Response surface plot showing the interactive effect of reaction time and temperature on biodiesel yield	113
Figure. 4.7: Response surface plot showing the interactive effect of reaction time and catalyst loading on biodiesel yield	115
Figure 4.8: Response surface plot showing the interactive effect of reaction time and methanol ratio on biodiesel yield	116
Figure 4.9: Response surface plot showing the interactive effect of temperature and catalyst loading on biodiesel yield	117
Figure 4.10: Response surface plot showing the interactive effect of temperature and methanol ratio on biodiesel yield	118
Figure 4.11: Response surface plot showing the interactive effect of catalyst loading and methanol ratio on biodiesel yield	119
Figure 4.12: Effect of reaction time on biodiesel yield	121
Figure 4.13: Plot for First order determination based on effect of time	122
Figure 4.14: Plot for Second order determination based on effect of time	122
Figure 4.15: Arrhenius plot for activation energy determination	123

Figure 4.16: Optimum Reaction Conditions	125
Figure 4.17: GC–MS chromatogram of fatty acid methyl esters (FAME) from optimized reaction	128

LIST OF PLATES

Plate 3.1: Washed Banana Peels	75
Plate 3.2: Dried Banana Peels	76
Plate 3.3: Catalyst blend of Banana peel ash, Calcined Periwinkle shell and Zeolite ...	76
Plate 3.4: Viscosity Test for Neem Oil	85
Plate 3.5: Tranesterification Run 24	88
Plate 3.6: Washing of Biodiesel	89

LIST OF TABLES

Table 2.1: Advantages and disadvantages of catalysts used in the transesterification reaction (Bohlouli & Mahdavian, 2021).....	55
Table 3.1: Raw materials and Reagents	71
Table 3.2: Apparatus and Equipment.....	73
Table 4.1: Physical and Chemical Properties of Neem Oil and Waste Cooking Oil	92
Table 4.2: X-Ray Diffraction Quantitative Analysis	94
Table 4.3: Mixture Component Design	100
Table 4.4: FFA Reduction ANOVA for the Quartic model	103
Table 4.5: Components Fit Statistics	104
Table 4.6: Coefficients in Terms of Coded Factors	107
Table 4.7: Biodiesel Yield ANOVA for Quadratic model	109
Table 4.8: Fit Statistics	110
Table 4.9: Physicochemical Properties of Produced Biodiesel	126
Table 4.10: Fatty acid methyl ester composition of produced biodiesel	129

LIST OF EQUATIONS

Equation 2.1: Tranesterification reaction rate	64
Equation 2.2: Pseudo first order kinetic equation	65
Equation 2.3: Arrhenius equation	65
Equation 3.1: Acid value formula	78
Equation 3.2: Free fatty acid formula	79
Equation 3.3: Peroxide Value formula	79
Equation 3.4: Iodine Value formula	80
Equation 3.5: Specific Gravity formula	81
Equation 3.6: Saponification Value formula	81
Equation 3.7: FFA Reduction Percentage formula	84
Equation 3.8: Biodiesel yield formula	88
Equation 4.1: FFA Reduction (%) in terms of L-pseudo coded components	104
Equation 4.2: Biodiesel yield Percentage	111

NOMENCLATURE

Abbreviation	Meaning
AV	Acid Value
FFA	Free Fatty Acid
IV	Iodine Value
SV	Saponification Value
PV	Peroxide Value
SG	Specific Gravity
ρ (rho)	Density
η (eta)	Viscosity
BP	Banana Peel
PS	Periwinkle Shell
ZL	Zeolite
WCO	Waste Cooking Oil
NO	Neem Oil

Abbreviation	Meaning
RSM	Response Surface Methodology
DOE	Design of Experiment
ANOVA	Analysis of Variance
ASTM	American Society for Testing and Materials
FAME	Fatty Acid Methyl Ester
GC-MS	Gas Chromatography–Mass Spectrometry
XRD	X-ray Diffraction
FTIR	Fourier Transform Infrared Spectroscopy
wt%	Weight Percentage
T	Temperature
t	Time
N	Normality of solution

Abbreviation	Meaning
V	Volume
W	Weight of sample
Yb	Biodiesel Yield

CHAPTER 1

INTRODUCTION

1.1: BACKGROUND OF STUDY

The rapid escalation of population growth, industrialization, and urbanization in recent years has led to a global energy crisis and increased concerns about the reliance on non-renewable energy sources. In 2019, fossil fuels such as coal, diesel, petrol and natural gas constituted 84% of the global primary energy consumption, thereby establishing them as the dominant energy source worldwide. The use of fossil fuels, which began with the industrial revolution, has been pivotal in fulfilling global energy needs (M. A. H. Khan et al., 2021). From an environmental perspective, the combustion of fossil fuels releases gaseous pollutants, including carbon dioxide (CO₂), carbon monoxide (CO), nitrogen oxides (NO_x), sulfur oxides (SO_x), volatile organic compounds (VOCs), and particulate matter (PM), which can alter atmospheric composition and have harmful effects on climate and public health. To address the negative impacts of climate change due to greenhouse gas (GHG) emissions, the Paris Agreement, introduced in 2015, set a goal to "limit global temperature rise to 2 °C above pre-industrial levels, whilst pursuing efforts to limit the increase to 1.5°C (Matemilola et al., 2023).

Transitioning from conventional fossil fuels to renewable energy sources is a promising strategy to reduce GHG emissions, stabilize the global climate, and enhance energy security. Key renewable energy sources include solar, wind, hydro, geothermal, and biofuel, all of which have the potential to provide energy services with reduced emissions of GHGs and air pollutants (Owusu & Asumadu-Sarkodie, 2016). Among these, biofuels are particularly promising for the transportation sector. Most of the other renewable energies, such as solar, wind, hydro, and nuclear power, primarily generate

electricity and thus cannot compete directly with oil (Arutyunov et al., 2017). Challenges associated with electricity, such as long-distance transmission and conversion to different energy forms, make these sources less appealing. Furthermore, biofuels can be integrated into existing infrastructures and require fewer technological advancements compared to other energy sources (M. A. H. Khan et al., 2021).

Bioenergy is acknowledged as sustainable and clean choice of energy source that plays an important role as not just a complementary but also a substitute form of energy in the immediate future (Su et al., 2017). Bioenergy is one of the many several resources accessible to satisfy the required need for energy. It is readily obtained from materials of organic nature, commonly known as biomass (A. R. Singh et al., 2022).

Biomass is regarded as a renewable source as a result of its limited lifespan, and biofuels sourced from biomass are sustainable alternatives to fossil fuels (W. H. Chen et al., 2019) Biofuels in their gaseous state are majorly utilized for the generation of heat and energy however, liquid biofuels are used in the transportation industry. Examples of biofuels includes; biomethanol, biochar, bioethanol, biodiesel, bio-dimethyl ether, charcoal, biogas, synthetic natural gas, Fischer-Tropsch (FT) fuels and H₂ fuels (Chen et al., 2019). These biofuels can be categorized into first, second, third and fourth generation biofuels (Sikarwar et al., 2017.).

Additionally, biofuels can be incorporated into established infrastructures and need a reduced number of technological developments compared to alternative sources of energy (Khan et al., 2021). One of the most prospective sources of renewable energy is Biodiesel owing to its sustainability, biodegradability, non-toxicity and its reduced impact on environment. Biodiesel has attracted interest as a substitute to fossil fuels over the last few decades (Rodionova et al., 2017.). It can be described

as monoalkyl ester of long-chain fatty acids obtained from lipid raw materials that can be renewed, produced through the transesterification of oils with short-chain alcohols, namely methanol or ethanol, in the existence of basic or acid catalysts (da Silva et al., 2018). In addition to transesterification, other techniques that have been applied to the production of biodiesel are ultrasound-assisted, microwave-assisted, membrane-assisted methods, in situ transesterification, pyrolysis and micro-emulsification. Decrease in the emissions of greenhouse gases and reduced national dependence on fossil energy are two notable strengths of the life cycle of biodiesel (Živković et al., 2018.). Other benefits of biodiesel include improved storage, simplicity of forming blends with diesel oil, compatibility with current engine cycles. Moreover, the production technology is economically feasible and user-friendly, and existing infrastructure can be utilized (Agarwal et al., 2018.). For application in the Transportation industry, biodiesel appears promising as a result of its non-toxicity, carbon neutrality and biodegradability characteristics. Additionally, a variety of edible and non-edible oils such as castor oil, waste cooking oil, animal fats serve as sources of biodiesel (Thangaraj et al., 2019).

There is a number of disadvantages that are associated with biodiesel such as low calorific value, high viscosity, hygroscopicity, volatility and low oxidation stability and when utilized as a solvent can pose the danger of attacking some plastic materials used for hoses and coatings as well as corroding components. The associating cost of the process is a primary constraint to the production of biodiesel. The cost of raw materials contributes up to 80% to the net cost of biodiesel generation (Etim et al., 2020). The utilization of conventional edible feedstocks such as corn oil, palm oil, sunflower oil, soybean oil, and palm oil are being discouraged due to the food versus fuel debate and the availability of land. There needs to be a decrease in the elevated cost of production in order for biodiesel to be competitive in the energy market worldwide. This has prompted the exploration of

more readily available and less expensive feedstocks with bulk of the focus currently on cost-reduced nonedible oils such as yellow oleander seed oil, rubber seed oil (Sai et al., 2020), castor seed oil (Roy et al., 2020.), jatropha seed oil, waste cooking oil (Sahar et al., 2018), crude neem oil (Budhwani et al., 2019), and kapok oil (Pooja et al., 2021.) among others.

As a result of the production of soap which leads to a decrease in the yield of biodiesel, the conventionally used homogeneous liquid catalysts are not well-suited for oils possessing an elevated free fatty acid content (Chuah, Klemeš, et al., 2017.). The incapability of recovering the homogeneous catalysts and the necessity for extra purification and product separation leads to the production of biodiesel wash water which needs to be handled properly (Balajii & Niju, 2020). Heterogeneous catalysts have gained considerable interest as better substitutes due to their characteristics of thermal stability, noncorrosivity, reusability, nontoxicity and being environmentally friendly (D. Singh et al., 2020.). The generation of heterogeneous catalysts from waste materials possesses the potential to lessen the associated cost of biodiesel production (Chuah, Amin, et al., 2016.).

The transition towards renewable energy sources is pivotal for the future of energy acquisition. The finite availability of fossil fuels necessitates their gradual substitution with alternative resources, such as agricultural, industrial, and other waste materials, which are inexhaustible and require ongoing, effective management (Perea-Moreno & Kalak, 2023). In the current energy landscape, biodiesel emerges as a vital element in diminishing reliance on fossil fuels. The economic feasibility of cleaner biodiesel is largely contingent upon the costs associated with feedstock and catalysts. The expenses related to catalysts can be curtailed by utilizing catalysts that are simple to synthesize and necessitate minimal or no purification (Maheshwari et al., 2022). Recently, to mitigate the costs of biodiesel synthesis, effective heterogeneous catalysts have been derived from biomass waste materials, including banana peels, wood, cocoa pod husk, neem husk, rice husk, peanut shell, pomelo peel,

tucumã peel, waste cupuaçu, walnut shell, kola nut pod, and banana peduncle (Jitjamnong et al., 2021). As the second most produced tropical fruit globally, bananas generate a significant amount of waste by-products, particularly banana peels. The non-edible banana peel has been applied in various domains, including as bio-sorbents, in bioethanol production, and other energy-related activities. Recently, the application of banana peel biochar as a catalyst for biodiesel production has attracted considerable interest (Jitjamnong et al., 2021). These catalysts can support a sustainable and environmentally friendly approach to biodiesel production (Rizwanul Fattah et al., 2020).

1.2 PROBLEM STATEMENT

The diminishing reserves of non-renewable energy sources have spurred extensive research into alternative fuels and environmentally responsible energy solutions that produce minimal pollutants (Suresh et al., 2024.). It is crucial to develop an energy system that is not reliant on fossil fuels, ensuring it is ecologically sound, cost-efficient, stable, regenerative, and emits minimal pollutants. However, the primary obstacle in biodiesel production is the high cost of raw materials, which accounts for approximately 75–80% of the total production expenses (Balajii & Niju, 2020).

Conventional edible feedstocks, such as palm oil, rapeseed oil, sunflower oil, corn oil, and soybean oil, offer higher yields and simpler processing due to their low free fatty acid (FFA) content (Atabani, Silitonga, Ong, et al., 2012.). Nevertheless, their use has resulted in land availability challenges, food versus fuel conflicts, and ecological imbalances in numerous developing nations (Atabani, Silitonga, Ong, et al., 2012.). In recent decades, non-edible oils have been investigated as a cost-effective renewable feedstock to reduce biodiesel production costs and address these issues (Balajii & Niju, 2020).

Homogeneous catalysts are commonly employed in biodiesel production due to their rapid reaction rate at moderate temperatures, low cost, and high catalytic activity. However, they are vulnerable to the presence of water, leading to saponification reactions that complicate separation and necessitate substantial water for purification (Mohandass et al., 2025.). Heterogeneous catalysts have been developed to address these issues, offering advantages such as ease of separation, environmental friendliness, and greater stability at high temperatures and pressures (Fitriana et al., 2018). Utilizing heterogeneous catalysts derived from agricultural waste is more cost-effective than synthetic homogeneous types. Ash-based agricultural waste containing alkali and alkaline earth metal oxides exhibits high catalytic activity and recyclability for biodiesel production (H. Khan et al., 2021.). Several ash catalysts derived from banana plant parts have demonstrated excellent performance in biodiesel synthesis, including those from *Musa balbisiana* peel, *Musa acuminata* peel, and acai seed. However, heterogeneous base catalysts produced from Awak (*Musa paradisiaca* L. Var) banana peel ash have not been extensively documented. The banana peel ash generates substantial waste from peels and stems post-harvest (Meriatna et al., 2023).

1.3 AIM AND OBJECTIVES

The aim of this study is to synthesize a bifunctional heterogeneous catalyst from banana peels, zeolite, and periwinkle shell, and to optimize its application in biodiesel production from a blend of neem oil and waste cooking oil through statistical modeling and process parameter optimization.

OBJECTIVES

To achieve this aim, the following specific objectives were pursued:

1. To synthesize a heterogeneous catalyst from banana peels, periwinkle shell, and zeolite through calcination.
2. To characterize the synthesized catalyst's physicochemical properties using X-ray diffraction (XRD) and Fourier-transform infrared spectroscopy (FTIR).
3. To determine the physicochemical properties of neem oil and waste cooking oil feedstocks including acid value, iodine value, saponification value, density, and viscosity.
4. To determine the optimal blending ratio of neem oil and waste cooking oil for maximum free fatty acid (FFA) reduction using simplex lattice mixture design.
5. To optimize the transesterification process parameters (reaction time, temperature, catalyst loading, and methanol-to-oil ratio) for maximum biodiesel yield using response surface methodology (RSM).
6. To investigate the kinetic behavior of the transesterification reaction by determining the reaction order and activation energy.
7. To characterize the produced biodiesel through gas chromatography-mass spectrometry (GC-MS) analysis and evaluate its physicochemical properties against ASTM D6751 and EN 14214 standards.

1.4 SCOPE OF STUDY

The scope of this research entails an investigation into the development and application of an effective and renewable heterogeneous base catalyst derived from banana peels, periwinkle shell and zeolite for biodiesel production. The study is centered on the use of a composite blend of neem oil and waste cooking oil as feedstocks.

The research is structured across several key dimensions, starting with the Materials Scope. This includes an investigation into the properties and characteristics of the heterogeneous catalyst, an analysis of the composition and compatibility of neem oil and waste cooking oil, an examination of catalyst-feedstock interactions and optimization parameters. The Methodological Scope involves the development and standardization of catalyst preparation protocols, the implementation of transesterification reaction procedures, the characterization of physical and chemical properties.

The study is confined to laboratory-scale experimentation, emphasizing fundamental research principles and practical applications. While investigating innovative approaches to sustainable biodiesel production, the research remains anchored in established scientific methodologies and analytical techniques.

1.5 SIGNIFICANCE OF STUDY

The relevance of this study stems from its strategic integration of multiple sustainable elements, with the selection of banana peels, periwinkle shell and zeolite as a catalyst source representing a critical innovation in waste valorization. This choice holds particular importance for energy security by promoting domestic energy independence; locally sourced banana peels and periwinkle shells can be converted into valuable catalysts, thereby reducing reliance on imported materials and enhancing national energy self-sufficiency. Additionally, the use of neem oil and waste cooking oil as feedstocks reinforces this framework by exploiting abundant regional resources, thereby establishing a robust foundation for sustainable biodiesel production that minimizes dependence on external inputs.

The environmental importance of this research is evident in its comprehensive approach to waste reduction and pollution mitigation. By transforming banana peels and periwinkle shells into functional catalysts, the research simultaneously addresses two pressing environmental issues: the management of organic waste streams and the advancement of cleaner industrial processes. This dual benefit aligns with circular economy principles by converting potential landfill materials into essential components of renewable energy production. Furthermore, incorporating waste cooking oil augments the environmental gains by offering an innovative solution to waste disposal challenges in the food service sector, thus fostering a closed-loop system wherein waste materials serve as valuable inputs for sustainable energy generation.

From an economic and technological perspective, this research exhibits considerable relevance by potentially establishing new value chains within sustainable energy production. The development of a cost-effective catalyst utilizing waste materials tackles a major obstacle to widespread biodiesel adoption—the high cost associated with conventional catalysts. This innovation has the capacity to stimulate local economies through the emergence of industries centered on waste collection and processing, while concurrently lowering production costs for biodiesel manufacturers.

Moreover, the study's broader societal implications are reflected in its potential to inform policy and practice in sustainable energy development by providing empirical evidence supporting renewable energy initiatives and waste management strategies.

This alignment with national sustainability goals enhances the study's significance, especially in regions where banana peels and periwinkle shells constitute a substantial organic waste stream and where achieving renewable energy targets remains a persistent challenge.

CHAPTER 2

LITERATURE REVIEW

2.1 ENERGY

Energy is essential for sustaining life, and it has become increasingly imperative to optimize the utilization of limited resources as the demand for energy sources continues to rise at an unprecedented rate (Ullah et al., 2016). The future will undoubtedly see a significant rise in energy demand. Presently, fossil fuels are responsible for generating 84% of the world's energy (Yusuf et al., 2021). The extensive utilization of fossil fuels on this scale is unparalleled in Earth's history. To address the detrimental impacts of global warming and meet the goals set by the Paris Agreement, it is essential to transition to a cleaner and more economically viable energy source (Maheshwari et al., 2022).

The pursuit of clean and affordable energy is integral to the seventeen Sustainable Development Goals (SDGs), with particular significance for African countries like Nigeria. SDG 7, which emphasizes affordable and clean energy, is a critical factor in socio-economic advancement. In recent years, the demand for energy in African nations has surged, driven by rapid population growth, technological advancements, and the expansion of small-scale industries (Adewuyi, 2020). Nigeria, as the most populous black nation with an estimated population of around 200 million, faces a significant energy demand. However, numerous obstacles impede access to affordable and clean energy. The lack of availability and accessibility to energy results in several adverse consequences, including poverty, a decline in economic growth, inadequate health services, poor research development, and imbalances in socio-economic affairs (Oyedepo, 2012). To address these issues, Nigeria is actively exploring sustainable, eco-friendly energy alternatives, with a focus on renewable resources (Owunna et al., 2022.).

2.2 BIOFUELS

The global scientific community is increasingly focusing on the production of biofuels from biomass resources through environmentally sustainable methods. Presently, a range of gaseous and liquid biofuels, including biodiesel, ethanol, methanol, methane, bio-oil, and Fischer–Tropsch, H₂, are being produced from biomass (Joshi et al., 2019; Prasad et al., 2012.). These biofuels are seen as promising candidates for future energy supply and for ensuring sustainable energy security (Choi et al., 2010.). The use of biofuels as renewable energy sources contributes to the reduction of air pollutant emissions, including greenhouse gases such as CO₂, during combustion, thereby lessening overall pollution and other environmental impacts (Anukam et al., 2019.; Prasad et al., 2012.). Additionally, the production and utilization of biofuels are regarded as carbon-neutral processes because they originate from biomass, which absorbs more CO₂ than it emits into the atmosphere (Prasad et al., 2012.).

The biofuel sector is anticipated to grow by 41 billion liters, culminating in a total volume of 186 billion liters by the year 2026. This expansion corresponds to an average annual growth rate of 4% throughout the projected period (Ashok et al., 2024). Both industrialized and developing nations are becoming interested in sustainable energy management. Biofuels become viable alternatives to petroleum-based fuels in such a scenario. According to predictions, 7% of global transportation fuels will originate from renewable sources, such as biofuels, by 2030 (Ullah et al., 2016).

Biofuels are an energy source that is made from organic materials (also known as biomass) produced by plants and other living organisms that can be repeatedly cultivated and collected. In the absence of fossil fuels, biofuels are a viable alternative that have the benefit of non-toxicity and the absence

of sulfur owing to their origin from renewable resources. Biofuels can be categorized into two primary types: primary and secondary biofuels. Primary biofuels are naturally derived from sources such as firewood, plants, forests, animal waste, and crop residues. Secondary biofuels, on the other hand, are directly generated from plants and microorganisms and can be further classified into three generations (Rodionova et al., 2017.).

The most common types of biofuels are bioethanol, which is made by fermenting sugar and starch crops like corn; biogas and biodiesel, which is made from vegetable oils, recycled wax, or animal fats. Agricultural and critical harvesting, woods, and residual streams are the main sources of biofuels utilized to substitute non-renewable energy fuels (Agarwal et al., 2018; Polburee et al., 2015.; S. J. Xue et al., 2018). The first generation of biofuels involves the production of ethanol from starch-rich food crops like wheat, barley, corn, potato, and sugarcane, or biodiesel from soybean, sunflower, and animal fat. The second generation encompasses the production of bioethanol and biodiesel from various plant species such as jatropha, cassava, miscanthus, straw, grass, and wood. The third generation focuses on the production of biodiesel from microalgae and microbes (Slade et al., 2013.) .

2.2.1 BIOETHANOL

Bioethanol, a plant-derived fuel, is obtained through the fermentation of simple sugars into alcohol. It can be used in blends with fossil fuels or in nearly pure form in specially adapted vehicles (E-85, flex-fuel technology), particularly developed in Brazil. From a technological perspective, three generations coexist, depending on the origin of the sugars used for fermentation (from edible plants, lignocellulosic residues, or algae) (Bertrand & Dussap, 2022). First-generation ethanol was primarily produced from plant sugars or starches (Al-Maamary et al., 2017.). First-generation biofuels are directly produced from food crops, with corn, wheat, and sugarcane being the major feedstocks (Aro, 2016). First-generation biofuels offer CO₂ benefits and remain commercially available today.

Most commercially available biofuels are derived from first-generation feedstocks. Vegetable oil, corn sugar, and similar feedstocks are used to produce first-generation biofuels such as fatty acid methyl ester (FAME) or biodiesel, corn ethanol, or sugar alcohol (Niphadkar et al., 2018). Currently, corn is the predominant source for ethanol production, particularly in the United States, where 40% or more of the corn crop is utilized for this purpose. The primary issue with this crop is its status as a staple food in many developing and developed countries, leading to a global increase in food prices and even hunger. A similar problem arises when sugarcane is used as a feedstock. Both corn and sugarcane cultivation require pesticides and fertilizers, which are costly and result in soil and water contamination. This has necessitated the identification and utilization of feedstocks that do not present food-versus-fuel conflicts and are renewable for future bioethanol production; this is the central theme of second-generation techniques (Niphadkar et al., 2018).

Second-generation bioethanol production utilizes plant biomass that is relatively inexpensive, widely available, and does not generate food security concerns. These processes are specifically designed to

circumvent the food-versus-fuel dilemma by primarily relying on agricultural residues and forest wastes, which are predominantly composed of various lignocellulosic materials. A key advantage of second-generation biofuels lies in their use of abundant, low-cost, non-food plant-based feedstocks, thereby mitigating competition with food supply. However, significant challenges remain, particularly regarding sugar degradation and the high energy demands associated with pretreatment steps, which contribute to increased production costs. Additionally, the development of efficient microorganisms capable of fermenting both pentose (C5) and hexose (C6) sugars simultaneously continues to be a critical bottleneck in optimizing bioethanol yields (Niphadkar et al., 2018).

The production of third-generation bioethanol relies on biomass with high carbon content. Research indicates that seaweed and marine algae, including species like *Enteromorpha*, possess approximately 70% carbohydrates on a dry weight basis, making them viable candidates for bioethanol production. This generation of bioethanol focuses on utilizing microalgae for biofuel production, contingent upon the establishment of cost-effective processes (Niphadkar et al., 2018). Currently, fourth-generation bioethanol is being developed to enhance algae's ability to capture CO₂ and improve the synthesis of specific compounds. However, the high costs associated with processing non-edible feedstocks continue to pose a barrier to making bioethanol economically competitive with traditional gasoline (Inambao, 2021).

2.2.2 Biogas

The prediction of the global demand for biogas is continuously on the rise (Chaemchuen et al., 2016). Biogas, a combustible gas, is produced through the anaerobic digestion of organic materials. It predominantly comprises 60–70% methane and 30–40% carbon dioxide, with minor quantities of gases such as hydrogen, nitrogen, oxygen, carbon monoxide, and hydrogen sulfide. The biogas

composition is affected by factors like the raw materials used, reactor temperature, and the retention time of materials in the fermentation tank. Elevated carbon dioxide levels in biogas diminish its heating value and flammability, necessitating CO₂ removal to enhance its energy content (Thanigaivel et al., 2022). Methane fuel, or biogas, is recognized as a promising clean energy carrier due to its higher hydrogen-to-carbon (H/C) ratio and its role in reducing CO₂ emissions (Chaemchuen et al., 2016).

The significance of biogas energy sources is growing, given their impact on global warming and national economies. The production and use of biogas are pivotal in achieving renewable energy goals and environmental benefits. Biogas can be directly utilized as fuel for generating heat, steam, and electricity on-site in industrial settings. Additionally, refined biogas can be integrated into natural gas grids and used as vehicle fuel. Environmentally, biogas emits less CO₂ compared to fossil fuels. Furthermore, it serves as a fundamental material for producing synthesis gas, hydrogen, and chemicals (Jürgensen et al., 2017.).

2.3 BIODIESEL

Biodiesel emerges as a cleaner substitute to traditional petroleum products, significantly lowering emissions of unburnt hydrocarbons (68%), particulate matter (40%), carbon monoxide (44%), sulfur oxides (100%), and polycyclic aromatic hydrocarbons (80–90%) (Brito et al., 2020.). It is a prominent environmentally sustainable substitute for petroleum-based diesel (Bokhari et al., 2016.). It is distinguished by several beneficial attributes, such as renewability, non-toxicity, biodegradability, inherent lubricity, and low sulfur content, all of which contribute to its advantageous emission profile.

Additionally, biodiesel can be employed in existing diesel engines without requiring extensive modifications (D. Singh et al., 2022.). Its ability to blend seamlessly with petrodiesel in varying ratios further enhances its utility (Amenaghawon et al., 2022). As a biofuel alternative for diesel-powered vehicles, biodiesel is appreciated for its renewability, biodegradability, and carbon neutrality. It is predominantly synthesized from vegetable oils or animal fats through the transesterification process, which involves a catalyst. Importantly, biodiesel can be sourced from a wide array of materials, including edible oils (Mahfud et al., 2018), non-edible plant oils (Silitonga et al., 2019), animal fats (Banković-Ilić et al., 2014) , waste cooking oil (WCO), and algae oil (Ong et al., 2021.).

The utilization of biodiesel in the transportation sector is well-established, with its adoption spanning over 60 countries globally. Many nations are actively promoting biodiesel to decrease dependence on non-renewable fossil fuels. Edible oils, such as palm oil (PO), are considered promising due to their high yield and compatibility with diesel engines. Presently, there is a growing focus on using non-edible crops as future feedstocks for biodiesel production, which could reduce reliance on edible oils and alleviate pressure on the human food supply over time (Yusoff et al., 2022).

Biodiesel is defined as a monoalkyl ester of long-chain fatty acids derived from renewable lipid raw materials, produced by the transesterification of oils with short-chain alcohols, such as methanol or ethanol, in the presence of acid or basic catalysts (da Silva et al., 2018). It is a fuel composed of monoalkyl esters formed by the transesterification of triglycerides (oils or fats) with light alcohols, which may be catalyzed or not (methanol or ethanol). Virgin or used edible oils, such as soybean oil, palm oil, vegetable oil, or sunflower oil, can serve as triglyceride sources (Abdulmumin et al., 2021).

2.3.1 Factors Affecting Biodiesel Yield

The factors influencing the yield of biodiesel include FFA content, the molar ratio of alcohol to oil, the type and concentration of the catalyst, reaction temperature, and reaction duration. Among these variables, the molar ratio, temperature, and catalyst concentration are particularly critical in determining biodiesel yield (Verma & Sharma, 2016).

2.3.1.1 Effect of free fatty acid and moisture

The influence of free fatty acid (FFA) and moisture content is critical in the transesterification process, serving as key determinants for the suitability of vegetable oil (Mishra & Goswami, 2018). Both FFA and water negatively impact this process by promoting soap formation, which depletes the catalyst and diminishes its effectiveness, thereby reducing the overall conversion rate to biodiesel (Demirbas et al., 2007). Moisture presence adversely affects methyl ester yields in catalyzed transesterification techniques (Demirbas, 2006).

In acid-catalyzed transesterification, fatty acids may form through reactions involving carbocation II in the presence of water within the reaction mixture. The interaction of FFAs with alkaline catalysts results in soap production, which complicates the separation of biodiesel, glycerin, and wash water during alkali-catalyzed transesterifications. For a continuous base-catalyzed reaction to reach completion, the FFA content must be kept below 3%. Notably, the presence of water exerts a more detrimental effect on the transesterification process than FFAs themselves (Mishra & Goswami, 2018).

2.3.1.2 The effect of molar ratio and type of alcohol

The molar ratio of alcohol to triglyceride and the type of alcohol employed are crucial factors influencing the yield of esters in transesterification reactions. Although the stoichiometric molar ratio of methanol to triglyceride is 3:1, elevated molar ratios are commonly utilized to improve solubility and enhance molecular interaction between triglycerides and alcohol (Noureddini et al., 1998). Increased molar ratios typically lead to higher ester conversion within shorter reaction times. For example, in the transesterification of peanut oil with ethanol, a 6:1 molar ratio produced significantly more glycerine than the standard 3:1 ratio (Feuge et al., 1949). Furthermore, the appropriate molar ratio depends on the catalyst type; acid-catalyzed reactions often require higher alcohol-to-oil molar ratios to achieve satisfactory yields within practical durations. However, this increase in molar ratio does not correspond to a proportional increase in ester yield (Mishra & Goswami, 2018).

2.3.1.3 Catalyst effect

Catalyst selection plays a significant role in transesterification efficiency. Alkali catalysts, acids, and enzymes are commonly used, with alkali-catalyzed transesterification generally proceeding at a faster rate and being the preferred method in commercial production (Salvi et al., 2012.). A study on methanolysis of RBD palm oil (with FFA content <0.1%) identified sodium (Na), sodium hydroxide (NaOH), and potassium hydroxide (KOH) as the most effective catalyst. Additionally, the influence of catalyst concentration on base-catalyzed transesterification was explored using ultrasonic energy to optimize biodiesel synthesis from vegetable oils (YuenMay, 2004).

2.3.1.4 The effect of temperature and time

Temperature and reaction time also significantly affect the transesterification process. The optimal temperature varies depending on the type of vegetable oil or fat employed (Salvi et al., 2012, (L. C.

Meher et al., 2006). Microwave-assisted heating has been investigated as a method to accelerate reaction rates in both laboratory and industrial scales. Transesterification can be conducted in batch or continuous-flow modes, with batch processing being more prevalent due to its operational simplicity. Compared to conventional heating, microwave heating offers a more efficient means of speeding up the transesterification reaction (Soltani et al., 2015a).

2.3.2 Properties and Qualities of Biodiesel

Biodiesel quality improvements are being pursued worldwide to achieve reliable engine performance across different production scales and feedstock sources. When biodiesel is produced from plants of varying capacities and origins, it is essential to standardize biodiesel quality to prevent operational issues (Atabani, Silitonga, ..., et al., n.d.) (Balat & Balat, 2010).

The evaluation of biodiesel properties or quality is primarily conducted through physicochemical parameters. These include cetane number (CN), caloric value (MJ/kg), density (kg/m^3), viscosity (mm^2/s), cloud and pour points ($^{\circ}\text{C}$), flash point ($^{\circ}\text{C}$), acid value (mg KOH/g-oil), ash content (%), water content and sediment, copper corrosion, distillation range, carbon residue, sulphur content, glycerine presence (% m/m), phosphorus (mg/kg), and oxidation stability. The chemical and physical characteristics of biodiesel depend largely on the type of raw material (i.e., feedstock) and the composition of fatty acids (Atabani, Silitonga, et al., 2012.).

2.3.2.1 Viscosity

Viscosity refers to a fuel's capacity to flow and is critical in the functioning of fuel injection systems and spray atomization, especially at lower temperatures where increased viscosity impacts fuel fluidity. Biodiesel's viscosity is approximately 10–15 times higher than that of fossil diesel, attributed to its larger molecular mass and chemical structure (Atabani, Silitonga, et al., 2012.). At cold temperatures, biodiesel may become very viscous or even solidify, which can impair volume flow and fuel injection spray behavior in engines (Mishra & Goswami, 2018)

2.3.2.2 Fuel density and relative density

Density measures a fuel's weight per unit volume, with denser oils providing greater energy content (Atabani, Silitonga, et al., 2012.). Biodiesel density is measured following EN ISO 3675/12 185 and ASTM D1298 standards, typically at reference temperatures of 15 or 20°C (Torres-Jimenez et al., n.d.). Relative density compares the fuel's density to that of water, which is essential for mass-to-volume conversions, flow and viscosity calculations, and assessing biodiesel tank homogeneity (Atabani, Silitonga, et al., 2012.).

2.3.2.3 Cetane number

The cetane number (CN) represents a fuel's ignition quality—its ability to auto-ignite promptly after injection. A higher CN signifies better ignition characteristics (Atabani, Silitonga, et al., 2012). CN is crucial in selecting methyl esters for biodiesel production (L. C. Meher et al., 2006) (Qin et al., 2010) (M. B.-E. conversion and management & 2011, 2011). CN increases with longer fatty acid

chains and higher saturation, meaning biodiesel generally has a higher CN than petroleum diesel, correlating to improved combustion efficiency (Karmakar et al., 2010.) (Lapuerta et al., 2008).

2.3.2.4 Flash point

Flash point refers to the temperature at which a fuel ignites upon exposure to a flame. Fuel volatility decreases as flash point increases. Biodiesel exhibits a flash point above 150°C, exceeding petroleum diesel's 55–66°C, making it safer for transport, handling, and storage (Atadashi, Aroua, energy, et al., 2013.) (L. C. Meher et al., 2006). Demirbas (A. D.-E. conversion and management & 2009, 2008) notes that fatty acid methyl esters have significantly lower flash points than their original vegetable oils.

2.3.2.5 Titre

Titre defines the temperature at which oil transitions from solid to liquid (Atabani, Silitonga, et al., 2012.). This property is vital since biodiesel production via transesterification is a liquid-phase process, and oils with high titre require heating, which raises energy consumption and production costs (Karmakar et al., 2010.).

2.3.2.6 Cloud point, pour point, and cold filter plugging point (cfpp)

Low-temperature behavior of biodiesel is a key quality measure. Wax crystallization at colder temperatures can block fuel lines and filters, causing engine startup failures, driving issues, and

lubrication problems. The cloud point marks the temperature when wax crystals first appear on cooling; pour point is the lowest temperature at which fuel can flow before gelling occurs; CFPP indicates the temperature when filters begin to plug due to crystallization or gel formation. CFPP is a reliable indicator of fuel performance in cold weather, more so than cloud point, affecting flow in fuel lines, pumps, and injectors (Mishra & Goswami, 2018).

2.3.2.7 Oxidation stability of fuel

Oxidation stability assesses biodiesel's resistance to degradation upon exposure to oxygen. The presence of unsaturated fatty acid chains with double bonds makes biodiesel more prone to oxidative reactions compared to fossil diesel (Atabani, Silitonga, et al., 2012.). This property indicates the necessity for antioxidants to maintain fuel quality (Atadashi, Aroua, energy, et al., 2010.).

2.3.2.8 Lubrication properties of fuel

Biodiesel generally exhibits superior lubrication properties over diesel, contributing to enhanced engine longevity (Atabani, Silitonga, et al., 2012.). However, biodiesel (FAAE) may cause deposit formation or filter plugging depending on its degradability, glycerol content, and cold flow attributes (Lapuerta et al., n.d.). Improved lubricity reduces friction losses, potentially increasing brake effective power (J. Xue et al., 2011).

2.3.2.9 Acid value of fuel

Also known as the neutralization number, acid value measures free fatty acids (FFA) in fresh fuel, which are naturally occurring saturated or unsaturated monocarboxylic acids not bonded to glycerol

(Atabani, Silitonga, et al.,2012.). Higher acid values correspond to increased FFA levels and are expressed in mg KOH needed to neutralize 1 g of FAME. Elevated acid content can severely corrode engine fuel systems (Mishra & Goswami, 2018).

2.3.2.10 Free glycerin

Refers to the glycerol remaining in the completed biodiesel. Its concentration depends on the production process and may result from incomplete separation after washing. Glycerol's insolubility in biodiesel allows removal by settling or centrifuging. Excess free glycerol risks injector coking and damage to fuel injection systems (Mishra & Goswami, 2018).

2.3.2.11 Available water and sediment in fuel

Water contamination exists as either dissolved or suspended droplets, with biodiesel absorbing significantly more water (up to 1500 ppm) than diesel (around 50 ppm). Sediments may be rust, dirt, or insoluble compounds formed during oxidation (Zheng et al., n.d.). Water induces corrosion, rust, and acid formation in storage tanks, and promotes microbial growth, which generates sludges and plugging agents; some microbes convert sulfur into corrosive sulfuric acid (Mishra & Goswami, 2018).

2.3.2.12 Ash or sulfate content

Ash content quantifies inorganic contaminants such as abrasive solids, catalyst residues, and metal soaps present in the fuel. This is determined after burning biodiesel and treating the residue with sulfuric acid to measure sulfated ash levels (Mishra & Goswami, 2018).

2.3.2.13 Total glycerol

Total glycerin measures residual triglycerides, diglycerides, and monoglycerides remaining after transesterification, representing bound and free glycerol (Maceiras et al., 2011). Incomplete reactions leave these glycerol-containing compounds, where total glycerol equals the sum of free and bound glycerol (Mishra & Goswami, 2018).

2.3.2.14 Carbon residue

Indicates the propensity of fuel to leave carbon deposits after combustion. It correlates strongly with FFA content, unsaturated fatty acids, soaps, glycerides, polymers, and inorganic impurities. Despite the name, carbon residue includes more than just carbon and is recognized in all standards (Mishra & Goswami, 2018).

2.3.2.15 Corrosion of copper strip

This test evaluates how corrosive biodiesel is towards copper, brass, or bronze components. A copper strip is exposed to fuel at 50°C for three hours, then compared with a standard strip to assess corrosion extent. Copper corrosion may result from sulfur compounds or acids, linked to the acid number (Mishra & Goswami, 2018).

2.3.2.16 Cold soak filtration

A recent addition to ASTM D6751 standards, this test determines whether crystals that form at low temperatures persist upon rewarming, potentially impacting fuel filterability (Mishra & Goswami, 2018).

2.3.2.17 Presence of phosphorus, calcium and magnesium

According to ASTM D6751, phosphorus in biodiesel must be below 10 ppm, while combined calcium and magnesium should not exceed 5 ppm. Phosphorus content is measured using ASTM D4951, and calcium plus magnesium via EN Standard 14 538 (Atabani, Silitonga, et al., 2012).

2.3.3 Advantages of Biodiesel

Several benefits are associated with biodiesel fuel, notably its oxygen content of 10–11%. This oxygen concentration facilitates improved combustion properties in the fuel (Atadashi, Aroua, energy, et al., 2010.).

There are numerous advantages to using biodiesel, including the following:

1. Biodiesel is the world's most diverse fuel. Different types of fat and oil like Soybean oil, animal fats, and leftover cooking oil are all used in its production. Since biodiesel can repurpose fats and oils, it is an excellent advanced biofuel, cutting emissions by more than 50% when compared to petroleum-based fuels. It also encourages the development of novel feedstocks. Microalgae, for example, is a future feedstock that may help meet the world's energy needs (Abdulmumin et al., 2021).

2. Biodiesel reduces greenhouse gas emissions by an average of 80% compared to petroleum diesel, even when land-use consequences are considered. It has been established by government agencies and national laboratories that biodiesel reduces greenhouse gas emissions significantly across its whole lifecycle (Abdulmumin et al., 2021)

3. With ultra-low sulfur heating oil, biodiesel can be blended to form bioheat, a fuel for home heating. It is a simple decision that provides better fuel for the home and the environment. Bioheat is heating oil for the future, and it is currently sweeping the industry. Bioheat fuel blends range from B20 up to B100, with most businesses now offering blends from B20 on up (Abdulmumin et al., 2021).

4. It fits seamlessly with today's diesel infrastructure. In other words, it fits in existing vehicles and technologies, biodiesel blends provide performance characteristics like conventional diesel, such as fuel economy, horsepower, and torque. Depending on the fuel type and concentration, biodiesel may also provide the following extra performance advantages like longer engine life due to improved lubricity. Enhanced combustion because of increased Cetane numbers, emissions reductions when compared to petroleum-based alternatives (Abdulmumin et al., 2021).

In conclusion, biodiesel can be said to have the potential to provide some perceived advantages over the conventional diesel derived from fossil fuel including political, economic, and agricultural benefits, as well as environmental (due to its biodegradability, lower toxicity, and renewability) and health benefits (greenhouse gas-saving, less harmful exhaust emissions) (Abdulmumin et al., 2021).

2.4 BIODIESEL PRODUCTION TECHNOLOGIES

Biodiesel production typically involves an oil extraction step following feedstock preparation. This extraction yields crude oil and byproducts such as seed or kernel cakes. Common extraction techniques include:

1. Mechanical pressing
2. Solvent extraction and
3. Enzymatic methods.

Mechanical extraction, using expellers or presses on whole seeds or kernels, achieves yields of 68–80% (Atabani et al., 2012). Solvent extraction employs liquid solvents with variations in particle size, extraction temperature, agitation, and solvent type affecting efficiency, using approaches like hot water extraction, Soxhlet extraction, and ultrasonication. Enzymatic extraction, especially with alkaline proteases, has shown promising results and can be enhanced by ultrasonication pretreatment (Atabani et al.,)

The principal challenges of using crude vegetable oils as fuel—such as high viscosity, low volatility, and high polyunsaturation—can be mitigated through several methods:

1. Direct use and blending
2. Pyrolysis
3. Microemulsification
4. Transesterification (Atabani et al., 2012)

2.5 BIODIESEL PRODUCTION METHODS

2.5.1 Pyrolysis

Pyrolysis, also referred to as thermal cracking, involves a chemical transformation induced by thermal energy in the presence of a catalyst and the absence of air or nitrogen. The feedstocks for biodiesel production via pyrolysis can include vegetable oils, animal fats, natural fatty acids, or methyl esters of fatty acids. Studies have indicated that pyrolyzing triglycerides yields biodiesel compatible with diesel engines, with temperature-dependent liquid fractions from vegetable oils closely resembling diesel fuel. This decomposition results in various hydrocarbons such as alkanes, alkenes, alkadienes, aromatics, and carboxylic acids (Atabani et al., 2012) (Ma & Hanna, 1999a) (Balat et al., 2008). Moreover, pyrolyzates typically exhibit lower viscosity, flash point, and pour point compared to petroleum diesel while maintaining comparable calorific values (Atabani et al., 2012). Pyrolysis can be categorized into conventional, fast, and flash pyrolysis based on operating conditions, with the triglyceride pyrolysis mechanism described by Schwab et al. (A. W. Schwab et al., 1988).

In an oxygen-free environment, pyrolysis converts materials through heat and catalysis (Higman et al., 1973). Compared to alternative cracking techniques, this method provides benefits including speed, decreased pollution, and efficiency (A. W. Schwab et al., 1988). However, pyrolysis for biodiesel synthesis is considered outdated, prompting the adoption of newer technologies (Maheshwari et al., 2022).

2.5.2 Microemulsification

Microemulsification refers to a colloidal dispersion of optically isotropic fluids at the microstructural scale (1–150 nm), formed spontaneously by mixing two immiscible liquids with ionic amphiphiles (Likoazar et al., 2014.). Microemulsions improve spray characteristics by explosively vaporizing low boiling-point constituents within micelles (Maheshwari et al., 2022). This technique addresses the high viscosity challenge of vegetable oils, producing transparent and thermodynamically stable colloidal dispersions.

Solvents like methanol, ethanol, hexanol, butanol, and 1-butanol facilitate microemulsion formation, meeting diesel fuel viscosity standards. Typical droplet diameters range between 10 and 100 nm. Microemulsions can be prepared from vegetable oils combined with esters and dispersants or mixtures containing alcohols, surfactants, and cetane improvers, optionally blended with diesel. Butanol, hexanol, and octanol are effective in meeting viscosity requirements, with 2-octanol particularly efficient in solubilizing methanol in vegetable oils. Methanol is favored economically over ethanol (Mishra & Goswami, 2018).

2.5.3 Direct Use and Blending

The direct use and blending of vegetable oils or animal fats constitute some of the earliest and simplest approaches for employing these substances as alternative diesel fuels. This technique involves either using the oils directly in modified engines or blending them with conventional diesel to improve fuel properties, especially viscosity (Ma & Hanna, 1999a). As early as 1980, vegetable oils were proposed as fuels, positioning petroleum as the alternate fuel with vegetable oils and alcohols as renewable alternatives (Ma & Hanna, 1999b) (Bartholomew, 1981). During the South African oil embargo,

sunflower oil blends (10% vegetable oil) were successfully used in pre-combustion chamber engines without modifications (Ma & Hanna, 1999a) (Singh et al., 2010.). Although 100% vegetable oil substitution was impractical then, blends of up to 20% vegetable oil with diesel proved viable. Additionally, experimental use of 50:50 blends of vegetable oil and diesel has been documented (Mishra & Goswami, 2018).

2.5.4 Transesterification

Transesterification, the preferred method for biodiesel synthesis, involves the reaction of fatty acids or oils with alcohols to yield fatty acid esters and glycerol. This reaction can be catalyzed or non-catalyzed; however, the non-catalyzed process requires elevated temperature and pressure yet yields lower product quantities (Murugesan et al., 2019.). Catalysts significantly enhance both reaction rate and yield. Free fatty acids (FFAs) react with alcohols to form fatty acid methyl esters (FAME) and water. To drive the reversible reaction forward, excess alcohol is typically employed. Primary and secondary alcohols with carbon chain lengths from C1 to C8 are commonly used. Catalyst selection is dictated by factors including conversion efficiency, corrosion potential, and end-product separation (Maheshwari et al., 2022).

During biodiesel synthesis, triglycerides undergo transesterification with alcohol (commonly methanol), producing methyl esters of fatty acids (biodiesel) and glycerol across three sequential steps: triglycerides to diglycerides, diglycerides to monoglycerides, and monoglycerides to glycerol (Soltani et al., 2015b). Stoichiometrically, 3 moles of alcohol react with 1 mole of triglyceride to

yield 1 mole of glycerol and 3 moles of biodiesel. Industrial processes often utilize a 6:1 methanol-to-triglyceride molar ratio to shift equilibrium towards product formation (Fukuda et al., 2001).

Catalysts used in transesterification include acids, alkalis, and lipase enzymes (Fukuda et al., 2001) (Soltani et al., 2015b) (Chisti, 2007). Alkali-catalyzed reactions proceed approximately 4000 times faster than acid-catalyzed ones leading to commercial preference for sodium and potassium hydroxide at about 1% by weight of oil. Alkoxide catalysts such as sodium methoxide provide enhanced activity and are increasingly utilized. Although enzymatic catalysis offers distinct advantages, its high cost currently limits widespread application (Chisti, 2007) (Fukuda et al., 2001). To minimize saponification and consequent yield loss, both the oil and alcohol must be dry with minimal FFAs. Post-reaction, biodiesel is purified by repeated washing to eliminate glycerol and residual methanol. Transesterification methods are broadly classified into catalytic and non-catalytic approaches (Mishra & Goswami, 2018).

2.5.5 Catalytic Transesterification

Catalytic transesterification employs various catalyst types grouped as alkali, acid, enzymatic, or heterogeneous. Alkali catalysts including sodium hydroxide, sodium methoxide, potassium hydroxide, and potassium methoxide are notably effective (Meher et al., 2006.). Acid catalysts such as sulfuric acid, hydrochloric acid, and sulfonic acids are also utilized, though at higher alcohol-to-oil molar ratios and under moderate reaction conditions. Heterogeneous catalysts encompass

enzymes, titanium-silicates, alkaline-earth metal compounds, anion exchange resins, and organic polymer-supported guanidines (Vicente et al., n.d.). Methanolysis of vegetable oils or animal fats with methanol is well-established industrially, primarily catalyzed by acids or alkalis such as sulfuric acid or sodium hydroxide. These catalysts are less effective or inactive for long-chain alcohols, with sodium and potassium bases favored for their availability and catalytic effectiveness (Balat et al., 2008.).

2.5.6 Alkali Catalytic Transesterification

Alkali catalytic transesterification primarily uses alkaline metal alkoxides, hydroxides, and carbonates (A. Schwab et al., 1987.) (L. Meher, Sagar, et al., n.d.) (Balat et al., 2008.). Alkali catalysts efficiently convert vegetable oils with low FFA content; however, oils with significant FFA lead to soap formation, impeding separation of biodiesel, glycerin, and wash water (Canakci et al., 2003.). Typical conditions involve batchwise transesterification at atmospheric pressure and temperatures between 60–70°C with excess methanol (A. Srivastava & Prasad, 2000). Despite high conversion rates, alkali catalyst removal adds complexity and cost (Demirbaş, 2002). Although alkali hydroxides like KOH and NaOH are less active than alkoxides, they remain economical alternatives with increased catalyst concentrations (1–2 mole %) achieving comparable conversions (Schuchardt et al., 1998). Economic advantages include methanol recovery and glycerol by-product production, the latter used in pharmaceuticals, but requiring removal to prevent harmful emissions on combustion (Balat et al., 2008.).

2.5.7 Acid-Catalyzed Transesterification

Acid-catalyzed transesterification employs catalysts such as sulfuric acid, hydrochloric acid, and organic sulfuric compounds (Goff et al., 2004) (Liu et al., n.d.) [Acid-catalyzed alcoholysis of soybean oil, Effect of water on sulfuric acid catalyzed esterification]. Studies reveal that sulfuric acid exhibits optimal catalytic activity at 1.5–2.25 M concentration (Al-Widyan et al., 2002.). Acid-catalyzed processes require high alcohol-to-oil molar ratios, moderate temperatures, and relatively high catalyst concentrations to achieve acceptable yields. Despite their insensitivity to FFAs, these reactions have been less favored due to slower kinetics (Y. Zhang et al., 2003).

2.5.8 Enzymatic Transesterification

Enzymatic transesterification, predominantly catalyzed by lipases from organisms such as *Candida antarctica*, *Candida rugosa*, *Pseudomonas cepacia*, and *Rhizomucor miehei*, offers a biologically-driven alternative (Royon et al., 2007) (chemistry & 2003,) (Bernardes et al., 2007) (Ming et al., 1999.). Although enzymatic methods provide cleaner reaction profiles and can process aqueous or non-aqueous systems, their reaction rates are slower compared to chemical catalysts, and the cost of enzymes remains a significant barrier (Y. Zhang et al., 2003) (Mishra & Goswami, 2018).

2.5.9 Non-Catalytic Supercritical Methanol Transesterification

Non-catalytic supercritical methanol transesterification involves using supercritical conditions of methanol, ethanol, propanol, or butanol to produce biodiesel, demonstrating promising potential [Biodiesel production via non-catalytic SCF method and biodiesel fuel characteristics]. Critical temperatures and pressures vary with the alcohol employed (Balat et al., 2008.). Advantages include the simultaneous reaction of glycerides and free fatty acids, elimination of diffusion barriers via homogeneous phase, tolerance to water in feedstock without catalyst deactivation, obviation of catalyst removal, and rapid complete conversion under high methanol ratios. Disadvantages include the necessity for high operation pressures (25–40 MPa), elevated temperatures leading to increased energy costs, large alcohol-to-oil ratios increasing operational costs, and challenges in reducing free glycerol content below 0.02% (Mishra & Goswami, 2018).

2.6 BIODIESEL FEEDSTOCKS

Biodiesel can be derived from a diverse array of feedstocks, including [vegetable, algae, microbial oil and animal fats], with the resultant fuel exhibiting variations in purity and composition (Mahdavi et al., 2015.). The initial and critical step in biodiesel production involves feedstock selection, which directly influences several factors such as the purity, cost, composition, and yield of the final biodiesel. Furthermore, the availability and type of feedstock source are primary determinants in classifying biodiesel into edible, non-edible, or waste-based origins (bioenergy & 2009.).

The choice of feedstock for biodiesel production is also significantly influenced by regional factors, primarily considering a country's availability and economic viability. For instance, canola oil serves as the predominant feedstock in Canada, while soybean oil is widely utilized in Brazil and the USA.

Conversely, Indonesia and Malaysia primarily employ coconut and palm oils for biodiesel production, whereas rapeseed oil is favored in European nations like Italy, Germany, Finland, and the UK. Historically, oils such as sunflower, rapeseed, soybean, and mustard have been used, but concerns regarding their impact on food security have led to a reduction in their application as biodiesel feedstocks (A. Kumar et al., 2010). Non-edible oils offer considerable advantages, including biodegradability, low sulfur content, minimal impact on the food chain, low aromatic content, and widespread availability, making them preferable alternatives. Emerging feedstocks like tallow oil, animal fats, fish oil, and microalgae also present promising avenues for biodiesel synthesis (D. Singh et al., 2020).

Based on their raw material, biodiesels are categorized into four generations:

1. First-generation from edible oils;
2. Second-generation from non-edible plant oils;
3. Third-generation from microalgae lipids, used cooking oil, or waste animal fats; and
4. Fourth-generation from genetically modified microorganisms (Pikula et al., 2020a).

2.6.1 First-Generation Biodiesel

First-generation biodiesel, primarily sourced from edible feedstocks like rapeseed, canola, and soybeans, gained initial popularity due to their availability and relatively straightforward production processes. While over 90% of biofuels currently originate from edible biomass, drawbacks such as high material costs, dependence on food prices, land expropriation, and environmental sensitivity have rendered their extensive use less effective (Pikula et al., 2020b)

COMMONLY UTILIZED EDIBLE OIL FEEDSTOCKS

2.6.1.1 Palm Oil

Palm oil, sourced from the *Elaeis guineensis* fruit, yields two distinct oils: crude palm oil from the outer pulp and palm kernel oil from the internal kernels. Crude palm oil exhibits a semi-solid consistency at ambient temperatures, while palm kernel oil is characterized by its richness in lauric and myristic fatty acids, contributing to superior oxidative stability and a distinct melting profile (Karmakar et al., 2010.). Malaysia is a global leader in palm cultivation, with plantations encompassing approximately two-thirds of its agricultural land. Palm oil has proven to be an effective biodiesel source, demonstrating an average yield of about 6000 liters of palm oil per hectare, which can produce an estimated 4800 liters of biodiesel (Addison et al., 2009.). Both Nigeria and Brazil possess significant potential for palm oil production, and the demand for palm biodiesel oil is rapidly escalating in Europe. The primary advantages of palm oil include its exceptionally high oil yield per hectare and its economic viability when compared to other edible oils (D. Singh et al., 2020). However, a notable challenge with palm oil for biodiesel production is its high saturated fatty acid content, which necessitates an additional methanol transesterification step when employing alkali-catalyzed methods, thereby increasing production costs (Crabbe et al., 2001.). An effective solution to this issue involves implementing an acid-catalyzed pre-esterification method (S. L. Lee et al., 2015). Notably, farmers in Ghana have successfully utilized palm kernel oil to power farm vehicles and generators (Karmakar et al., 2010.).

2.6.1.2 Coconut

Coconut (*Cocos nucifera*) represents another significant edible feedstock for biodiesel production, particularly embraced in the Philippines. This tall tree, typically ranging from 15 to 18 meters in height (Karmakar et al., 2010.) (D. Kumar et al., 2010.), produces oil that is predominantly composed of saturated fatty acids (86%), with minor percentages of monounsaturated (6%) and polyunsaturated (2%) fatty acids. The key fatty acids present are lauric (45%), palmitic (8%), and myristic acid (17%), alongside a lesser amount of oleic acid (monounsaturated) and linoleic acid (polyunsaturated). Coconut oil is recognized for its high biodiesel yield (Li & Khanal, 2016). When utilized in automobiles, even a 1% blend of coconut biodiesel has been shown to enhance fuel efficiency by 1–2 km and reduce emission levels by 60% due to improved oxygenation (Ahmed et al., 2014.).

2.6.2 Second-Generation Biodiesel

The adverse impact of first-generation biomass feedstock on global food prices has led researchers to explore lignocellulosic biomass resources, also known as second-generation biomass feedstock. These feedstocks include crop residues, wood residues, and dedicated energy crops specifically developed for biofuel generation. As they do not compete with food crops, second-generation biomass feedstock is increasingly recognized globally as a sustainable alternative to fossil fuels (Abdulmumin et al., 2021).

Second-generation feedstocks offer a promising alternative to the use of edible plants for biodiesel production. These non-edible plant sources present numerous advantages:

- They can thrive in contaminated or agriculturally unsuitable areas, requiring minimal fertility and humidity.
- They exhibit stability across a wide range of climatic conditions, indicating robust environmental resilience.
- They incur lower environmental stress while yielding a final product of comparable quality to that derived from edible feedstocks.
- They require less dedicated land and can be cultivated alongside other plant species, promoting efficient land use.
- They possess the potential for rehabilitating degraded lands, contributing to environmental restoration.
- Critically, they avoid competition with agricultural food sources, addressing a major concern associated with first-generation biofuels.
- They demonstrate resistance to pests and diseases, reducing crop losses and the need for chemical interventions.
- They offer the possibility of producing valuable by-products, enhancing economic viability.
- They are characterized by availability, renewability, biodegradability, and low sulfur and aromatic hydrocarbon content (C.-H. Lee, 2012).

Despite these benefits, the primary disadvantages of second-generation feedstocks include a comparatively lower oil yield and a higher alcohol consumption during the production process when compared to edible sources. Nevertheless, the inherent ability of these non-edible plants to flourish under diverse climatic conditions facilitates the establishment of stable biofuel production systems in numerous countries (Pikula et al., 2020a).

COMMONLY UTILIZED NON-EDIBLE OILS

Globally, numerous sources of renewable oils exist that are not derived from conventional food crops or annual agricultural cultivation. Illustrative examples include oil extracted from the Honge (Indian beech or pongamia) tree and *Jatropha curcas* (physic nut) (Karmakar et al., 2010.). In many developing nations, the scarcity of edible oils necessitates imports to satisfy domestic demand, leading to higher prices compared to petro-diesel. This economic context renders edible oils unsustainable as biodiesel feedstocks, thereby advocating for the adoption of non-edible alternatives. Even with substantial edible oil consumption in certain countries, such as India, the availability of used cooking oil for biodiesel production remains minimal due to its complete utilization. Consequently, it is imperative to reorient research and development efforts towards non-edible resources (Karmakar et al., 2010.).

2.6.2.1 *Jatropha curcas*

Jatropha curcas has recently gained prominence as a highly promising prospective oil source for biodiesel production across Asia, Europe, and Africa. This species demonstrates remarkable resilience, flourishing under diverse climatic conditions, including intense heat, low precipitation, ample rainfall, and frost. *Jatropha* is typically cultivated on marginal and degraded lands, thereby eliminating potential land-use conflicts with food production. The oil yield from *Jatropha* varies based on the specific species, climatic parameters, and, notably, the altitudinal growth conditions. Furthermore, various components of the plant possess medicinal properties. Beyond its contribution to diesel replacement, the cultivation of *Jatropha* trees actively contributes to the reduction of

atmospheric CO₂ concentrations. In developing regions like India, it has been identified as a primary source for biodiesel (Karmakar et al., 2010.). Jatropha oil predominantly consists of unsaturated fatty acids, such as oleic (34.3–44.7%) and linoleic acid (31.4–43.2%), along with saturated components including palmitic acid (13.6–15.1%) and stearic acid (7.1–7.4%) (Reksowardojo et al., 2007).

2.6.2.2 Neem (*Azadirachta Indica*)

Neem oil presents a color range from light to dark brown and possesses a bitter taste. The neem tree is indigenous to India and Burma, with almost its entirety being utilized for diverse applications, including medicinal remedies, pesticides, and organic fertilizers. Neem exhibits the capacity to grow in highly marginal soils, encompassing those that are notably rocky, shallow, arid, or prone to pan formation. (Karmakar et al., 2010.).

Azadirachtin, the principal constituent of neem seed oil, exhibits concentration variations from 300 to 2500 ppm, influenced by the extraction methodology and the quality of the processed neem seeds. The oil contains sulfurous compounds, which contribute to its pungent aroma and a less efficient combustion profile compared to other vegetable oils (Karmakar et al., 2010.). Neem oil primarily contains a substantial proportion of unsaturated fatty acids, such as oleic acid (25–54%) and linoleic acid (6–16%), while its saturated components include stearic acid (9–24%) (Anyanwu et al., 2013.) (Ali et al., 2013.).

2.6.3 Third-Generation Biodiesel

Given the constraints associated with first and second-generation biofuels, the exploration for alternative feedstocks for biofuel production led to the discovery of microalgae's potential. Third-generation biofuels, derived from algal biomass such as microalgae and macroalgae, have been extensively investigated and considered due to their high lipid productivity (Mat Aron et al., 2020).

2.6.3.1 Microalgae

Microorganisms, including bacteria, yeasts, cyanobacteria, and microalgae, are viable for biofuel production. Cyanobacteria and microalgae are recognized as optimal candidates for this application (Moravvej et al., 2019.). The cultivation of microalgae is gaining significant attention as a source of lipids for biodiesel (Li et al., 2012). Algae cultures are specifically defined environments where microalgae are cultivated. This form of aquaculture focuses on growing algae to yield food or other valuable products. These unicellular aquatic plants possess the capacity to generate substantial quantities of lipids suitable for biodiesel production (Pienkos et al., 2009).

Microalgae exhibit a rapid growth rate, allowing for harvesting within approximately 5 to 6 days of cultivation (Srivastava et al., 2019.) (Tang et al., 2020.). A primary advantage of utilizing microalgae as a feedstock is the low cultivation cost, as they can be grown in moist marginal areas or wastewater (Wang et al., 2016). The cultivation of microalgae is environmentally beneficial, requiring minimal cultivation area while producing high oil content, oxygen, and hydrogen (ShirReen & HwaiChyuan, 2018) (Shah et al., 2018.). Microalgal growth is contingent upon cultivation conditions and factors such as temperature, CO₂ concentration, light intensity, pH, and the nutrient composition of the culture medium (Metsoviti et al., 2019.). Three classifications of microalgae exist: autotrophic

microalgae (utilizing inorganic carbon), heterotrophic microalgae (utilizing organic carbon), and mixotrophic microalgae (utilizing both inorganic and organic carbon) (Shah, Raja, Mahmood, et al., 2016.).

2.6.3.2 Animal fat

Animal fat is a co-product of the fishery and meat industries, derivable from sources such as fish, cattle, chicken, and hogs. Currently, animal fat co-products are primarily used for biodiesel production due to their low retail prices, particularly as a substitute fuel for automobile fleets developed by companies utilizing these raw materials. Due to various animal health concerns and scandals, the use of animal fat sources for human consumption is no longer permitted. Consequently, its suitability for biodiesel development has been verified. Tallow obtained from diseased livestock has also emerged as a significant feedstock for biodiesel production. A major challenge for these feedstocks is an irregular supply, as animal fat is not exclusively produced for biodiesel. Beef tallow, mutton, yellow grease, lard, and residues from omega-3 fatty acid extraction are employed in the production of third-generation biodiesel (Abishek et al., 2014).

These represent primary by-products of the leather and meat industries. These sources offer advantages in terms of food security, economic viability, and environmental benefits compared to edible oils. However, animal waste fats with higher saturated fatty acids and free fatty acids necessitate complex processing methods. Conversely, animal waste fats with lower saturated fatty acid content offer several benefits, including a shorter ignition delay, good oxidation stability, and an elevated calorific value (Adewale et al., 2015.).

2.6.3.3 Waste oil

The production of biodiesel can effectively utilize a diverse range of waste oils. These materials are generally cost-effective and contribute to environmental sustainability by repurposing substances that would otherwise require disposal (Elkady et al., 2015). Waste oils are broadly categorized into three types: those originating from the food industry, non-food industry, and household and restaurant sources. Common examples include waste oils derived from rapeseed, coconut, soybean, and palm, which are frequently employed in biodiesel development. However, processing these waste oils necessitates additional steps to manage the high acid content at elevated temperatures and to remove residues. Furthermore, numerous co-products from food processing facilities can also be valorized for biodiesel production. In the non-food sector, waste plastic oil and waste tire oil are utilized to generate biodiesel through the pyrolysis process (Knothe et al., 2009.).

2.6.4 Fourth Generation Biofuels

Fourth-generation biofuels primarily derive from genetically modified microalgae. These microorganisms are engineered to enhance carbon dioxide uptake for photosynthesis, thereby creating an artificial carbon sink, and to augment biofuel production (Abdullah et al., 2019.) (Vassilev et al., 2016). Several algal strains, such as *Chlamydomonas reinhardtii* sp., *Phaeodactylum tricornutum* sp., and *Thalassiosira pseudonana* sp., have undergone genetic modifications to improve their growth rates and adaptability to nutrient-poor environments (Abdullah et al., 2019.). The genetic manipulation of microalgae primarily targets lipid and carbohydrate metabolism, enhanced nutrient utilization, hydrogen production, improved photosynthetic efficiency, increased stress tolerance, facilitated cell disintegration, and optimized flocculation (Bharadwaj et al., n.d.). Additionally, genetic modifications can assist in oil extraction from microalgal biomass by inducing autolysis and enabling product secretory systems (Moravvej et al., 2019.).

CULTIVATION SYSTEMS FOR GENETICALLY MODIFIED MICROALGAE

Genetically modified microalgae can be cultivated in either closed or open systems (Adeniyi et al., 2018.). Closed systems offer enhanced security by protecting the cultivation environment from external elements and minimizing contamination risks (Adeniyi et al., 2018.). However, the higher operational costs associated with closed systems often render them less economically viable. Conversely, open systems are susceptible to leakage, which poses a risk of microalgae escaping or leaching into the surrounding environment (Hannon et al., 2010).

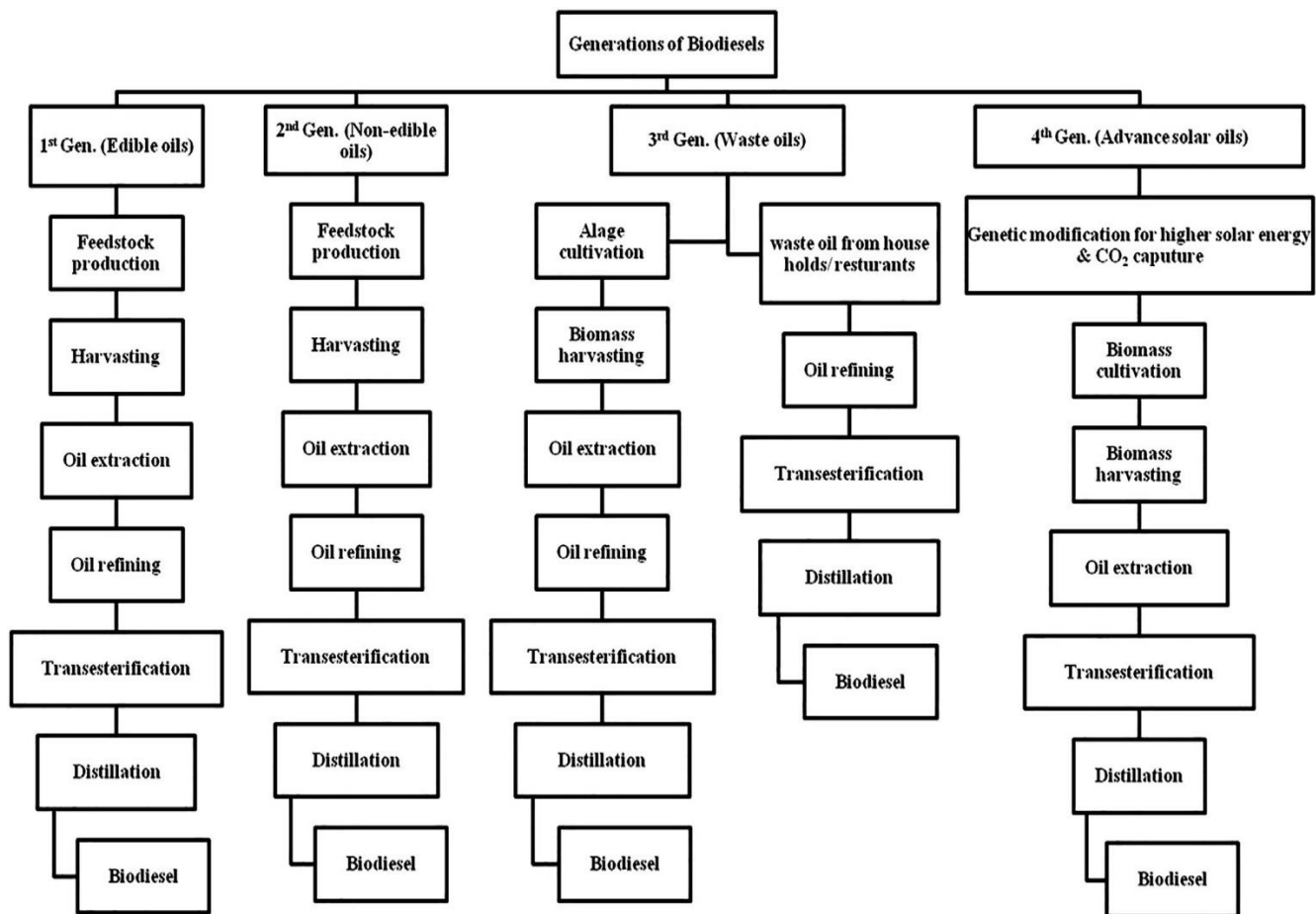


Figure 1: Biodiesel production process for different generations. (S. Singh et al., 2010.)

2.7 CATALYSTS IN BIODIESEL PRODUCTION

While various established methods exist for biodiesel synthesis, transesterification is widely recognized as the prevalent pathway. This process entails a catalyzed chemical reaction involving either vegetable or animal oils and an alcohol, yielding fatty acid alkyl esters (biodiesel) and glycerol (Y. Zhang et al., 2003). This approach is favored due to its efficiency in converting triglycerides into biofuel components.

A catalyst is defined as a substance that accelerates the rate of a chemical reaction without undergoing permanent chemical transformation itself. Theoretically, a catalyst is practically not consumed in a single reaction cycle. Catalysts modify the reaction speed of thermodynamically feasible processes; however, they cannot enable reactions that are thermodynamically unfavorable (Bohlouli & Mahdavian, 2021). Essentially, a catalyst functions as a chemical entity capable of influencing both the reaction rate and the thermodynamic progression of a reaction.

In reversible reactions, a catalyst similarly impacts the rates of both forward and reverse reactions, thus not altering the equilibrium constant. When multiple reaction mechanisms are plausible, catalyst selection is crucial to enhance the proportion of desired products relative to unwanted byproducts. Although catalysts are ideally expected to remain unchanged during a reaction, practical applications reveal that they are reactive substances susceptible to irreversible physical and chemical alterations over time, which can diminish their efficacy, especially after facilitating numerous reactions (Bohlouli & Mahdavian, 2021). Catalysts employed in the transesterification of vegetable oils and animal fats are generally categorized into three main types: homogeneous, heterogeneous, and enzymatic catalysts (Helwani et al., 2009.).

2.7.1 Homogeneous Catalysts

Homogeneous catalysts share the same phase as the reactants and products, typically exhibiting high solubility in alcohol during biodiesel production (De Boer, 2010). These catalysts are further classified into homogeneous alkaline and homogeneous acidic categories (Bohlouli & Mahdavian, 2021). While transesterification with homogeneous catalysts can be conducted at moderate temperatures and atmospheric pressures, this method often presents drawbacks, including the typical inability to recycle the catalyst (De Boer, 2010) and the necessity for separation from the product streams (biodiesel and alcohol/glycerol). Furthermore, homogeneous catalysts have been observed to react with impurities, particularly free fatty acids (FFAs), leading to soap formation as a side reaction (Bohlouli & Mahdavian, 2021).

2.7.1.1 Homogeneous alkaline catalysts

Sodium hydroxide (NaOH), potassium hydroxide (KOH), sodium methoxide (NaOCH₃), potassium methoxide (KOCH₃), sodium ethoxide (NaOC₂H₅), sodium peroxide (Na₂O₂), and sodium butoxide (C₄H₉NaO) are among the most frequently utilized homogeneous alkaline catalysts in the transesterification of edible oils (Kulkarni et al., 2006). The formation of water, a byproduct of transesterification with potassium hydroxide and sodium hydroxide, can diminish biodiesel yield. Conversely, transesterification with sodium methoxide and potassium methoxide results in superior performance due to the absence of water as a reaction byproduct (Sharma et al., 2009.). Homogeneous alkaline catalysts are most effective with refined oils possessing FFA values below 0.5%, as higher FFA levels promote soap formation and complicate separation processes (Issariyakul et al., 2014.) (Tariq et al., 2012.). While some studies suggest alkaline catalysts may tolerate elevated FFA

concentrations, it is generally accepted that for optimal performance in transesterification, the FFA content in the oil should ideally remain between 0.5 wt.% and 2 wt.% (Bohlouli & Mahdavian, 2021).

2.7.1.2 Homogeneous acidic catalysts

Homogeneous acid catalysts demonstrate greater tolerance to the presence of water or moisture during the reaction. They are frequently employed to reduce the FFA content in used cooking oils and animal fats before full transesterification with an alkali catalyst (Tariq et al., 2012.). However, their corrosive nature necessitates specialized and more costly processing equipment. The reaction rate catalyzed by homogeneous acidic catalysts is considerably slower, approximately 4000 times less efficient than that of alkaline catalysts (Wang et al., 2006.). Additionally, acidic catalysts require higher reaction temperatures and a greater alcohol-to-oil molar ratio, which collectively limit their widespread application in this field (De Boer, 2010). Common acidic catalysts used in transesterification include sulfuric acid (H_2SO_4), sulfonic acid (HSO_3R), and hydrochloric acid (HCl) (Atadashi et al., 2013.).

2.7.2 Heterogeneous Catalysts

In heterogeneous catalysis, the reactants and the catalyst exist in distinct phases, with the chemical reaction primarily occurring at the catalyst's surface (Dalvand & Mahdavian, 2018). Typically, heterogeneous catalysts are solid materials, contrasting with homogeneous catalysts which operate within the same phase as the reactants. Similar to homogeneous catalysts, heterogeneous catalysts employed in biodiesel production are broadly categorized into alkaline and acidic types (Mardhiah et

al., 2017.). A significant advantage of these solid catalysts is their facile separation from the final product, enabling convenient recycling for subsequent reaction cycles and thereby offering a more economically viable route to biodiesel production (Meher et al., 2013.). Furthermore, the utilization of heterogeneous catalysts for biodiesel synthesis is regarded as an environmentally benign process (Meher et al., 2013.), as it streamlines the biodiesel filtration process, consequently reducing energy and water consumption (YieHua & Abdullah, 2015).

2.7.2.1 Heterogeneous alkaline catalysts

Various metal oxides have been investigated for their efficacy as heterogeneous alkaline catalysts, including calcium oxide (CaO), magnesium oxide (MgO), and composite oxides such as (CaO/ZnO), (Li/CaO), mixed metal oxides, and hydrotalcites (Borges et al., 2012.). Mixed metal oxides, specifically Mg/Al and Mg/Zr, have also demonstrated commendable performance in the transesterification process (Fraile et al., 2009.). Notably, heterogeneous alkaline catalysts can be derived from diverse waste materials like bone, ash, fruit peels, and shells, which exhibit significant potential as catalytic agents for biodiesel synthesis (YieHua & Abdullah, 2015). These catalysts offer a solution to limitations associated with homogeneous alkaline catalysts, particularly the issue of soap formation which impedes the separation of the glycerol layer from the methyl ester layer (Hassani et al., 2016.). Moreover, these alkaline catalysts are readily separable and reusable; despite potential destruction of active sites due to their low solubility during reaction, these sites can often be regenerated through straightforward methods (Chen et al., 2013.). However, a notable disadvantage of heterogeneous alkaline catalysts is their susceptibility to moisture absorption during storage (Mardhiah et al., 2017.).

Recent research has explored the application of waste materials as catalysts in chemical reactions, with low-cost solid-waste materials showing promise for sustainable biodiesel production. Dominant mineral wastes, such as cement waste from concrete and mortar containing quartz, calcite, sodium/calcium aluminosilicates, albite, and portlandite, possess an inherent alkaline nature suitable for catalysis (Kumar et al., 2018.). Eggshells, rich in calcium carbonate, can be calcined at 900°C to yield CaO, which has demonstrated high catalytic activity in transesterification, achieving biodiesel yields up to 93.5%. The utilization of waste materials for catalyst preparation not only addresses waste disposal challenges but also provides value-added materials for various industrial applications. Furthermore, organic waste-based solid catalysts, including plantain peels, wood, coconut shells, palm trunks, and sugarcane bagasse, have been successfully developed and applied. Banana peels, for instance, contain potassium and sodium oxides that can be converted into their corresponding catalytic forms (Thangaraj et al., 2019).

2.7.2.2 Heterogeneous acidic catalysts

Heterogeneous acidic catalysts primarily comprise zeolites, heteropoly acids, pure oxides, or modified transition metals such as zirconium, molybdenum, silica, and alumina (Galadima & Muraza, 2014). These catalysts are generally more stable and environmentally friendly than their homogeneous counterparts (Galadima & Muraza, 2014). Ideal heterogeneous acidic catalysts should possess a high density of accessible active sites, moderate acidity, hydrophobicity, and sufficient porosity to mitigate diffusional limitations. Key advantages of these catalysts include their reusability, efficient conversion capabilities, and ease of separation and product filtration (Guldhe et

al., 2017.). The substitution of homogeneous catalysts with heterogeneous acidic catalysts can eliminate several separation processes, reduce hazardous wastewater generation, and prevent corrosion phenomena (Hassani et al., 2016). Nevertheless, a drawback of heterogeneous acidic catalysts is their requirement for elevated temperatures and extended reaction times to achieve high conversion yields (Thangaraj et al., 2019).

2.7.2.3 Heterogeneous nano-catalysts

In recent decades, significant research has focused on the development of novel and cost-effective nanomaterials for various applications, including carbon nanotubes, nanoclays, nanofibers, nanocomposites, porous nanomaterials, nanowires, and nanoparticles (Bohlouli & Mahdavian, 2021). Nanoparticles, defined as spherical or pseudo-spherical particles with diameters less than 100 nm, play a critical role in numerous catalytic processes, representing one of the earliest applications of nanotechnology (Banković–Ilić et al., n.d.). The utility of nanoparticles in catalysis is underscored by their distinctive characteristics, such as enhanced selectivity, high durability, and recyclability, making them highly significant from environmental, social, technological, and scientific perspectives. The most salient features of nanocatalysts include 100% selectivity, high levels of activity, prolonged operational lifespan, and ultra-low energy consumption (Today & 2006.).

A reduction in catalyst particle size inherently increases the relative active surface area, a crucial catalytic property. Consequently, as particle size diminishes and the surface-to-volume ratio increases, reaction efficiency improves, and the required catalyst quantity decreases (Amini et al., 2013). The synthesis of transition metal nanoparticles has been extensively explored, largely due to

their substantial catalytic activities, which scale proportionally with their high surface-to-volume ratio. Despite their pronounced catalytic efficacy, the application of metal nanoparticles faces certain limitations, particularly concerning the separation of products from residues and the reusability of the nanocatalysts (Chaturvedi et al., 2012.).

2.7.3 Biocatalysts (Enzymatic)

The application of biocatalysts represents an innovative and practical methodology that has effectively addressed numerous human and environmental challenges. Several distinguishing factors set biocatalysts apart from conventional catalysts. Notably, enzymes, unlike alkaline catalysts, do not induce soap formation and yield high-purity biodiesel, even when utilizing lower-grade feedstocks such as cooking oil (MacEiras et al., 2010.).

Traditional transesterification processes have historically encountered difficulties due to the presence of free fatty acids (FFAs) and water in raw materials (Brask et al., 2011). However, these issues can be circumvented through the employment of enzymes as catalysts in the transesterification process. Enzymatic transesterification is particularly well-suited for raw materials containing elevated levels of FFAs, including waste oils, beef, and pork suet, because FFAs are directly converted into alkyl esters by the enzymatic catalysts (Christopher et al., 2014.) Broadly, enzymatic catalysts are categorized into two types: extracellular and intracellular lipases. Factors such as thermal stability, high selectivity, efficiency, minimal adverse reactions, and excellent recyclability are posited as reasons for the high effectiveness of biocatalysts. Nevertheless, significant drawbacks include the substantial production cost of biocatalysts, their protracted reaction times, and limitations concerning

their utilization and recycling, which collectively diminish their overall efficiency (Fukuda et al., 2001).

A notable challenge associated with biocatalyst application is the inactivation of most lipases by methanol, which is the preferred acyl acceptor in alcoholysis. This inactivation restricts the permissible concentration of methanol or ethanol during the conversion reaction (Reviews & 2013, n.d.). Unspecific binding of solvent molecules to the protein structure can induce unfolding or aggregation, leading to irreversible enzyme inactivation. Additionally, solvent molecules may non-covalently bind to the enzyme's substrate binding site or substrate entrance channel, resulting in competitive inhibition. A comprehensive understanding of these mechanisms is foundational for devising engineering strategies to surmount these limitations (Lotti et al., 2018). One efficacious approach to mitigate this problem involves enzyme immobilization, utilizing various supports such as polymeric matrices, colloidal suspensions, powdered materials, metallic and glass surfaces, carbon nanotubes, and porous or non-porous inorganic materials (e.g., mesoporous silicates, mesocellular foam).

Table 2.1: Advantages and disadvantages of catalysts used in the transesterification reaction (Bohlouli & Mahdavian, 2021).

Catalyst	Types of catalysts	Advantages	Disadvantages
Homogeneous alkaline	NaOH, KOH	<ul style="list-style-type: none"> * High catalytic activity * Quick reaction time * Cheap * Desirable kinetics * Moderate operating conditions 	<ul style="list-style-type: none"> * Highly sensitive to water and free fatty acid * Soap-making as a reaction * Non-recyclable catalyst
Homogeneous acidic	H ₂ SO ₄ , HCL, HF, H ₃ PO ₄ , ρ-sulfonic acid	<ul style="list-style-type: none"> * They are not sensitive to free fatty acids and the amount of water in the oil. * The esterification and transesterification reactions are performed in the presence of catalysts. * There is no soap-making process. 	<ul style="list-style-type: none"> * Slow reaction rate * Lengthy reaction time * High levels of reaction temperature and pressure * High levels of molar ratio of alcohol to oil * Weak catalytic activity * Difficulty in recycling the catalysts
Heterogeneous alkaline	CaO, MgO, SrO, mixed oxide and hydrotalcite	<ul style="list-style-type: none"> * Eco-friendly * Non-corrosive * Recyclable * Easily separated * Higher levels of selectivity * Longer durability 	<ul style="list-style-type: none"> * Compared to homogeneous counterparts, they have a slower reaction rate. * They are sensitive to water and free fatty acids. * Soap-making is observed during a given reaction. * Their synthesis is complex and expensive.
Heterogeneous acidic	ZrO, TiO, ZnO, ionexchange resin, sulfonic modified mesostructured silica, sulfonated carbonbased catalyst, heteropolyacids and zeolites	<ul style="list-style-type: none"> * Not sensitive to free fatty acid and the amount of water in oil * The esterification and transesterification reactions are performed in the presence of catalysts. * Recyclable and eco-friendly * Resistant to corrosion to reactor and reactor parts 	<ul style="list-style-type: none"> * Slow reaction rate * Lengthy reaction time * High levels of reaction temperature and pressure * High levels of molar ratio of alcohol to oil * Weak catalytic activity * Their synthesis is complex and expensive.
Nano-catalyst	KF/CaO-Fe ₃ O ₄ K ₂ O/γ-Al ₂ O ₃ Ca/Al/Fe ₃ O ₄	<ul style="list-style-type: none"> * Maximum active surface per units of mass and volume * Controllable shape and size * The possibility to separate them from the reaction mixture * Highly selectable and efficient * Highly variable and chemically modifiable 	<ul style="list-style-type: none"> * Susceptible to clogging
Enzyme	Candida antarctica fraction B lipase, Rhizomucor miehei lipase	<ul style="list-style-type: none"> * Transesterification can be carried out at a low reaction temperature, even lower than the homogeneous alkaline catalysts. * Not sensitive to free fatty acid and the amount of water in the oil * No soap-making process * Not-contaminated * Easy filtration 	<ul style="list-style-type: none"> * The reaction rate is very slow, even slower than the acidic catalysts. * It is very expensive. * It is sensitive to alcohol. It is usually methanol that can disable the enzyme.

2.8 OPTIMIZATION TECHNIQUES IN BIODIESEL PRODUCTION

The development of any product or process fundamentally relies on a meticulously planned experimental design. A robust experimental design necessitates a comprehensive understanding of

the system under investigation (Bell, 2012). When considering factorial designs, it is essential to discern both independent and dependent factors. Once these factors are identified, experiments are systematically designed and analyzed to ascertain the technique yielding a maximal response, with optimization serving as a widely employed process for identifying the most advantageous alternative among available options (Alonso et al., 2012). Contemporary research frequently utilizes various optimization techniques to facilitate a clearer understanding and selection of the most appropriate outcomes (Reji et al., 2022.).

2.8.1 Design of Experiments (Doe)

The Design of Experiments (DOE), initially developed for agricultural applications by British statistician Sir Ronald Fisher in the 1920s (Antony, 2023), has since become a widely adopted statistical method across diverse scientific and industrial domains. Its application is particularly notable in supporting the design, development, and optimization of products and processes (Antony, 2023). DOE encompasses a suite of applied statistical tools systematically used to categorize and quantify the causal relationships between variables and the outputs of a studied process or phenomenon. This ultimately allows for the identification of optimal settings and conditions. Standardized guidelines and procedures are available to facilitate the implementation of DOE methods (Antony, 2023), which typically involve defining objectives and response variables, determining factors and levels, selecting an experimental design type, and executing the experiment.

The selection of variables, including the number of factors, levels, and their specific logic, is generally contingent on the type of investigation (e.g., screening, characterization, or optimization), the nature of the process, and the available resources. While a multitude of DOEs can theoretically align with

an investigation type, it is challenging to readily identify the design that offers the most profound insights with the fewest resources. Fundamentally, a well-structured experimental design ensures the validity of the derived insights, with distinctions between good and excellent DOEs often lying in their efficiency—the ratio of extracted information to invested resources (Jankovic et al., 2021).

Each DOE typically progresses through a series of stages: planning, execution of the experiment, and analysis of the collected experimental data utilizing various statistical methods to derive valid and objective conclusions (Mojib Zahraee et al., 2013). The process commences with the selection of the system or process and the precise identification of the research problem. The problem statement then guides the establishment of objectives, which in turn dictate the definition of the performance indicator (response variable) as a quantitative measure of system behavior. A crucial subsequent step involves defining the factors influencing the performance indicator, how they are discretized, the number of experimental runs, and an appropriate experimental array (Farooq et al., 2016).

The third stage involves conducting the experiment in accordance with the designed array and collecting the necessary data. The final stage comprises data analysis using statistical tools, such as ANOVA and related methods, and the interpretation of results, leading to an enhanced understanding of system behavior or its optimization (Jankovic et al., 2021). DOE serves as a systematic approach for establishing the correlation between processing parameters and process output, aiming to pinpoint design variables that exert significant influence for further in-depth investigation (engineering & 2021.). Commonly employed first-order designs include (2^k) factorial, simplex, and Plackett-Burman designs, whereas prevalent second-order designs encompass central composite, (3^k) factorial, and Box-Behnken designs (Reji et al., 2022.).

The Design of Experiments (DOE) offers a diverse range of approaches to efficiently explore process parameters and their effects on outcomes. Each design type is tailored for specific research objectives, balancing the need for comprehensive data with experimental resources. Understanding the characteristics of these designs is crucial for selecting the most appropriate methodology for a given optimization task.

2.8.1.1 Prominent Doe Designs

1. (2^k) Factorial Design:

- Evaluates each of (k) variables at two levels, typically coded as -1 (low) and 1 (high).
- Often used as a "screening design" to identify significant main effects and interactions, assuming a roughly linear relationship within the interval of interest (Pais et al., 2014)

2. Plackett-Burman Design:

- Similar to the (2^k) design, it allows two levels for each of the (k) control variables.
- Requires significantly fewer experimental runs, especially for a large number of factors, making it more cost-effective than the full (2^k) design (Kaur & Kaur, 2013).
- These designs are "saturated," meaning the number of design points equals the number of variables approximated in the model, and are often recommended for investigating more than seven factors (Reji et al., 2022.).

3. Simplex Design:

- A saturated design consisting of $(n = k + 1)$ points, where (k) is the number of variables (Reji et al., 2022.).

- Its design points form the vertices of a (k)-dimensional regular-sided figure, characterized by an angle of ($\cos \theta = -1/k$) between any two points and the design center (Reji et al., 2022.).

4. (3^k) Factorial Design:

- Includes all possible permutations of three levels for each of the (k) control variables.
- The total number of trial runs is (3^k), which can become very large, particularly for higher (k) values.
- The cost of such experiments can be mitigated by employing fractional (3^k) designs (Reji et al., 2022.) (Bezerra et al., 2008.)

5. Central Composite Design (CCD):

- A highly preferred design, often referred to as a Box-Wilson central composite design (Sahoo et al., 2012.).
- Comprises central points (at the design space's center), factorial points (with factor levels -1 and +1), and axial points (symmetrically arranged on the coordinate system's axes relative to the central point) (Sahoo et al., 2012.).
- CCD is advantageous for sequential trials, allowing for expansion upon prior factorial assessments by adding axial and center points (Sahoo et al., 2012.).

6. Box-Behnken Design (BBD):

- Defined by Box and Behnken, this design utilizes three levels for each factor, derived from a specific subset of the factorial combinations from a (3^k) factorial design (Reji et al., 2022.) (Bezerra et al., 2008.).
- It is popular in industrial research due to its cost-effectiveness, requiring only three levels for each element with configurations typically set at -1, 0, and 1 (Bezerra et al., 2008.).

- BBD allows for the sequential analysis of the impact of various design parameters by keeping other elements constant while examining specific factors.

Several software tools facilitate the implementation and analysis of these experimental designs:

1. **Design-Expert:** A specialized statistical software package from Stat-Ease Inc., exclusively focused on the execution of Design of Experiments (DOE) (Akram et al., 2021).
2. **ECHIP:** Offers a user-friendly interface for conducting statistically planned experiments with its state-of-the-art software package (Hahn et al., 2006.).
3. **Nemrodw:** Provides a wide array of experiment matrices to meet specific needs and accommodate both technical and financial experimental constraints (Mazerolles et al., 1989.).
4. **Minitab:** A comprehensive program for statistical analysis, suitable for both learning and conducting statistical research (Rostamiyan et al., 2015.).
5. **Systat:** Delivers an unparalleled selection of scientific and technical graphing possibilities, enabling the creation of individualized graphs for more meaningful results (X. Zhang et al., 2018).

2.8.2 Response Surface Methodology (RSM)

Response Surface Methodology (RSM) is a powerful statistical and mathematical technique widely used for the design, optimization, and analysis of experiments in various processes (Baş et al., 2007.). It is frequently employed to develop and improve new products and processes, especially when multiple input variables influence a process's performance (Chan et al., 2017.) RSM establishes a

series of experiments to fit an empirical model, allowing for the determination of optimal conditions for input variables that yield maximum or minimum responses within a specified region of interest (Myers, 1999). By correlating a response to the levels of various influencing factors through experimental design and analysis, RSM utilizes one or more polynomial regression equations to model the functional relationships between factors and response values, thereby optimizing process parameters and predicting response outcomes (Kaur & Kaur, 2013). This approach enhances result reproducibility and facilitates process improvement, making it valuable in diverse optimization scenarios where the effects of multiple factors and their interactions on several response variables need to be analyzed [(Ba & Boyaci, 2007) (Reji et al., 2022.).

2.8.2.1 Applications of RSM

1. Statistical Optimization Tool: RSM is primarily utilized as a statistical tool for the optimization of various processes and experiments (Chan et al., 2017.).
2. Improvement of Existing Studies and Products: It efficiently enhances existing research and products by yielding significant information with minimal effort, making it highly resource-effective.(Reji et al., 2022.)
3. Design, Development, and Examination: RSM plays a crucial role in the design, development, and thorough examination of specific scientific studies and products.(Reji et al., 2022.)
4. Response Surface Topography and Optimization: It is used to map the topography of a response surface and identify the regions that yield the best possible responses (Khuri et al., 2010).

5. Integration with Large-Scale Simulation Systems: RSM can be effectively integrated with various large-scale simulation systems, including Bio War, ORA, Vista, Construct, and DyNet, expanding its utility in complex modeling scenarios (Box & Draper, 1987).

2.8.2.2 Advantages of RSM

1. Cost-Effective Knowledge Acquisition: A relatively small number of experimental trials can provide a substantial amount of knowledge in a cost-efficient manner (Reji et al., 2022.).
2. Interaction Effects Determination: It is capable of identifying and quantifying the interaction effects among independent input parameters, offering a more complete understanding of system dynamics (Reji et al., 2022.).
3. Illustrative Data-Driven Model Equation: The data-driven model equations derived from RSM can clearly illustrate how different combinations of input factors influence process or product outcomes (Reji et al., 2022.).
4. Approximation of Responses: RSM can effectively approximate both experimental and numerical responses, making it versatile for different types of data (Raissi et al., 2009.).
5. Efficiency in Resource Management: It helps maintain high efficiency by optimizing cost, time, and other operational restrictions (Reji et al., 2022.).
6. Superior Mathematical Modeling: Compared to methods like Taguchi and one-factor-at-a-time, RSM often provides more promising mathematical modeling for forecasting responses (Myers, 1999).

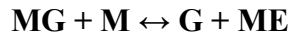
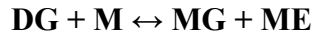
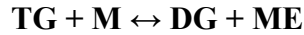
2.8.2.3 Disadvantages of RSM

1. Limited Explanation of Interactions: RSM cannot inherently explain the underlying reasons or mechanisms behind the development of observed interactions (Reji et al., 2022.).
2. Necessity of Appropriate Parameter Ranges: The method requires careful selection of appropriate operating parameter ranges, and the optimization results are confined to these specific scales (Reji et al., 2022.).
3. Poor Extrapolation Capability: RSM is not effective in predicting outcomes for systems operated outside the range of the particular study from which the model was derived (Myers, 1999).
4. Limitations with Larger Models: It is generally not well-suited for handling or operating with larger, more complex models (Khuri et al., 2010).
5. Risk of Poor Optimization with Multiple Responses: As the number of responses increases, there is a higher probability of obtaining less optimal or poor optimization results (Reji et al., 2022.).

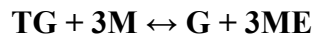
2.9 KINETIC STUDY OF THE BIODIESEL PROCESS

The kinetics of the transesterification process for a mixture of neem oil and waste cooking oil was examined utilizing a pseudo-first-order kinetic model to determine the correlations among the rate constant, activation energy, temperature, and reaction duration. Transesterification, a reversible reaction involving triglycerides (TGs) and methanol (M), transpires in three primary stages, resulting in the production of diglycerides (DGs), monoglycerides (MGs), glycerol (G), and methyl esters (MEs) (D. Singh et al., 2020.). In this study, a bifunctional catalyst synthesized from banana peels, zeolite, and periwinkle shell was used to facilitate the reaction.

The stoichiometric equation for the transesterification reaction is represented by the following equations:



The transesterification reaction leads to the overall stoichiometric equation (Ambat et al., 2018.):



Three moles of methanol and one mole of triglyceride react to generate three moles of methyl ester and one mole of glycerol for transesterification reaction rate (Thangaraj et al., 2019):

$$r = -d[\text{TG}]/dt = k[\text{TG}][\text{M}]^3 \dots\dots\dots (2.1)$$

In the transesterification reaction, [TG] shows the triglyceride concentration, [TG₀] the starting concentration, [M] the methanol concentration, r the reaction rate, and k the rate constant. To examine the catalyst ratio's effect on transesterification kinetics and simplify kinetic analysis, the following assumptions were established (Amenaghawon et al., 2022):

1. To determine rate constants, the transesterification reaction process, as defined in Eq. (6), was examined without intermediary phases.
2. Le Chatelier's principle states that excess methanol shifts transesterification equilibrium towards the product side, promoting biodiesel synthesis (Shafinaz & Embong, 2019).

- Reverse reactions were ignored, and methanol content was expected to remain constant due to its high concentration. The kinetic model became a pseudo-first-order reaction after this simplification (Naveenkumar et al., 2020.).

Triglyceride transesterification kinetics are given by Eqs. 8–12. Since the excess methanol maintained a virtually constant concentration throughout the reaction, pseudo-first-order kinetics was assumed for the triglyceride concentration.

$$r = -d[TG]/dt = k[TG]$$

$$-\ln([TG]/[TG_0]) = kt$$

$$X = 1 - [TG]/[TG_0]$$

$$-\ln(1 - X) = kt$$

$$\ln(1 - X) = -kt \dots\dots\dots (2.2)$$

A plot of $-\ln(1-X)$ against t yields the rate constant k as the slope of the linear equation (Betiku, Omilakin, et al., 2014.). The activation energy (E_a) was ascertained utilizing the Arrhenius equation, which delineates the correlation among temperature, activation energy, and the rate constant (LiPing et al., 2010):

$$\ln k = \ln A - (E_a/R)(1/T) \dots\dots\dots (2.3)$$

Plotting $\ln k$ against $1/T$ enables the calculation of the activation energy E_a (kJ/mol) from the slope of the line. Experiments were performed at various temperatures (40°C, 45°C, 50°C, 55°C, and 60°C, corresponding to 313 K, 318 K, 323 K, 328 K, and 333 K) utilizing the gas constant $R = 8.314$

J/mol·K to determine the correlations among temperature, activation energy, and the rate constant (Akhiero et al., 2021).

2.10 RESEARCH GAPS

This research project is poised to address several significant gaps within the realm of heterogeneous catalysis for sustainable biodiesel production, particularly through the innovative utilization of waste materials and complex oil feedstocks. By developing a novel bifunctional catalyst from banana peels, calcined periwinkle shells, and zeolite, specifically tailored for the conversion of waste cooking oil and neem oil, this work directly confronts existing limitations in catalyst design, performance, and application, while also addressing critical sustainability concerns regarding feedstock competition.

BRIDGING THE GAP IN SYNERGISTIC BIFUNCTIONAL CATALYST DESIGN FROM WASTE-DERIVED MATERIALS

Current literature often presents heterogeneous catalysts derived from single waste streams or binary composites, which frequently exhibit either predominantly acidic or basic functionalities (Petro Chem Eng, 2023). This presents a challenge for feedstocks like waste cooking oil and neem oil, characterized by varying free fatty acid (FFA) content, necessitating a catalyst capable of simultaneous esterification (acid-catalyzed) and transesterification (base-catalyzed) (Bharti et al., 2023). A critical research gap exists in the rational design and synthesis of truly bifunctional catalysts that synergistically combine multiple waste-derived components to achieve an optimized balance of acidic and basic sites (Changmai et al., 2022).

This work directly addresses this gap by synthesizing a multi-component bifunctional catalyst integrating banana peels, calcined periwinkle shells, and zeolite. The rationale behind this combination is to leverage the distinct catalytic precursors within each component: potassium from banana peels for basic sites, calcium from periwinkle shells for basic sites, and the inherent acidity of zeolite (Amenaghawon et al., 2022). The project will systematically investigate the precise proportions and synthesis conditions required to maximize the synergistic effects among these components, thereby optimizing the density, strength, and distribution of both acid and base sites (Enguilo Gonzaga et al., 2021). This methodical approach to multi-component catalyst design offers a novel pathway to develop a robust bifunctional material, an area where comprehensive studies utilizing this specific combination of waste-derived precursors are currently lacking (Petro Chem Eng, 2023).

ADVANCING CATALYTIC PERFORMANCE AND DURABILITY WITH COMPLEX, HIGH-FFA NON-EDIBLE FEEDSTOCKS

The majority of catalyst performance studies often employ refined oils or simplified model lipid mixtures, which do not fully replicate the complexities of real-world feedstocks such as waste cooking oil (WCO) and crude neem oil (Amenaghawon et al., 2022). These practical feedstocks are characterized by high FFA content, varying moisture levels, and the presence of diverse impurities, all of which can significantly impact catalyst activity, selectivity, and long-term stability (Amenaghawon et al., 2022). Furthermore, the reliance on edible oil feedstocks, such as palm oil, for biodiesel production raises ethical concerns regarding food security and contributes to increased commodity prices and land-use change. Therefore, a significant research gap persists in the development and rigorous evaluation of catalysts specifically optimized for, and robust against, the

challenges posed by complex, high-FFA non-edible lipid sources, thereby mitigating competition with the food chain (Banković-Ilić et al., 2012).

This project directly confronts this gap by evaluating the synthesized bifunctional catalyst using a blend of WCO and neem oil as the primary feedstock (Mhetras & Gokhale, 2025). Both of these are non-edible oils; WCO is a discarded resource, and neem oil is an agricultural product not suitable for human consumption. This approach moves beyond idealized conditions to assess the catalyst's ability to efficiently facilitate simultaneous esterification and transesterification reactions in a complex, industrially relevant matrix, while simultaneously promoting the sustainable utilization of non-edible resources (Amenaghawon et al., 2022). The research will meticulously characterize the catalyst's performance metrics, including conversion efficiency, biodiesel yield, and selectivity, while specifically scrutinizing its tolerance to the inherent impurities and elevated FFA content of these oils.

ELUCIDATING REACTION MECHANISMS AND ENHANCING CATALYST DURABILITY FOR INDUSTRIAL RELEVANCE

While the general principles of esterification and transesterification are well-established, the intricate reaction mechanisms occurring concurrently on the surface of complex bifunctional catalysts, particularly those derived from multi-component waste streams, when processing heterogeneous feedstocks, remain incompletely understood (Changmai et al., 2022).

This work aims to bridge these gaps by undertaking detailed kinetic studies and catalyst characterization. These analyses will provide fundamental insights into the rate-determining steps and the interplay between the acidic and basic sites of the novel catalyst during simultaneous esterification and transesterification of the WCO-neem oil blend (Bharti et al., 2023).

CHAPTER 3

MATERIALS AND METHODS

3.1 RAW MATERIALS AND REAGENTS

The major materials utilized in this work are presented in Table 3.1

Table 3.1: Raw materials and Reagents

Materials	Use
Neem Oil	Used for biodiesel production
Waste Cooking Oil	Used for biodiesel production
Banana Peels (<i>Musa paradisiaca</i>)	Used for catalyst production.
Periwinkle shell	Used for catalyst production.
Zeolite	Used for catalyst production.
Ethanol	Used for acid and saponification value test.
Deionized water	Used for chemical reaction, solution preparation and laboratory equipment maintenance.
Benzene	Used for acid value test.
Potassium hydroxide solution (KOH)	Used for acid value test and saponification value test
Hydrochloric Acid (HCl)	Used for saponification value test
Phenolphthalein Indicator	Used as indicator for acid value and saponification value determinations.

Methanol	Used for esterification and transesterification to produce biodiesel.
Tetraoxosulphate(VI) Acid (H_2SO_4)	Used as an acid catalyst for esterification to reduce free fatty acids in the oil.
Sodium thiosulphate	Used as a titrant for iodine value determination.
Iodine monochloride	Used for iodine value determination to measure the degree of unsaturation in oil.
Chloroform	Used as a solvent for dissolving oil and reagents during iodine value determination.
Acetic acid	Used as a solvent and acidic medium for iodine and acid value determinations.
Potassium iodide	Used to liberate iodine from unreacted iodine monochloride during iodine value determination.
Starch	Used as an indicator for detecting the end point in iodine value titration.

3.1.2 APPARATUS AND EQUIPMENT

Table 3.2: Apparatus and Equipment

Apparatus and Equipment	Use
Beaker	Used for mixing, heating, and holding liquid samples and reagents.
Conical flask (Erlenmeyer flask)	Used for titration and mixing solutions to prevent spillage.
Round-bottom flask	Used for heating oil and methanol mixtures during esterification and transesterification.
Reflux condenser	Used to condense methanol vapors and prevent loss during heating reactions.
Separating funnel	Used for separating biodiesel from glycerol after transesterification.
Measuring cylinder	Used for accurately measuring liquid volumes.
Burette	Used for titration to deliver precise volumes of titrant.
Pipette	Used to measure and transfer small volumes of liquid accurately.
Retort stand with clamp	Used to hold glassware such as burettes, condensers, or flasks securely during experiments.
Hot plate with magnetic stirrer	Used for heating and stirring mixtures uniformly during reactions.
Thermometer	Used for measuring and monitoring reaction temperature.
Weighing balance	Used for accurately measuring the mass of oil, catalysts, and reagents.
Filter paper	Used for separating solid catalyst residues or impurities from liquids.
Funnel	Used for transferring liquids or for filtration with filter paper.

Desiccator	Used for cooling and storing samples in a moisture-free environment after drying.
Oven	Used for drying catalyst samples or oil before characterization.
Muffle furnace	Used for calcining catalyst materials such as banana peel, zeolite, and periwinkle shell.
Magnetic stir bar	Used inside flasks for uniform stirring during transesterification.
pH meter	Used to measure the acidity or alkalinity of oil and reaction mixtures.
Viscometer	Used to determine the viscosity of the produced biodiesel.
X-ray diffractometer (XRD)	Used to identify crystalline phases in the synthesized catalyst.
Gas chromatograph (GC)	Used to analyze the composition and purity of the biodiesel produced.
Water bath	Used to maintain a constant temperature for controlled heating of samples.
Centrifuge	Used to separate biodiesel and glycerol phases more efficiently.
Micropipette	Used for transferring small and precise amounts of reagents.
Glass rod	Used for stirring solutions manually.
Wash bottle	Used for rinsing glassware and adding small amounts of distilled water.
Wash brush	Used for cleaning glassware after experiments.
Stopwatch	Used for timing reaction durations accurately.
Safety gloves and face mask	Used for protecting the hands and face during chemical handling.

3.2 METHODOLOGY

3.2.1 PREPARATION OF RAW MATERIALS

3.2.1.1 Banana Peel Pre-Treatment

Banana peels were thoroughly washed with water to remove surface dirt and adhered fruit pulp, then rinsed with distilled water. The cleaned peels were cut into small pieces (approximately 2 cm × 2 cm) to increase surface area for drying. The cut peels were spread uniformly on aluminum trays and sun-dried for five days until constant weight was achieved, indicating complete moisture removal. The dried peels were subsequently oven-dried at 105°C for 6 hours to eliminate residual moisture. After cooling in a desiccator, the dried peels were ground using a laboratory blender and passed through a 250 μm (60 mesh) sieve. The powdered banana peel was stored in airtight polyethylene containers until further use.



Plate 3.1: Washed Banana Peels



Plate 3.2: Dried Banana Peels



Plate 3.3: Catalyst Blend of Banana Peel Ash, Calcined periwinkle shell and Zeolite.

3.2.1.2 Periwinkle Shell Pre-treatment

Periwinkle shells were washed extensively with water to remove sand, mud, and organic matter, followed by rinsing with distilled water. The cleaned shells were boiled in distilled water for 30 minutes to eliminate any remaining organic tissues and to sterilize the shells. After boiling, the shells were drained and sun-dried for seven days until completely dry. The dried shells were crushed manually using a mortar and pestle, then ground in a ball mill for 2 hours at 300 rpm to obtain fine powder. The ground shell powder was sieved through a 250 μm sieve, and the fraction passing through was collected and stored in sealed containers.

3.2.1.3 Zeolite Pre-treatment

Commercial zeolite was used in its as-received form after verification of particle size. The zeolite powder was dried in an oven at 110°C for 4 hours to remove adsorbed moisture. After drying, the zeolite was cooled in a desiccator and stored in airtight containers to prevent moisture reabsorption.

3.2.2 CATALYST SYNTHESIS

3.2.2.1 Physical Mixing and Homogenization

The catalyst was prepared by physical mixing of the three pre-treated components in a specific mass ratio. Based on preliminary screening experiments, the optimal composition was determined to be 66.67 wt% banana peel powder, 16.67 wt% periwinkle shell powder, and 16.67 wt% zeolite. For a typical batch, 66.67 g of banana peel powder, 16.67 g of periwinkle shell powder, and 16.67 g of zeolite were weighed accurately using an analytical balance. The three components were transferred to a porcelain mortar and mixed manually using a pestle for 15 minutes to ensure uniform distribution. The mixture was then transferred to a planetary ball mill and homogenized at 400 rpm for 1 hour with

zirconia grinding balls (10 mm diameter) at a ball-to-powder ratio of 10:1. This mechanical mixing ensured intimate contact between the three components and reduced particle size further.

3.2.2.2 Calcination Process

The homogenized powder mixture was transferred to a ceramic crucible and placed in a muffle furnace for calcination. The furnace temperature was programmed to increase from ambient temperature to 800°C at a heating rate of 10°C/min. Once the target temperature was reached, it was maintained for 3 hours to allow complete thermal decomposition of organic matter in the banana peel biochar and conversion of calcium carbonate in the periwinkle shell to calcium oxide. The calcination was conducted under atmospheric conditions without controlled gas flow. After the holding period, the furnace was switched off and allowed to cool naturally to room temperature overnight. The calcined catalyst was removed from the furnace, ground gently using a mortar and pestle to break any agglomerates, and sieved through a 150 µm (100 mesh) sieve. The final catalyst powder was stored in airtight glass bottles and kept in a desiccator to prevent moisture absorption and carbonation from atmospheric CO₂.

3.2.3 CATALYST CHARACTERIZATION

3.2.3.1 X-ray diffraction (XRD) Analysis

The crystalline structure and phase composition of the synthesized catalyst were determined using X-ray diffraction. A powder sample of the catalyst was placed on a silicon zero-background sample holder and analyzed using a Rigaku MiniFlex 600 X-ray diffractometer. The instrument was operated at 40 kV and 15 mA with Cu-K α radiation ($\lambda = 1.5406 \text{ \AA}$). Diffraction patterns were recorded over a 2θ range of 10° to 80° with a step size of 0.02° and a scanning rate of 2°/min. Phase identification

was performed by comparing the obtained diffraction peaks with standard reference patterns from the International Centre for Diffraction Data (ICDD) database. Quantitative phase analysis was conducted using the Rietveld refinement method with HighScore Plus software (PANalytical) to determine the weight percentages of crystalline phases present in the catalyst.

3.2.3.2 Fourier-Transform Infrared Spectroscopy (FTIR)

Functional group analysis of the catalyst was performed using a PerkinElmer Spectrum Two FTIR spectrometer equipped with an attenuated total reflectance (ATR) accessory. A small amount of catalyst powder (approximately 5 mg) was placed directly on the diamond crystal of the ATR accessory, and pressure was applied using the built-in clamp to ensure good contact between the sample and crystal. Spectra were recorded in the wavenumber range of 4000 to 400 cm^{-1} with a resolution of 4 cm^{-1} and 32 scans per spectrum. Background correction was performed before each measurement using an empty ATR crystal. The obtained spectra were analyzed using Spectrum software to identify characteristic absorption bands corresponding to functional groups such as hydroxyl (O–H), carbonate (CO_3^{2-}), silicate (Si–O), aluminate (Al–O), and metal-oxygen (M–O) bonds.

3.2.4 Feedstock Preparation

3.2.4.1 Waste cooking oil pre-treatment

Waste cooking oil was pre-treated to remove suspended food particles, water, and other impurities. The oil was first filtered to remove large particulates, then heated to 110°C for 30 minutes under gentle stirring to evaporate water. The oil was then filtered again. The clarified oil was allowed to cool and stored in amber glass bottles.

3.2.4.1 Neem oil pre-treatment

Neem oil was heated to 110°C for 30 minutes under gentle stirring to evaporate water. The clarified oil was allowed to cool and stored in amber glass bottles.

3.2.5 Feedstock Characterization

Both neem oil and waste cooking oil were characterized for key physicochemical properties following standard ASTM and AOCS methods. The characterization of the oils was conducted through the following tests, with all procedures adapted from existing literature:

3.2.5.1 Acid value or Acid number (Canesin et al., 2014.) ASTM D 664

Exactly 0.05M KOH solution was prepared by dissolving 2.805g KOH (pellet) with 1000ml distilled water. Furthermore, a mixture of 99.7% pure ethanol and 98% pure benzene in a ratio of 1:1 by volume was prepared by mixing 10 ml benzene and 10 ml of ethanol. About 1g of the oil was weighed and dissolved in the mixture of ethanol and benzene. The solution was titrated with 0.1N KOH solution in presence of 2 drops of phenolphthalein as indicator until the end point with the appearance of a pale permanent pink. The titre volume of 0.1 N KOH (V) was noted. The total acidity (acid number) in mgKOH/g was calculated using the following equation

$$AV = \frac{MW \times N \times V}{W} \dots\dots\dots (3.1)$$

Where:

MW ≡ Molecular weight of potassium hydroxide (56.1g).

N≡ Normality of potassium hydroxide solution (0.05N).

V ≡ Volume of potassium hydroxide solution used in titration.

W ≡ Weight of oil sample.

$$\%FFA = \frac{AV}{2} \dots\dots\dots (3.2)$$

3.2.5.2 Peroxide value (Canesin et al., 2014.)

About 2.5g of the sample was weighed into a conical flask. 30ml of 3:2 acetic acid and chloroform was added. This was stirred (swirl) to dissolve. 1.5ml of saturated KI solution was then added with constant shaking for about 1 minute. 30ml distilled water was then added. The mixture was immediately titrated with 0.1N sodium thiosulphate with constant and vigorous shaking until the disappearance of the yellow iodine colour. 0.5ml starch indicator was added and the titration was continued with constant agitation to liberate all the iodine from the solvent layer. Thiosulphate solution was then added drop wise until the disappearance of the blue colour.

Blank titration was the conducted on the reagents with exactly 0.1ml of the 0.1N sodium thiosulphate solution. The peroxide value was thus estimated from the formula in meq/Kg

$$PV = \frac{(S - B) \times N \times 1000}{weight.of.oil} \dots\dots\dots (3.3)$$

Where:

S = Sample titre value

B = Blank titre value

N = mol of thiosulphate

3.2.5.3 Iodine value (Canesin et al., 2014.)

0.25g of the oil sample was weighed into a 250 mL conical flask and added 10ml of chloroform followed by 15 mL of Wiljs reagent (iodine monochloride). The flask was securely closed and the solution was left shaking for 30 minutes in the dark. This was followed by adding 10 mL of 15% potassium iodide solution and then shaken, after which 100mL of distilled water was added. The mixture was then titrated with the iodine solution against 0.1 N Sodium thiosulfate solution till a yellow colour formed. This was followed by addition of 1ml of starch solution after which a blue solution formed. The titration continued until the blue colour disappeared while the volume of Na₂S₂O₃ at end point was recorded. The Iodine value (I.V) in I₂g/100g was calculated as reported by other workers.

$$I.V = \frac{126.9 \times c \times (b - v) \times 100}{m \times 1000} \dots\dots\dots (3.4)$$

Where:

c = Normality of sodium thiosulphate (Na₂S₂O₃) used;

b = Vol of Na₂S₂O₃ used for the blank;

v = Vol of Na₂S₂O₃ used for sample;

m = mass of the sample.

126.9 = Equivalent weight of iodine

3.2.5.4 Density and specific gravity (Canesin et al., 2014.)

Density bottle was used in determining the specific gravity of the oil. A clean and dry stoppered bottle of 25 mL capacity was weighed (W_0) and then filled with the oil stoppered and reweighed to give (W_1). The oil was substituted with distilled water after washing and drying the bottle and weighed to give (W_2). The expression for specific gravity (Sp.gr) is:

$$Sp.gr = \frac{W_1 - W_2}{W_2 - W_0} \dots\dots\dots (3.5)$$

Where:

W_0 = weight of dry empty density bottle;

W_1 = weight of density bottle + oil;

W_2 = weight of density bottle + distilled water

3.2.5.5 Saponification value (Canesin et al., 2014.)

A one-gram (1 g) sample of the oil was weighed into a 250 mL glass conical flask, and then 10 mL of ethanol and benzene mixture (1:1) was added to the same flask followed by 25 mL of 0.5 N ethanolic potassium hydroxide. The flask was then fitted to a reflux condenser and refluxed using a boiling water bath for 30 min with occasional shaking. To the warm solution were added 2 - 3 drops of phenolphthalein indicator and the warm solution was titrated against 0.5 M HCl to the disappearance of pink coloration. The same procedure was used for other samples and blank. The expression for saponification value (S.V) is given by equation:

$$S.V = \frac{(b - s) \times 56.1 \times n}{w} \dots\dots\dots (3.6)$$

Where:

b = the volume of the solution used for blank test;

s = the volume of the solution used for determination;

n = Actual normality of the HCl used;

w = Mass of the sample.

3.2.5.6 Viscosity value (Canesin et al., 2014.)

A measured volume of the oil sample was poured into the viscometer cup. The viscometer was placed in a water bath set to a controlled temperature of 40°C. The oil was allowed to reach thermal equilibrium for about 10–15 minutes. The torque reading displayed on the viscometer was then recorded.



Plate 3.4: Viscosity Test for Neem oil

3.2.6 Experimental Design And Optimization

3.2.6.1 Esterification reaction

About 200g of oil in a glass reactor was esterified with 25 wt% of methanol using 1.0 wt% H₂SO₄ as catalyst to reduce the free fatty acids to less than 1% FFA. The mixtures were placed on a constant temperature magnetic stirrer set to heat at a constant temperature 60°C for 1 hour transesterification reaction.

3.2.6.2 Simplex lattice mixture design for feedstock blending

A simplex lattice mixture design was employed to optimize the blending ratio of neem oil and waste cooking oil for maximum free fatty acid reduction during acid-catalyzed pre-treatment. The design

was implemented using Design-Expert software (Version 13, Stat-Ease Inc., USA). Two mixture components were defined: neem oil (Component A) and waste cooking oil (Component B), with the constraint that $A + B = 50$ g. A quadratic simplex lattice design was selected, generating 8 experimental runs including pure vertices, edge midpoints, and centroid replicates. The response variable was FFA reduction percentage, calculated as:

$$\text{FFA Reduction (\%)} = [(\text{FFA}_0 - \text{FFA}_t) / \text{FFA}_0] \times 100 \dots\dots\dots (3.7)$$

where FFA_0 is the initial FFA content and FFA_t is the FFA content after pre-treatment. The experimental runs were conducted in randomized order to minimize systematic errors.

3.2.6.3 Response surface methodology for process optimization

A central composite design (CCD) within response surface methodology was used to optimize transesterification process parameters. Four independent variables were investigated: reaction time (A: 30–150 min), reaction temperature (B: 40–80°C), catalyst loading (C: 1–10 wt% based on oil weight), and methanol-to-oil ratio (D: 3:1–10:1 by weight). The response variable was biodiesel yield (wt%). A quadratic model was fitted to the experimental data, and the design matrix consisted of 29 runs including 16 factorial points, 8 axial points ($\alpha = 2$), and 5 center point replicates. Design-Expert software was used for experimental design generation, statistical analysis, and numerical optimization.

3.2.7 Transesterification Procedure

3.2.7.1 Feedstock preparation and pre-treatment

Based on the optimized blend ratio from the mixture design (12.5 g neem oil + 37.5 g waste cooking oil for 50 g total), the feedstock mixture was prepared by weighing the oils accurately and mixing them thoroughly in a beaker under magnetic stirring for 10 minutes at room temperature. For runs using pure oils, 50 g of either neem oil or waste cooking oil was used directly.

3.2.7.2 Transesterification reaction

The transesterification reaction was conducted in a 1000 mL three-neck round-bottom flask equipped with a reflux condenser, thermometer, and magnetic stirring bar. The flask was placed on a magnetic stirrer with heating plate. For a typical run, 50 g of oil (or oil blend) was transferred to the flask and heated to the desired reaction temperature with stirring at 600 rpm. Once the target temperature was reached, a pre-calculated amount of synthesized catalyst (based on wt% of oil) was added to the oil. Separately, the required amount of methanol (based on methanol-to-oil ratio) was measured and added to the reaction mixture. The addition of methanol marked the start of the reaction (time zero). The mixture was maintained at constant temperature with continuous stirring for the specified reaction time.

During the reaction, samples were periodically withdrawn using a syringe to monitor conversion progress. The reaction mixture initially appeared turbulent due to the immiscibility of methanol and oil, but as the reaction proceeded, the mixture became more homogeneous. Upon completion of the reaction, the stirring and heating were stopped, and the flask was removed from the hot plate.



Plate 3.5: Tranesterification Run 24

3.2.7.3 Product separation and purification

The reaction mixture was transferred to a 500 mL separating funnel and allowed to settle for 12 hours at room temperature to facilitate phase separation. Three distinct layers formed: the upper layer containing fatty acid methyl esters (biodiesel), a middle layer of catalyst particles, and a lower layer of glycerol. The glycerol layer was drained first, followed by separation of the catalyst through filtration using Whatman No. 1 filter paper. The biodiesel layer was collected and subjected to purification.

Purification was performed by washing the biodiesel with warm distilled water (50–60°C) at a ratio of 1:1 (v/v). The mixture was stirred gently for 5 minutes and then allowed to settle for 30 minutes.

The aqueous phase was drained, and the washing process was repeated three times until the wash water became clear and neutral (pH 6.5–7.5). Residual water in the biodiesel was removed by heating at 105°C for 30 minutes, followed by filtration through anhydrous sodium sulfate to ensure complete dryness. The purified biodiesel was stored in sealed amber glass bottles at room temperature for further analysis.



Plate 3.6: Washing of Biodiesel

3.2.8 Biodiesel Yield Calculation

Biodiesel yield was calculated gravimetrically using the following equation:

$$\text{Biodiesel Yield (wt\%)} = (\text{Mass of purified biodiesel} / \text{Mass of oil feedstock}) \times 100 \dots\dots\dots (3.8)$$

The mass of purified biodiesel was determined by weighing the dried and filtered product using an analytical balance. All yield determinations were performed in triplicate, and the average value was reported.

3.2.9 Biodiesel Characterization

3.2.9.1 Physicochemical properties

The produced biodiesel was characterized for key quality parameters following ASTM D6751 standard test methods. Density was measured at 15°C using a pycnometer (ASTM D1298). Kinematic viscosity was determined at 40°C using a calibrated Ostwald viscometer (ASTM D445). Acid value was measured by titration method (ASTM D664).

3.2.9.2 Gas chromatography-mass spectrometry (GC-MS) analysis

The fatty acid methyl ester (FAME) composition of the biodiesel was determined using gas chromatography-mass spectrometry. Analysis was performed on an Agilent 7890B GC coupled with 5977A mass selective detector. A 1 µL sample of biodiesel diluted in n-hexane (1:10 v/v) was injected in split mode (split ratio 50:1) into an HP-5MS capillary column (30 m length × 0.25 mm internal diameter × 0.25 µm film thickness). The oven temperature was programmed as follows: initial temperature 150°C held for 2 min, then ramped to 250°C at 5°C/min and held for 10 min. Helium was used as carrier gas at a constant flow rate of 1.0 mL/min. The injector temperature was 250°C

and the MS transfer line temperature was 280°C. The mass spectrometer was operated in electron ionization mode at 70 eV with a scan range of 50–550 m/z. FAME components were identified by comparing their mass spectra with the NIST library database, and their relative concentrations were determined from peak area percentages.

3.2.10 Statistical Analysis And Data Processing

Analysis of variance (ANOVA) was performed using Design-Expert software to evaluate the significance of model terms, with statistical significance set at $p < 0.05$. Model adequacy was assessed using coefficient of determination (R^2), adjusted R^2 , predicted R^2 , and adequate precision. Response surface plots and contour diagrams were generated to visualize the effects of process variables and their interactions on response variables. Numerical optimization was performed using the desirability function approach to identify optimal operating conditions that maximize biodiesel yield.

CHAPTER 4

RESULTS AND DISCUSSION

4.1 OIL CHARACTERIZATION

Table 4.1: Physical and Chemical Properties of Neem Oil and Waste Cooking Oil

Property	Neem Oil	Waste Cooking Oil
Acid Value (mg KOH/g)	10.97	7.70
Free Fatty Acid Content (%)	5.52	3.87
Iodine Value (g I ₂ /100 g)	28.43	18.06
Saponification Value (mg KOH/g)	209.05	268.41
Peroxide Value (meq/kg)	0.80	0.20
Density at 25°C (g/cm ³)	0.9622	0.9614
Specific Gravity at 25°C	0.9664	0.9656
Kinematic Viscosity at 40°C (mm ² /s)	7.18	24.2

From Table 4.1, neem oil exhibited an acid value of 10.97 mg KOH/g (5.52% FFA), while waste cooking oil showed 7.70 mg KOH/g (3.87% FFA). Both values significantly exceed the maximum acid value specification of 0.5 mg KOH/g by ASTM D6751 and 0.6 mg KOH/g by EN 14214. This high FFA content is attributed to enzymatic lipolysis in neem oil and thermal/hydrolytic degradation in waste cooking oil, necessitating a pretreatment step to prevent soap formation during transesterification.

From Table 4.1, neem oil possessed an iodine value of 28.43 g I₂/100 g, and waste cooking oil exhibited 18.06 g I₂/100 g. Both values fall well below the maximum limit of 120 g I₂/100 g specified by EN 14214 for biodiesel. These low values indicate predominantly saturated and monounsaturated fatty acids, which is advantageous for biodiesel quality as it translates to enhanced oxidative stability and a longer shelf life for the final product.

From Table 4.1, neem oil demonstrated a saponification value of 209.05 mg KOH/g, while waste cooking oil showed a significantly higher 268.41 mg KOH/g. The 209.05 mg KOH/g for neem oil is consistent with literature values for oils containing C16–C18 fatty acids, while the higher value for waste cooking oil suggests a greater proportion of shorter-chain fatty acids, likely formed from thermal cracking during frying. This influences the stoichiometry of the transesterification reaction and the properties of the resulting biodiesel.

From Table 4.1, neem oil possessed a peroxide value of 0.80 meq/kg, and waste cooking oil exhibited a notably lower 0.20 meq/kg. Both demonstrate exceptionally low peroxide values, well below conventional thresholds, indicating minimal primary oxidative degradation. The low peroxide value in neem oil reflects its natural antioxidant content, and while waste cooking oil has a history of thermal stress, its low value can be explained by peroxides decomposing into secondary oxidation products. These low values are highly favorable for transesterification, preventing catalyst deactivation and promoting biodiesel stability.

From Table 4.1, neem oil exhibited a density of 0.9622 g/cm³ and a specific gravity of 0.9664, while waste cooking oil showed a marginally lower density of 0.9614 g/cm³ and specific gravity of 0.9656. These values are consistent with typical vegetable oil densities. The nearly identical densities, differing by only 0.0008 g/cm³, suggest similar molecular weight distributions. The slightly higher density of neem oil may reflect its higher content of long-chain saturated fatty acids, leading to greater intermolecular forces and efficient molecular packing.

From Table 4.1, neem oil exhibited a kinematic viscosity of 7.18 mm²/s at 40°C, and waste cooking oil demonstrated a considerably higher viscosity of 24.2 mm²/s at the same temperature. Both feedstock oils exhibit viscosities substantially higher than biodiesel specifications, which is expected for triglycerides due to their higher molecular weight and stronger intermolecular interactions. The unusually low viscosity of neem oil may result from its specific compositional characteristics, while the elevated viscosity of waste cooking oil, potentially from polymerization during heating, highlights the importance of feedstock characterization for process optimization

4.2 CATALYST CHARACTERIZATION

Table 4.2: X-Ray Diffraction Quantitative Analysis

Phase name	Formula	Figure of Merit	Space Group	Weight Fraction, wt%
Calcite	CaCO ₃	1.935	167 : R-3c:H	77(6) %
Portlandite	Ca(OH) ₂	1.646	164 : P-3m1	15(6) %
Muscovite	H ₂ KAl ₃ (SiO ₄) ₃	3.198	15 : C12/c1	2.7(15) %
Titanite,syn	CaTi(SiO ₄)O	3.115	15 : A12/a1	4.6(18) %

Phase Data View

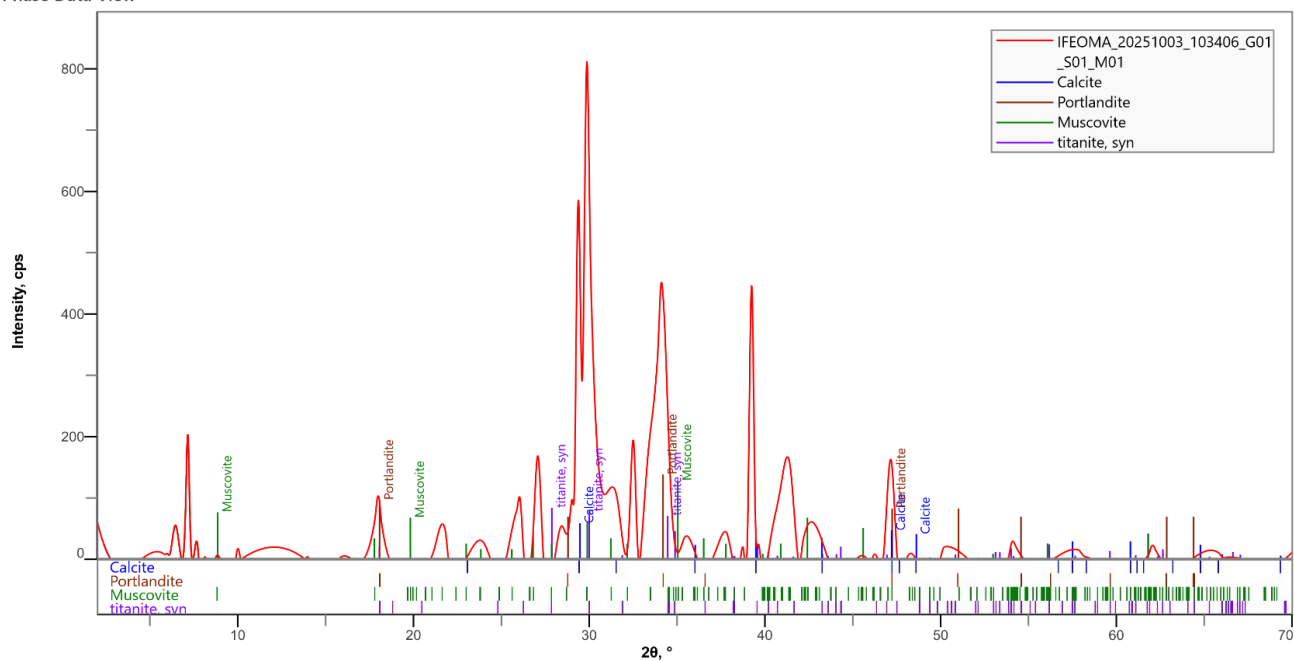


Figure 4.1: X-ray Diffraction phase composition of the synthesized catalyst

X-ray Diffraction Analysis

In Figure 4.1, the crystallographic composition of the synthesized catalyst was investigated using X-ray diffraction to identify the mineral phases present and their relative abundances. In Table 4.2, quantitative phase analysis revealed that the catalyst comprised primarily Portlandite (77 wt%), with minor contributions from Muscovite (15 wt%), Titanite (4.6 wt%), and Calcite (2.7 wt%). The dominant presence of Portlandite, chemically designated as calcium hydroxide $[\text{Ca}(\text{OH})_2]$, constitutes the principal basic catalytic phase responsible for transesterification activity.

Portlandite possesses strong Lewis basicity due to the hydroxyl groups bonded to calcium centers, which facilitates nucleophilic attack on the carbonyl carbon of triglycerides during methanol-mediated transesterification reactions. The high mass fraction of this phase correlates directly with the observed catalytic efficiency in biodiesel production. The detection of Muscovite $[\text{KAl}_2(\text{AlSi}_3\text{O}_{10})(\text{OH})_2]$, a phyllosilicate mineral, indicates successful incorporation of aluminosilicate mineral originating from the zeolite component. Muscovite contributes to the catalyst's structural integrity by providing a layered framework that enhances thermal stability and mechanical resistance during repeated calcination and reaction cycles.

Similarly, the presence of Titanite (CaTiSiO_5) suggests that titanium dioxide from the periwinkle shell matrix has undergone partial integration with calcium and silicon oxides, forming a complex oxide phase. Titanium-doped calcium catalysts have been reported by Hassan et al. (2023) to exhibit superior transesterification rates compared to pure CaO systems due to enhanced surface acidity and improved methanol activation. The synergistic combination of $\text{Ca}(\text{OH})_2$ (basic sites) with aluminosilicate and titanate phases (acidic sites) thus establishes the bifunctional character of the catalyst, enabling simultaneous esterification of free fatty acids and transesterification of triglycerides.

The minor Calcite (CaCO_3) fraction represents residual carbonate resulting from incomplete thermal decomposition or atmospheric carbonation of calcium hydroxide during cooling. While calcite exhibits reduced catalytic activity compared to Portlandite, it serves a structural function by maintaining catalyst stability and resisting sintering at elevated temperatures. Its low concentration (2.7 wt%) does not significantly impair overall catalyst performance.

4.2.2 Fourier-Transform Infrared Spectroscopy (FTIR)

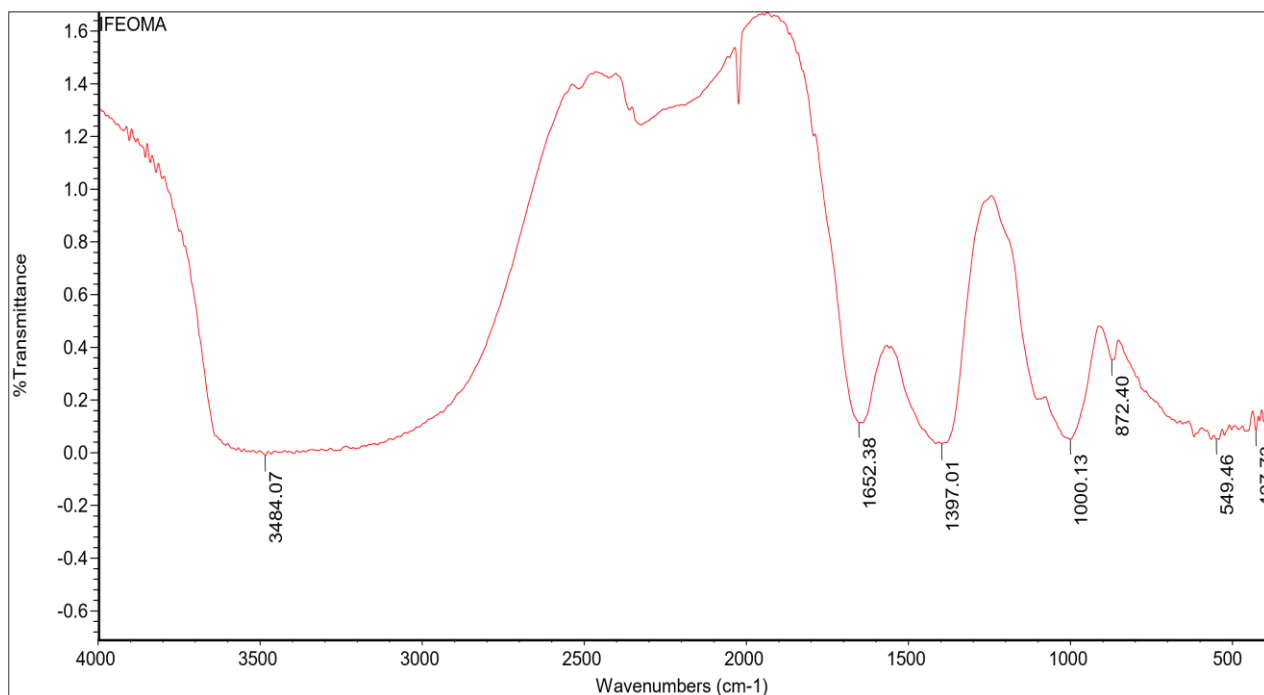


Figure. 4.2: Fourier-Transform Infrared Spectroscopy (FTIR) spectrum of banana peel-zeolite-periwinkle shell catalyst

As shown in Figure 4.2, Complementary Fourier-Transform Infrared Spectroscopy (FTIR) analysis was conducted to identify functional groups and bonding characteristics within the catalyst matrix. The spectrum exhibited distinct absorption peaks at 427.7, 549.5, 872.4, 1000.1, 1397.0, 1652.4, and

3484.1 cm^{-1} . The broad absorption band centered at 3484.1 cm^{-1} corresponds to the stretching vibration of hydroxyl groups (O–H), characteristic of $\text{Ca}(\text{OH})_2$ and adsorbed surface moisture. This peak confirms the presence of active hydroxyl species that serve as Brønsted base sites for catalysis.

The peak at 1652.4 cm^{-1} is attributed to the bending mode of water molecules physisorbed on the catalyst surface, which is typical for hygroscopic calcium compounds. The absorption at 1397.0 cm^{-1} indicates the presence of carbonate ions (CO_3^{2-}), consistent with the minor Calcite phase detected by XRD. Carbonate formation occurs when atmospheric carbon dioxide reacts with surface calcium hydroxide, a phenomenon commonly observed in alkaline earth metal catalysts exposed to ambient conditions. The peak at 872.4 cm^{-1} represents the symmetric stretching vibration of Ca–O bonds in calcium oxide and hydroxide phases, providing further evidence of the catalyst's calcium-rich composition.

Lower wavenumber peaks at 549.5 and 427.7 cm^{-1} correspond to metal-oxygen (M–O) vibrations in the aluminosilicate and titanate lattices. Specifically, the 549.5 cm^{-1} band is associated with Si–O–Al bending vibrations in Muscovite, while the 427.7 cm^{-1} peak reflects Ti–O stretching in Titanite. The presence of these peaks confirms the successful integration of zeolite and periwinkle shell components into a composite oxide structure. The peak at 1000.1 cm^{-1} is assigned to asymmetric Si–O–Si stretching vibrations, characteristic of silicate frameworks. This absorption is particularly important as it indicates that the zeolite structure retained partial crystallinity despite high-temperature calcination, thereby preserving some of its microporous characteristics.

The FTIR data corroborate the XRD results by confirming that the catalyst comprises a multi-phase Ca–Ti–Si–O system containing hydroxyl-functionalized calcium oxide, aluminosilicate, and titanate species. The coexistence of these functional groups supports the bifunctional nature of the catalyst,

wherein basic $\text{Ca}(\text{OH})_2$ sites catalyze transesterification while acidic aluminosilicate sites facilitate esterification of free fatty acids present in waste cooking oil and neem oil feedstocks.

4.3 MIXTURE DESIGN AND FEEDSTOCK OPTIMIZATION

Table 4.3: Mixture Component Design

Run	Neem Oil (g)	WC Oil (g)	FFA Reduction (%)
1	12.5	37.5	86.62
2	50	0	68.85
3	0	50	66.43
4	25	25	7.93
5	50	0	73.95
6	37.5	12.5	47.05
7	0	50	74.03
8	25	25	13.92

Table 4.3 presents the experimental matrix comprising eight runs designed to investigate the effect of blending neem oil and waste cooking oil on free fatty acid reduction. The table displays three columns: neem oil mass (g), waste cooking oil mass (g), and the corresponding FFA reduction (%). Each run represents a different blend composition, with the constraint that the total oil mass remained constant at 50 g across all experiments. The design included pure component formulations where only neem oil or only waste cooking oil was used (Runs 2, 3, 5, and 7), as well as various binary

blends at different proportions (Runs 1, 4, 6, and 8). This experimental strategy allowed for comprehensive evaluation of how feedstock composition influences FFA reduction performance.

Analysis of the experimental results reveals substantial performance variation across the eight runs. Runs 2 and 5, which utilized pure neem oil (50 g neem oil, 0 g waste cooking oil), achieved FFA reductions of 68.85% and 73.95%, respectively. The replicate runs demonstrate reasonable reproducibility, with an average FFA reduction of 71.4% for pure neem oil. Similarly, Runs 3 and 7, employing pure waste cooking oil (0 g neem oil, 50 g waste cooking oil), yielded FFA reductions of 66.43% and 74.03%, averaging 70.23%. These results indicate that both feedstocks individually support moderate FFA reduction, with comparable performance between the two oils. The slight variation between replicates (approximately 5–7 percentage points) reflects normal experimental variability associated with manual catalyst addition, temperature fluctuations, and titration endpoint determination.

The most striking observation from Table 4.3 is the dramatic difference in performance between various blend compositions. Runs 4 and 8, which represent 50:50 blends (25 g neem oil + 25 g waste cooking oil), exhibited severely depressed FFA reduction of 7.93% and 13.92%, respectively. These values are substantially lower than either pure component, indicating strong antagonistic interactions when the oils are mixed in equal proportions. This antagonism suggests that at intermediate compositions, unfavorable physicochemical interactions occur that inhibit the esterification reaction.

In contrast, Run 1 (12.5 g neem oil + 37.5 g waste cooking oil) and Run 6 (37.5 g neem oil + 12.5 g waste cooking oil) demonstrated markedly different outcomes. Run 1 achieved the highest FFA reduction in the entire experimental set at 86.62%, representing a substantial improvement of approximately 15–16 percentage points over either pure feedstock. This result indicates synergistic blending effects at the 1:3 neem-to-waste cooking oil ratio, wherein the combination of the two oils

produces superior performance compared to individual components. Conversely, Run 6, with the inverse 3:1 ratio, yielded only 47.05% FFA reduction, falling well below the performance of pure components. This asymmetry confirms that the order and proportion of blending are critical, and that the specific ratio of 25% neem oil to 75% waste cooking oil represents an optimal composition.

The experimental data from Table 4.3 were subsequently used to develop a predictive mathematical model that describes the relationship between blend composition and FFA reduction.

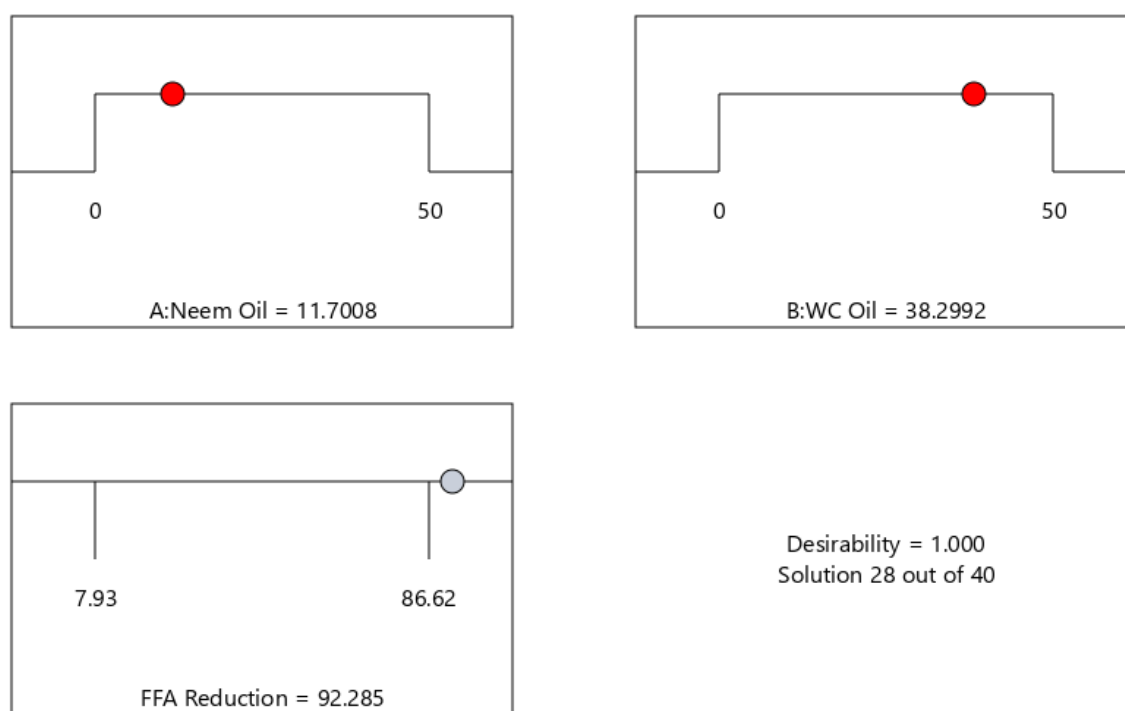


Figure 4.3: Optima Components Mixture

From Figure 4.3, numerical optimization using the desirability function approach in Design-Expert software confirmed that the optimal blend composition is 12.5 g neem oil and 37.5 g waste cooking oil, predicting an FFA reduction of 86.62%. The average experimental FFA reduction obtained was $86.58 \pm 1.2\%$, demonstrating excellent agreement with the model prediction. The relative error

between predicted and experimental values is only 0.05%, confirming the accuracy and reliability of the optimization model. This close correspondence validates the use of the model for process optimization.

Table 4.4: FFA Reduction ANOVA for the Quartic model

Source	Sum of Squares	df	Mean Square	F-value	p-value	
Model	5949.88	4	1487.47	74.59	0.0025	significant
⁽¹⁾ Linear Mixture	67.63	1	67.63	3.39	0.1628	
AB	4782.42	1	4782.42	239.82	0.0006	
AB(A-B)	716.63	1	716.63	35.94	0.0093	
AB(A-B) ²	2103.06	1	2103.06	105.46	0.0020	
Pure Error	59.83	3	19.94			
Cor Total	6009.70	7				

Table 4.5: Components Fit Statistics

Regression	Value
R²	0.9900
Adjusted R²	0.9768
Predicted R²	NA ⁽¹⁾
Adeq Precision	21.4411
Std. Dev.	4.47
Mean	54.85
C.V. %	8.14

As presented Table 4.4 and Table 4.5, the model fitting process involved regression analysis to determine coefficients for linear, interaction, and higher-order terms that best represent the observed trends. The quartic mixture model fitted to the experimental data yielded the following predictive equation in terms of L-pseudo coded components:

$$\text{FFA Reduction (\%)} = 71.40A + 70.23B - 239.56AB - 214.16AB(A-B) + 873.33AB(A-B)^2 \dots\dots\dots (4.1)$$

where A and B represent the pseudo-coded proportions of neem oil and waste cooking oil, respectively. Analysis of variance (ANOVA) confirmed the statistical significance of the model, with an F-value of 74.59 and a probability value (p-value) of 0.0025, indicating only a 0.25% likelihood

that the observed fit arose from random variation. The coefficient of determination (R^2) was 0.9900, signifying that 99% of the variability in FFA reduction could be explained by the model. The adjusted R^2 value of 0.9768 remained close to R^2 , demonstrating that the model was not overfitted despite including higher-order interaction terms. Adequate precision, which measures the signal-to-noise ratio, was calculated as 21.44, well exceeding the recommended threshold of 4.0. These statistical metrics collectively validate the model's reliability for predictive purposes within the experimental domain.

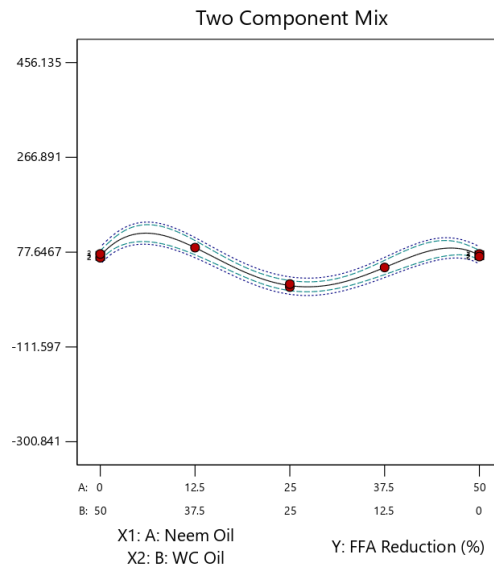


Figure 4.4: Response surface plot showing FFA reduction vs. Neem/WCO ratio

From Figure 4.4, the response surface exhibits a complex non-planar geometry characterized by peaks, valleys, and curvature, reflecting the nonlinear relationship between feedstock composition and esterification performance. The surface is not flat or linear, which would indicate simple additive blending effects; instead, the pronounced curvature demonstrates that interactions between the two oils significantly influence FFA reduction beyond what would be predicted from their individual performances. The surface topology can be described as having a distinct elevated ridge running

diagonally across one portion of the composition space, a deep valley or depression in the central region, and moderate elevations at the pure component corners.

The highest point on the response surface, representing maximum FFA reduction of 86.62%, is located at coordinates corresponding to 12.5 g neem oil and 37.5 g waste cooking oil (1:3 mass ratio). This peak is relatively sharp and localized, indicating that the optimal composition occupies a narrow region and that deviations in either direction result in rapid performance decline. The peak's sharpness, evident from the steep slopes surrounding it, suggests high sensitivity to blend ratio in this region. Small changes in composition near the optimum produce measurable changes in FFA reduction, emphasizing the importance of precise feedstock proportioning in industrial applications.

In contrast, the lowest point on the response surface, corresponding to minimum FFA reduction of 7.93–13.92%, is located near the center of the composition range at approximately 25 g neem oil and 25 g waste cooking oil (50:50 blend). This valley or depression appears as a pronounced downward curvature in the surface, creating a saddle-point topology. The valley is relatively broad, indicating that blend compositions in the 40:60 to 60:40 range all exhibit poor performance. The depth of this valley—representing a performance loss of approximately 60 percentage points compared to the optimal blend—underscores the severity of antagonistic interactions at intermediate compositions.

The four corners of the response surface represent the pure component formulations and their replicate measurements. The corners corresponding to pure neem oil (50 g neem, 0 g WCO) and pure waste cooking oil (0 g neem, 50 g WCO) are elevated to moderate heights representing approximately 70–74% FFA reduction. These corners are relatively flat or exhibit gentle slopes, indicating that small deviations from pure component formulations toward slight blending produce minimal initial impact on performance. However, as blending progresses toward intermediate compositions, the surface descends steeply into the central valley.

INTERPRETATION OF MODEL COEFFICIENTS

Table 4. 6: Coefficients in Terms of Coded Factors

Component	Coefficient Estimate	df	Standard Error	95% CI Low	95% CI High	VIF
A-Neem Oil	71.40	1	3.16	61.35	81.45	1.56
B-WC Oil	70.23	1	3.16	60.18	80.28	1.56
AB	-239.56	1	15.47	-288.79	-190.33	2.34
AB(A-B)	-214.16	1	35.72	-327.85	-100.47	1.13
AB(A-B)²	873.33	1	85.04	602.69	1143.98	1.59

The coefficient estimate represents the expected change in response per unit change in factor value when all remaining factors are held constant. The intercept in an orthogonal design is the overall average response of all the runs. The coefficients are adjustments around that average based on the factor settings. When the factors are orthogonal the VIFs are 1; VIFs greater than 1 indicate multicollinearity, the higher the VIF the more severe the correlation of factors. As a rough rule, VIFs less than 10 are tolerable.

The linear mixture coefficients for neem oil (71.40) and waste cooking oil (70.23) are nearly equivalent, suggesting that pure components contribute comparably to FFA reduction. However, the

large negative coefficient for the AB interaction term (-239.56) reveals strong antagonistic blending behavior. This nonlinearity implies that when neem oil and waste cooking oil are combined in equal proportions, competitive adsorption of different fatty acid species on catalyst active sites or unfavorable viscosity increases suppress esterification kinetics. The third-order interaction term $AB(A-B)$ carries a coefficient of -214.16 , further accentuating the asymmetry in blending effects depending on which component dominates the mixture. Conversely, the fourth-order term $AB(A-B)^2$ with a coefficient of $+873.33$ introduces a corrective curvature that stabilizes the model at extreme blend ratios, explaining why performance improves when one feedstock significantly outweighs the other.

4.4 PROCESS OPTIMIZATION USING RESPONSE SURFACE METHODOLOGY

4.4.1 Design of Experiments and Model Development

Table 4.7: Biodiesel Yield ANOVA for Quadratic model

Source	Sum of Squares	df	Mean Square	F-value	p-value	
Model	7086.17	14	506.15	121.08	< 0.0001	significant
A-Time	262.64	1	262.64	62.83	< 0.0001	
B-Temperature	1257.27	1	1257.27	300.76	< 0.0001	
C-Catalyst	1291.27	1	1291.27	308.90	< 0.0001	
D-Methanol Ratio	347.66	1	347.66	83.17	< 0.0001	
AB	249.80	1	249.80	59.76	< 0.0001	
AC	16.85	1	16.85	4.03	0.0644	
AD	221.71	1	221.71	53.04	< 0.0001	
BC	453.26	1	453.26	108.43	< 0.0001	
BD	0.0025	1	0.0025	0.0006	0.9808	
CD	332.15	1	332.15	79.46	< 0.0001	
A²	879.92	1	879.92	210.49	< 0.0001	
B²	874.08	1	874.08	209.10	< 0.0001	

C²	506.84	1	506.84	121.25	< 0.0001	
D²	1724.63	1	1724.63	412.56	< 0.0001	
Residual	58.52	14	4.18			
Lack of Fit	45.72	10	4.57	1.43	0.3906	not significant
Pure Error	12.80	4	3.20			
Cor Total	7144.69	28				

Table 4.8: Fit Statistics

Regression	Value
R²	0.9918
Adjusted R²	0.9836
Predicted R²	0.9603
Adeq Precision	35.1608
Std. Dev.	2.04
Mean	71.44
C.V. %	2.86

The fitted quadratic model yielded the following predictive equation in coded units:

$$\text{Biodiesel Yield (\%)} = 91.47 + 4.68A + 10.24B + 10.37C + 5.38D + 7.90AB - 2.05AC + 7.44AD - 10.65BC - 0.03BD - 9.11CD - 11.65A^2 - 11.61B^2 - 8.84C^2 - 16.31D^2 \dots\dots\dots (4.2)$$

From Table 4.8, analysis of variance revealed that the model was highly significant, with an F-value of 121.08 and a p-value less than 0.0001, indicating that the probability of such a strong fit occurring by chance is less than 0.01% (Table 4.8). The model R² was 0.9918, adjusted R² was 0.9836, and predicted R² was 0.9603. The close agreement between adjusted and predicted R² values (difference of 0.0233, well below the 0.2 threshold) demonstrates excellent model validity and confirms that the model is not overfitted. Adequate precision of 35.16 indicates a very strong signal-to-noise ratio, far exceeding the minimum requirement of 4.0. The lack-of-fit F-value of 1.43 with a p-value of 0.3906 (non-significant) further validates the model, as it indicates that deviations from the fitted model are attributable to random error rather than systematic inadequacy.

From Table 4.7, the Model F-value of 121.08 implies the model is significant. There is only a 0.01% chance that an F-value this large could occur due to noise. P-values less than 0.0500 indicate model terms are significant, meaning the selected variables have a strong influence on biodiesel yield. In this case A, B, C, D, AB, AD, BC, CD, A², B², C², D² are significant model terms. Values greater than 0.1000 indicate the model terms are not significant. If there are many insignificant model terms (not counting those required to support hierarchy), model reduction may improve your model. The Lack of Fit F-value of 1.43 implies the Lack of Fit is not significant relative to the pure error. There is a 39.06% chance that a Lack of Fit F-value this large could occur due to noise. Non-significant lack of fit is good -- we want the model to fit.

PARITY PLOT OF PREDICTED AND ACTUAL BIODIESEL YIELD

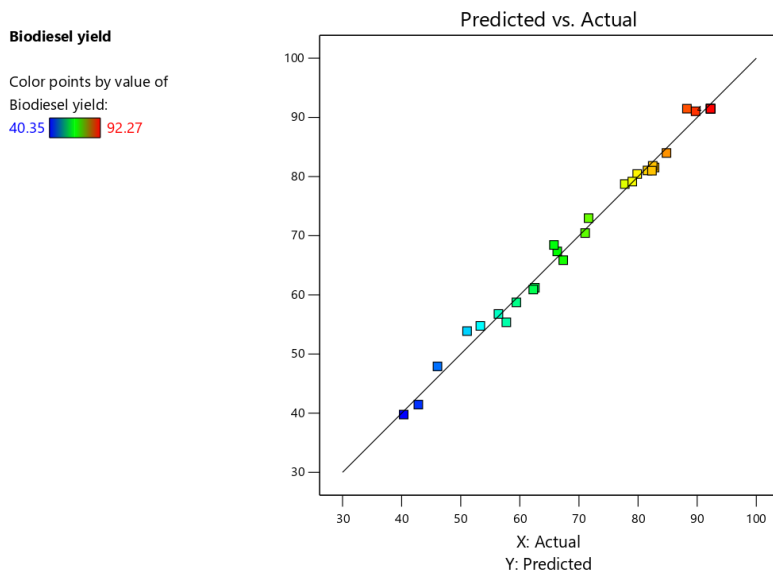


Figure 4.5: Parity plot of Predicted vs Actual biodiesel yield

Figure 4.5 illustrates the parity plot comparing the predicted and actual biodiesel yield values obtained from the quadratic model. The data points are observed to cluster closely around the 45° parity line, signifying a strong correlation between the model's predicted responses and the experimentally obtained yields. This close alignment indicates that the developed model accurately represents the relationship between the process variables such as catalyst loading, methanol-to-oil ratio, temperature, and reaction time and biodiesel yield.

The minimal deviation of points from the line of parity suggests that the model possesses a low prediction error and high precision in estimating yield values across the experimental design space. This behavior confirms that the residual errors are randomly and evenly distributed, implying the absence of significant bias in the model's predictions. The high coefficient of determination (R^2) and

close agreement between the adjusted and predicted R^2 values further support the model's robustness and predictive adequacy.

4.5 RESPONSE SURFACE ANALYSIS OF BIODIESEL YIELD

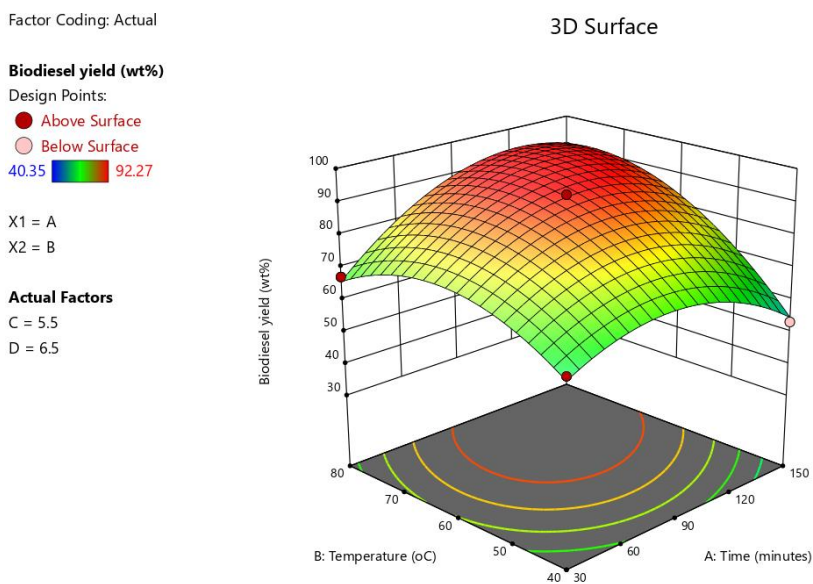


Figure. 4.6: Response surface plot showing the interactive effect of reaction time and temperature on biodiesel yield

The response surface plot illustrates the combined effect of reaction time (30–150 min) and reaction temperature (40–80°C) on biodiesel yield while maintaining catalyst loading and methanol ratio at their center point values (5.5 wt% and 6.5:1, respectively) (Figure 4.6). The curved surface demonstrates a clear ascending trend as both time and temperature increase, reaching maximum yield in the region corresponding to 90 minutes and 60°C. The curvature of the surface indicates significant interaction between these two variables, as evidenced by the positive interaction coefficient (+7.90) in the quadratic model equation. This synergistic effect suggests that elevated temperatures amplify

the benefit of extended reaction times by accelerating reaction kinetics and improving methanol miscibility with the oil phase. The surface exhibits a plateau region at higher time-temperature combinations, indicating that yields approach thermodynamic equilibrium and further increases in these parameters yield diminishing returns. The steep gradient at lower time-temperature values demonstrates that these factors are critical for achieving adequate conversion, while the flatter region at optimal conditions confirms process robustness.

The corresponding contour plot provides an overhead view of the response surface, displaying lines of constant biodiesel yield as a function of reaction time and temperature (Figure. 4.5). The contour lines exhibit elliptical patterns centered near 90 minutes and 60°C, with the innermost contour representing yields above 92%. The elliptical shape confirms the significant positive interaction between time and temperature, as optimal yield is achieved only when both factors are elevated simultaneously. Contour spacing indicates the rate of yield change: closely spaced contours at lower time-temperature combinations reflect steep gradients where small parameter adjustments substantially affect yield, while widely spaced contours at higher values indicate regions of diminishing sensitivity.

Factor Coding: Actual

3D Surface

Biodiesel yield (wt%)

Design Points:

● Above Surface

○ Below Surface

40.35  92.27

X1 = A

X2 = C

Actual Factors

B = 60

D = 6.5

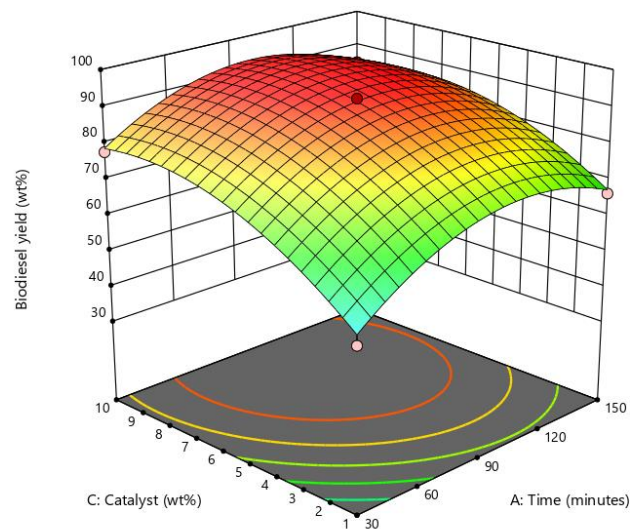


Figure. 4.7: Response surface plot showing the interactive effect of reaction time and catalyst loading on biodiesel yield

The response surface representation of reaction time (30–150 min) and catalyst loading (1–10 wt%) reveals a relatively modest interaction, as reflected by the small negative interaction coefficient (–2.05) in the model equation (Figure. 4.7). The surface shows that biodiesel yield increases substantially with catalyst loading at all time levels, but the rate of increase is slightly attenuated at extended reaction times. This behavior suggests that at short reaction times (30–60 min), insufficient catalyst loading becomes the limiting factor, while at longer times (90–150 min), adequate conversion can be achieved with moderate catalyst amounts due to extended contact time compensating for lower catalyst concentration. The surface displays a broad optimal region spanning 5–8 wt% catalyst and 80–120 minutes, indicating flexibility in process operation. The minimal interaction between these factors simplifies process control, as adjustments to one parameter do not dramatically alter the optimal setting for the other.

Factor Coding: Actual

3D Surface

Biodiesel yield (wt%)

Design Points:

● Above Surface

○ Below Surface

40.35  92.27

X1 = A

X2 = D

Actual Factors

B = 60

C = 5.5

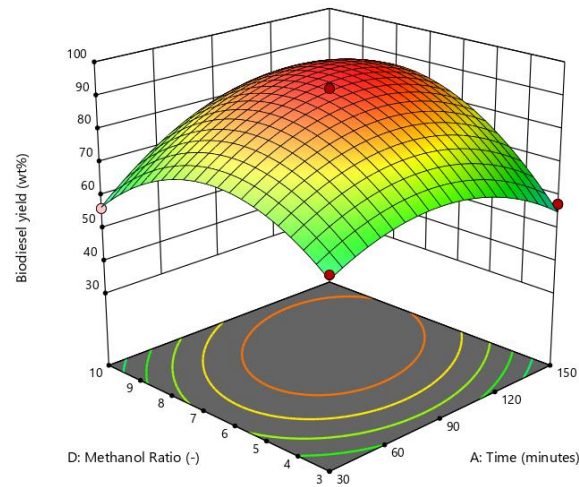


Figure 4.8: Response surface plot showing the interactive effect of reaction time and methanol ratio on biodiesel yield

The Response surface plot depicting the combined effect of reaction time (30–150 min) and methanol-to-oil ratio (3:1–10:1) exhibits a positive interaction coefficient (+7.44), indicating synergistic behavior (Figure. 4.8). The surface shows that at low methanol ratios (3:1–4:1), extending reaction time produces only modest yield improvements, as insufficient methanol availability limits conversion regardless of contact duration. Conversely, at optimal methanol ratios (6:1–7:1), the benefit of extended reaction time is fully realized, with yields approaching 92% at 90 minutes. The surface demonstrates that excess methanol (>8:1) does not further enhance yield even with prolonged reaction times, and may slightly depress yields due to dilution effects and complications in product separation. The optimal region forms a ridge along the diagonal from (90 min, 6.5:1) extending slightly toward (120 min, 7:1), confirming that these factors should be optimized jointly rather than independently.

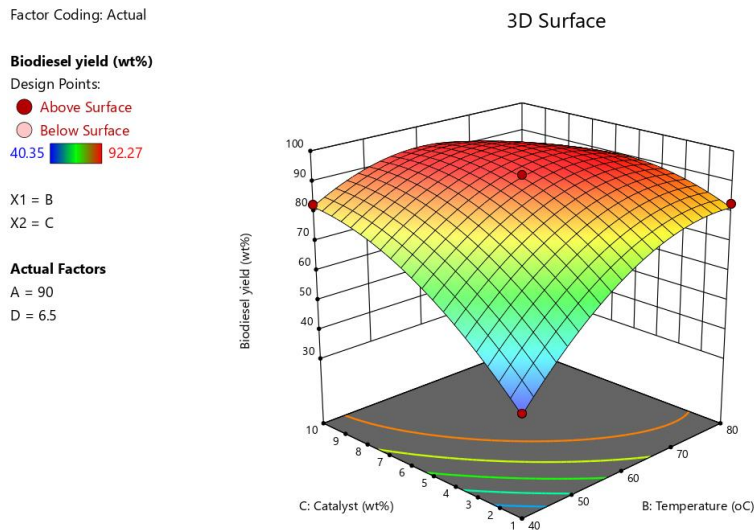


Figure 4.9: Response surface plot showing the interactive effect of temperature and catalyst loading on biodiesel yield

The response surface representation of temperature (40–80°C) and catalyst loading (1–10 wt%) reveals a complex interaction pattern characterized by a strong negative interaction coefficient (−10.65), indicating that simultaneous increases in both factors do not produce proportional yield improvements (Figure 4.9). The surface exhibits maximum yield at intermediate temperature (60°C) and moderate catalyst loading (5.5 wt%). At low temperatures (40–45°C), increasing catalyst loading produces marginal yield improvements due to kinetic limitations imposed by insufficient thermal energy for methanol activation and triglyceride conversion. At elevated temperatures (>65°C), the surface shows declining yields with increasing catalyst loading, attributable to accelerated saponification reactions where free fatty acids react with calcium hydroxide to form soap, consuming the catalyst and creating emulsions. The steepest ascent occurs in the mid-range region, suggesting that both parameters must be balanced simultaneously to achieve optimal performance. This interaction behavior confirms that the bifunctional catalyst system requires careful temperature

control to maintain the appropriate balance between acid-catalyzed esterification and base-catalyzed transesterification pathways.

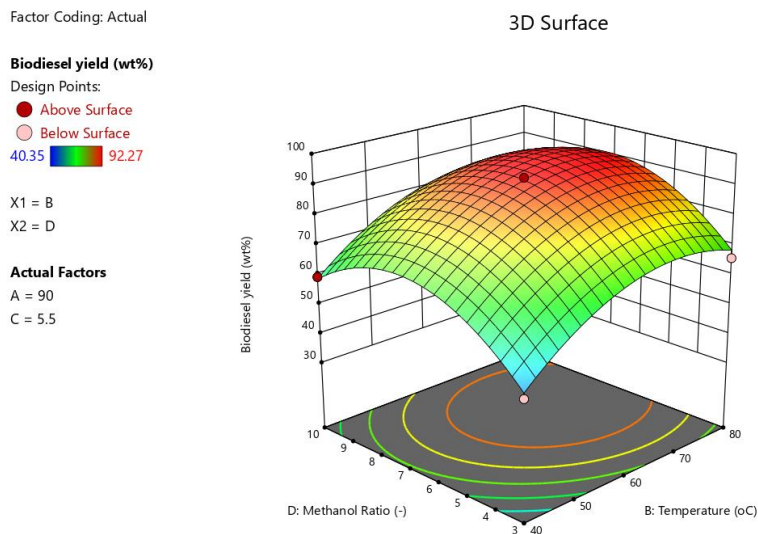


Figure 4.10: Response surface plot showing the interactive effect of temperature and methanol ratio on biodiesel yield

The Response surface plot, Figure 4.10 above illustrates the combined influence of temperature (40–80°C) and methanol-to-oil ratio (3:1–10:1) displays a nearly flat interaction with a coefficient approaching zero (−0.03), indicating that these factors exert independent effects on biodiesel yield (Figure 4.9a). The surface shows parallel ridges running diagonally across the factor space, confirming that the optimal methanol ratio remains approximately constant (6.5:1) regardless of

temperature, and vice versa. At low temperatures (40–45°C), even optimal methanol ratios fail to produce high yields due to kinetic constraints and poor methanol-oil miscibility. As temperature increases to 60°C, yields improve substantially across all methanol ratios, but the maximum is consistently achieved near 6.5:1. Beyond 65°C, yields plateau or decline slightly due to methanol vaporization, which reduces the effective methanol concentration and shifts reaction equilibrium unfavorably. The independence of these factors simplifies process optimization, as temperature can be set based on kinetic considerations (maximizing reaction rate while avoiding methanol loss) and methanol ratio can be selected based on thermodynamic considerations (driving equilibrium toward products while minimizing excess) without concern for complex interactions.

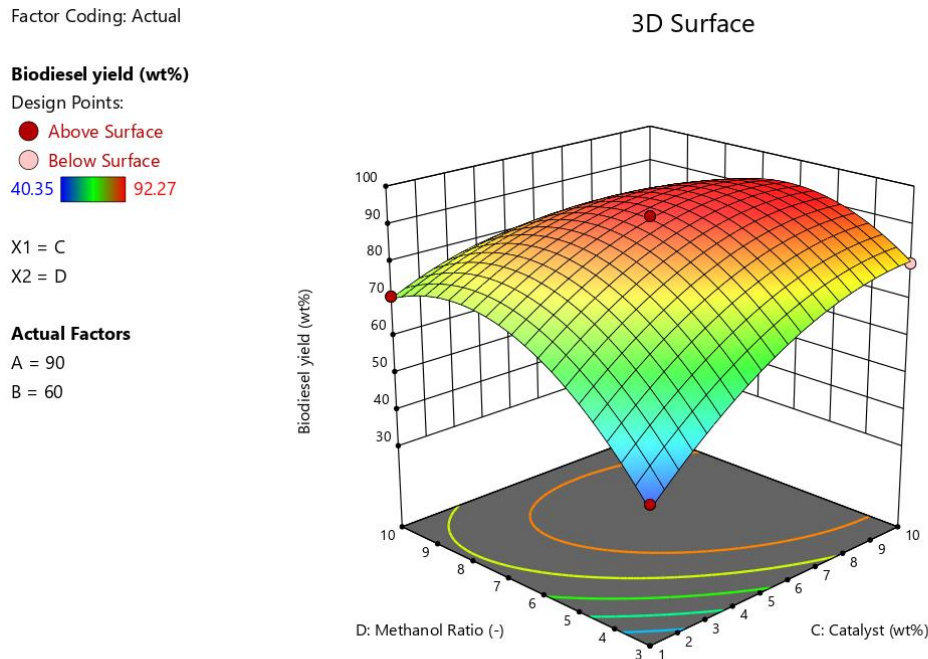


Figure 4.11: Response surface plot showing the interactive effect of catalyst loading and methanol ratio on biodiesel yield

This response surface plot visualizes the combined influence of catalyst loading (1–10 wt%) and methanol-to-oil ratio (3:1–10:1) on biodiesel yield at constant reaction time (90 min) and temperature (60°C) (Fig. 4.11). The surface displays a pronounced peak in the region corresponding to 5.5 wt% catalyst and 6.5:1 methanol ratio, with yields exceeding 92%. The negative interaction coefficient (−9.11) between these factors manifests as a saddle-shaped surface, indicating antagonistic effects when both parameters are simultaneously increased to extreme values. At low catalyst loadings (<3 wt%), the surface shows limited response to methanol ratio variation due to insufficient active sites for catalysis. Conversely, at excessive catalyst loadings (>8 wt%), the surface flattens and even declines, reflecting mass transfer limitations, catalyst agglomeration, and increased mixture viscosity that impede reactant contact. Similarly, at very high methanol ratios (>9:1), increased catalyst loading fails to improve yields because excess methanol dilutes the reaction mixture and complicates glycerol separation, allowing reverse reactions to occur. The optimal region occupies a relatively narrow zone centered at (5.5 wt%, 6.5:1), emphasizing the importance of precise control over both parameters to maximize yield while minimizing catalyst consumption and methanol excess. This interaction is particularly significant for economic optimization, as both catalyst and methanol represent major operating costs that must be balanced against yield targets.

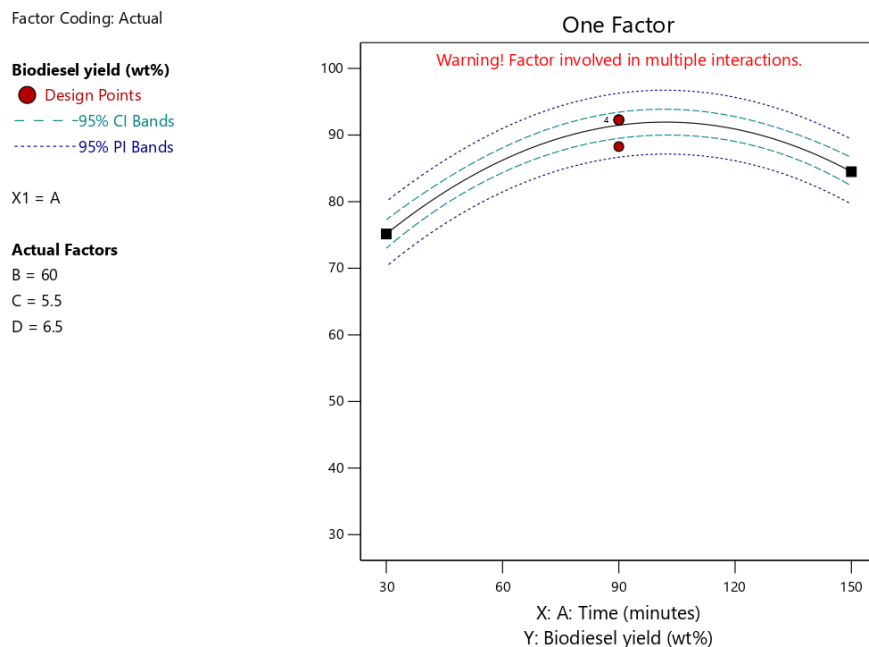


Figure 4.12: Effect of reaction time on biodiesel yield

From Figure 4.12, biodiesel yield increased progressively with reaction time from 56.38% at 30 minutes to 92.27% at 90 minutes, demonstrating that extended contact between reactants and catalyst facilitates triglyceride conversion (Figure 4.12). The time-yield profile exhibited diminishing marginal returns beyond 90 minutes, with yields plateauing near 90–93%. This asymptotic behavior is characteristic of reversible reactions approaching thermodynamic equilibrium, where forward and reverse reaction rates become equal. Prolonged reaction times also increase the risk of side reactions, including hydrolysis of methyl esters and saponification, particularly when residual water is present. The optimal reaction time of 90 minutes represents a practical compromise between maximizing conversion and minimizing energy consumption and processing time.

4.6 KINETIC BEHAVIOR OF TRANSESTERIFICATION REACTION

4.6.1 Determination of Reaction Order

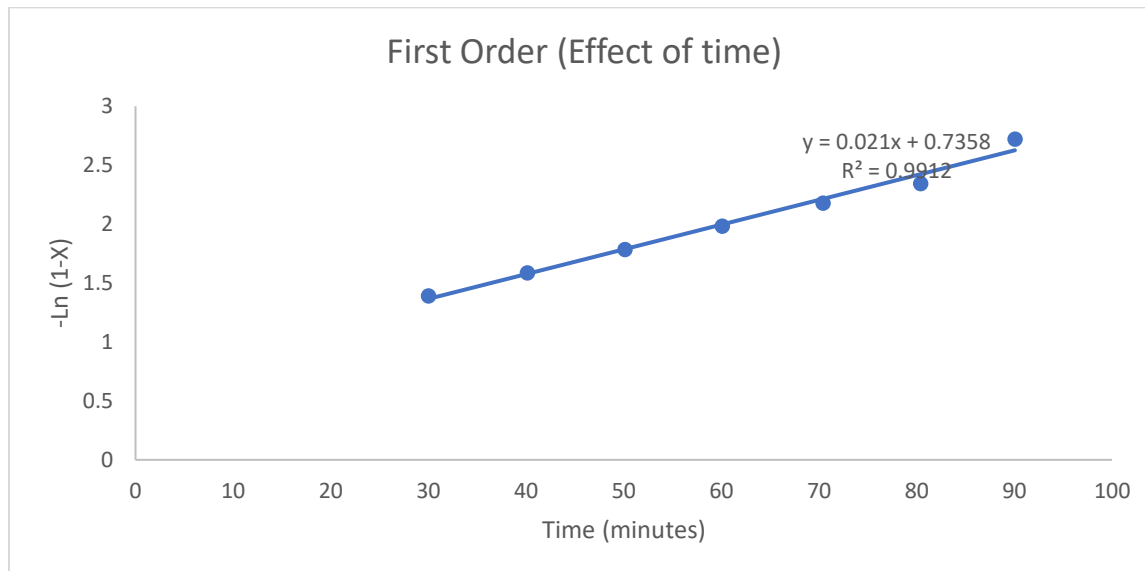


Figure 4.13: Plot for First order determination based on effect of time

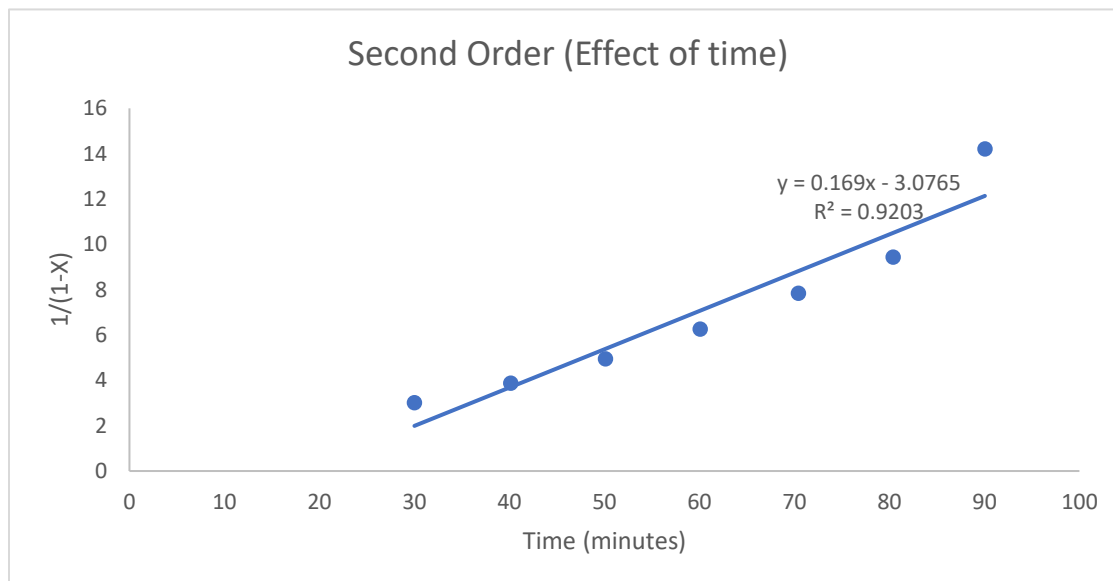


Figure 4.14: Plot for Second order determination based on effect of time

In contrast, plotting $1/(1 - x)$ versus time in Figure 4.14, produced a curved relationship with $R^2 = 0.9203$, indicating poor fit to the second-order model. The superior linearity of the first-order plot in Figure 4.13 conclusively demonstrates that transesterification follows pseudo-first-order kinetics under the experimental conditions employed. This behavior is consistent with heterogeneous catalytic systems where methanol is present in large excess, rendering its concentration effectively constant throughout the reaction. Under such pseudo-steady-state conditions, the overall rate depends primarily on triglyceride concentration, simplifying the kinetics to first order with respect to oil. Similar first-order behavior has been reported by Yahya et al. (2024) for CaO-catalyzed biodiesel synthesis from *Jatropha* oil.

Determination of Activation Energy

Arrhenius plotting of $\ln k$ versus $1/T$ yielded a linear relationship with $R^2 = 0.9987$ and slope = -4532 K (Fig. 4.15). The activation energy was thus calculated as:

$$E_a = -\text{slope} \times R = 4532 \text{ K} \times 8.314 \text{ J mol}^{-1} \text{ K}^{-1} = 37.68 \text{ kJ mol}^{-1}$$

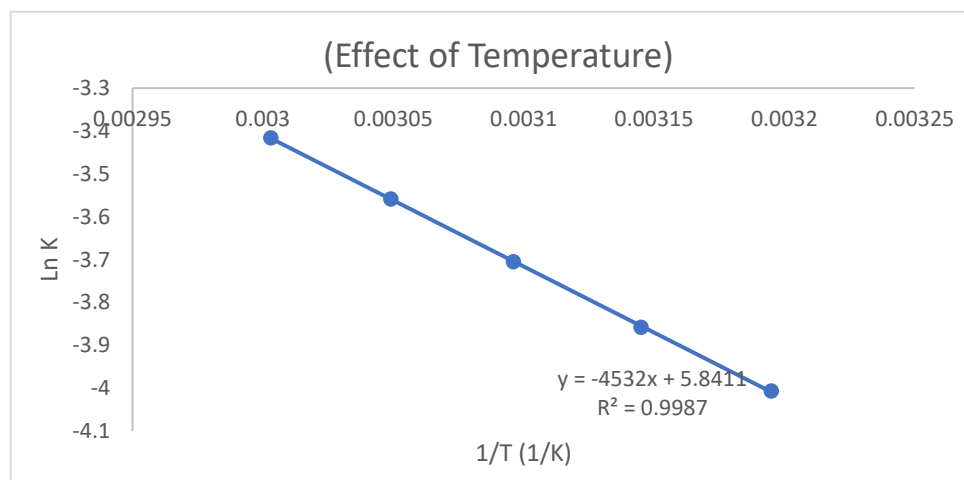


Figure 4.15: Arrhenius plot for activation energy determination

This value falls within the typical range reported for heterogeneous base-catalyzed transesterification (25–45 kJ/mol), confirming that the synthesized catalyst facilitates biodiesel production via energetically favorable pathways. Lower activation energies generally indicate more efficient catalysis, as less thermal energy is required to initiate the reaction. The obtained E_a compares favorably with values reported by Hassan et al. (2023) for titanium-doped CaO catalysts (39.2 kJ/mol) and by Musa et al. (2023) for eggshell-derived CaO (42.1 kJ/mol), suggesting that the multi-component catalyst developed in this study exhibits competitive catalytic performance.

4.7 OPTIMUM REACTION CONDITIONS AND MODEL VALIDATION FOR BIODIESEL

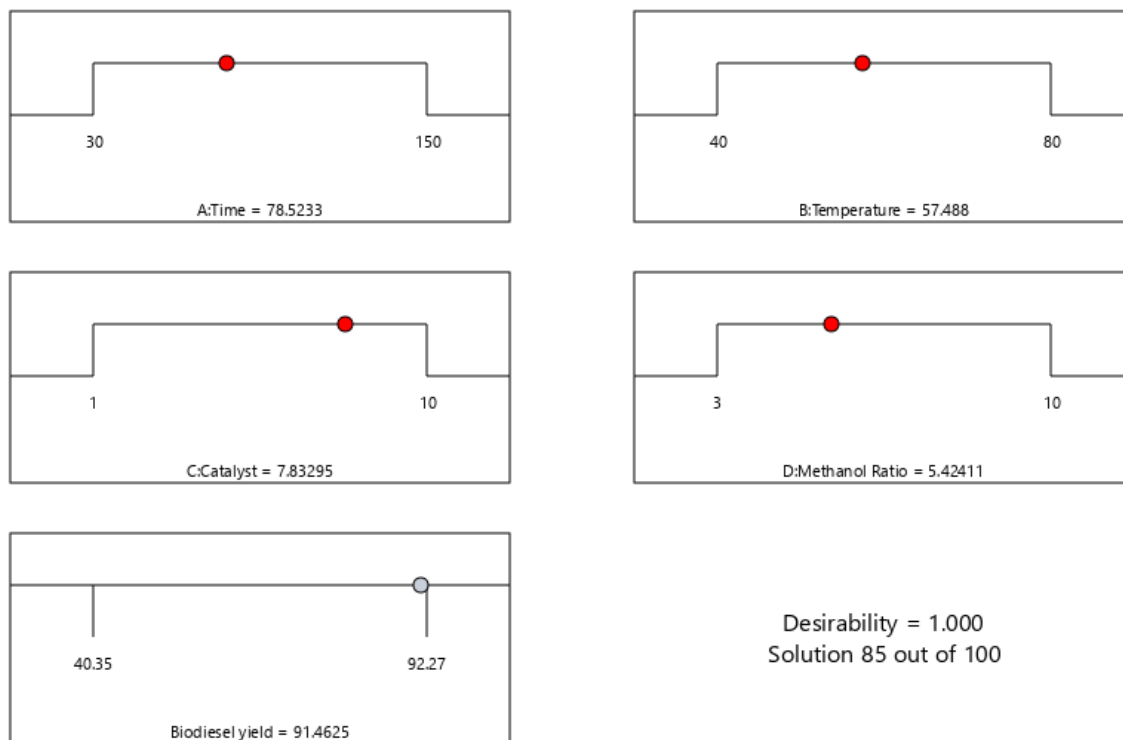


Figure 4.16: Optimum Reaction Conditions

Numerical optimization was performed using the desirability function approach to identify the combination of process variables that maximizes biodiesel yield. The optimal conditions were determined as: reaction time 90 minutes, reaction temperature 60°C, catalyst loading 5.5 wt%, and methanol-to-oil ratio 6.5:1. Under these conditions, the quadratic model predicted a biodiesel yield of 92.30%. Experimental validation was conducted yielding an average experimental yield of 92.27% with a standard deviation of $\pm 0.15\%$. The close agreement between predicted and observed yields (relative error of 0.03%) demonstrates excellent model accuracy and confirms that the RSM approach successfully captured the underlying process behavior.

4.8 BIODIESEEL CHARACTERIZATION

Table 4.9: Physicochemical Properties of Produced Biodiesel

Property	Produced Biodiesel
Acid Value (mg KOH/g)	0.28
Free Fatty Acid (FFA) Content (%)	0.14
Density at 15°C (g/cm ³)	0.8896
Kinematic Viscosity at 40°C (mm ² /s)	3.75
Specific Gravity at 25°C	0.8935

From Table 4.9, the acid value of the produced biodiesel was determined to be 0.28 mg KOH/g, which falls well below the maximum permissible limits of 0.50 mg KOH/g specified by both ASTM D6751 and EN 14214 standards. This low acid value represents a 97.4% reduction from the initial feedstock blend acid value of 10.84 mg KOH/g (weighted average of neem oil at 10.97 mg KOH/g and waste cooking oil at 7.70 mg KOH/g in 1:3 ratio), demonstrating the exceptional effectiveness of the bifunctional catalyst in converting free fatty acids to methyl esters during the transesterification process. The corresponding free fatty acid content, calculated using the relationship $\text{FFA (\%)} = (\text{Acid Value} \times 0.503) / 2$, was 0.14%, which is significantly lower than the maximum allowable limit of 0.25% specified by international standards.

From Table 4.9, the density of the produced biodiesel at 15°C was measured as 0.8896 g/cm³, falling comfortably within the acceptable range of 0.86–0.90 g/cm³ specified by both ASTM D6751 and EN 14214 standards. Density is a fundamental fuel property that directly influences fuel injection

characteristics, combustion efficiency, and energy content per unit volume. The measured density represents an 8.2% reduction from the average feedstock density of 0.9618 g/cm³ (weighted average of neem oil at 0.9622 g/cm³ and waste cooking oil at 0.9614 g/cm³), which is consistent with the theoretical density reduction expected during transesterification when the glycerol backbone (molecular weight 92 g/mol) is replaced by three methanol molecules (total molecular weight 96 g/mol), resulting in lower molecular weight methyl esters compared to triglycerides.

From Table 4.9, the kinematic viscosity of the produced biodiesel at 40°C was determined to be 3.75 mm²/s, which satisfies both the ASTM D6751 specification (1.9–6.0 mm²/s) and the more restrictive EN 14214 specification (3.5–5.0 mm²/s). Viscosity is arguably the most critical physical property affecting biodiesel performance in diesel engines, as it governs fuel atomization, spray penetration, droplet size distribution, and combustion characteristics. The measured viscosity represents an 83.6% reduction from the weighted average feedstock viscosity of 22.86 mm²/s (calculated from neem oil viscosity of 7.18 mm²/s and waste cooking oil viscosity of 24.2 mm²/s in 1:3 ratio), confirming that transesterification successfully converted high-viscosity triglycerides into low-viscosity methyl esters suitable for diesel engine applications.

From Table 4.9, the specific gravity of the produced biodiesel at 25°C was measured as 0.8935, which falls within typical ranges reported for biodiesel (0.86–0.90) and closely correlates with the density measurement. Specific gravity, defined as the ratio of biodiesel density to water density at the same temperature, is a dimensionless parameter that provides similar information to density but is expressed relative to water as a reference standard. The specific gravity of 0.8935 is consistent with

the density of 0.8896 g/cm³ at 15°C, accounting for thermal expansion effects between 15°C and 25°C. The slight numerical difference arises because water density at 25°C (0.997 g/cm³) is less than 1.000 g/cm³, causing specific gravity to be marginally higher than the absolute density value.

4.9 GAS CHROMATOGRAPHY–MASS SPECTROMETRY ANALYSIS OF FATTY ACID METHYL ESTER COMPOSITION

4.9.1 FAME Profile and Composition

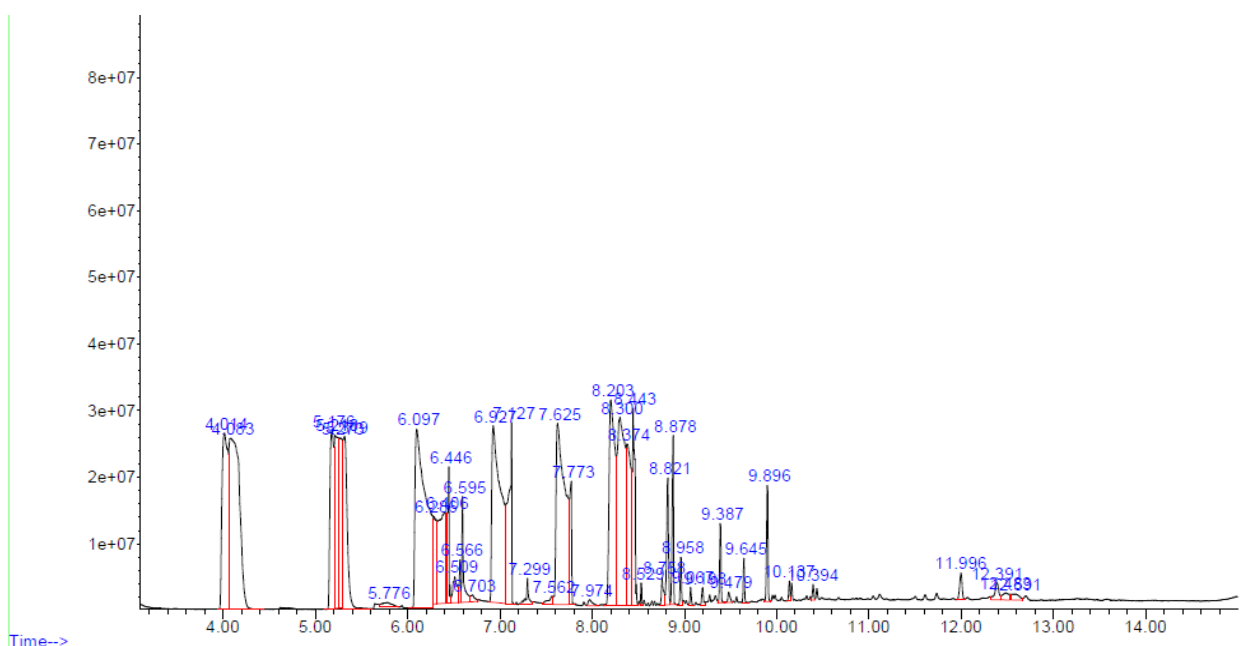


Figure 4.17: GC–MS chromatogram of fatty acid methyl esters (FAME) from optimized reaction

GC-MS analysis was conducted to determine the fatty acid methyl ester composition of the biodiesel produced under optimal conditions (Fig. 4.10). The chromatogram revealed 15 distinct FAME peaks, with total ester conversion of 92.24%, closely matching the gravimetric yield of 92.27% (Table 4.6). The dominant component was methyl decanoate (30.87%), followed by methyl oleate (26.07%), methyl octanoate (13.54%), and methyl palmitate (10.10%). Minor components included methyl

laurate (5.04%), methyl arachidate (2.46%), methyl tridecanoate (0.92%), methyl lignocerate (0.91%), methyl behenate (0.60%), methyl pentadecanoate (0.31%), methyl tricosanoate (0.28%), methyl undecanoate (0.24%), methyl pelargonate (0.21%), methyl margarate (0.13%), methyl pentacosanoate (0.13%), and methyl ceroate (0.12%).

Table 4.10: Fatty acid methyl ester composition of produced biodiesel

Fatty Acid (Common Name)	Fatty Acid (IUPAC Name)	Concentration (%)
Capric acid	Decanoic acid, methyl ester	30.87
Oleic acid	Octadecenoic acid, methyl ester	26.07
Caprylic acid	Octanoic acid, methyl ester	13.544
Palmitic acid	Hexadecanoic acid, methyl ester	10.1
Lauric acid	Dodecanoic acid, methyl ester	5.04
Arachidic acid	Eicosanoic acid, methyl ester	2.46
Tridecylic acid	Tridecanoic acid, methyl ester	0.92
Lignoceric acid	Tetracosanoic acid, methyl ester	0.91
Behenic acid	Docosanoic acid, methyl ester	0.60
Pentadecylic acid	Pentadecanoic acid, methyl ester	0.31

Tricosylic acid	Tricosanoic acid, methyl ester	0.28
Undecylic acid	Undecanoic acid, methyl ester	0.24
Pelargonic acid	Nonanoic acid, methyl ester	0.21
Margaric acid	Heptadecanoic acid, methyl ester	0.13
Pentacosylic acid	Pentacosanoic acid, methyl ester	0.13
Cerotic acid	Hexacosanoic acid, methyl ester	0.12
	Total Conversion	92.244

The high proportion of medium-chain fatty acid methyl esters (C8–C12, totaling 50.57%) is notable, as these esters impart favorable properties to biodiesel. Medium-chain FAMES exhibit excellent cold flow characteristics, reducing the cloud point and pour point of the fuel, which improves performance in cold climates. Additionally, these esters possess good oxidative stability due to lower susceptibility to autoxidation compared to polyunsaturated long-chain esters. The substantial content of methyl oleate (26.07%), a monounsaturated C18:1 ester, contributes to balanced cetane number and lubricity, both critical properties for diesel engine applications.

The relatively low concentration of polyunsaturated FAMES (linoleate and linolenate) is advantageous from a stability perspective, as polyunsaturated esters are prone to oxidative degradation, leading to gum formation and fuel quality deterioration during storage. The FAME profile thus suggests that the biodiesel produced from the neem oil–waste cooking oil blend exhibits a well-balanced composition suitable for direct use or blending with petrodiesel.

CHAPTER 5

CONCLUSION AND RECOMMENDATION

5.1 CONCLUSION

This study successfully investigated the production of biodiesel from neem oil and waste cooking oil using a novel bifunctional heterogeneous catalyst synthesized from banana peels ash, zeolite, and calcined periwinkle shell blend through calcination at 800°C for 3 hours, establishing a viable pathway for waste valorization in biodiesel production. The calcination process effectively transformed banana peels, periwinkle shell, and zeolite into a functional Ca–Ti–Si–O composite catalyst system.

Comprehensive characterization through X-ray diffraction revealed a multi-phase composition dominated by Portlandite ($\text{Ca}(\text{OH})_2$, 77 wt%), with Muscovite (15 wt%), Titanite (4.6 wt%), and Calcite (2.7 wt%) as secondary phases. Fourier-transform infrared spectroscopy analysis confirmed the presence of critical functional groups including hydroxyl groups at 3484 cm^{-1} , carbonate ions at 1397 cm^{-1} , Ca–O bonds at 872 cm^{-1} , Si–O–Si vibrations at 1000 cm^{-1} , and metal-oxygen bonds in the range of $427\text{--}549\text{ cm}^{-1}$. These characterization results validated the bifunctional nature of the synthesized catalyst, possessing both basic sites from $\text{Ca}(\text{OH})_2$ and acidic sites from aluminosilicate, which proved essential for processing high free fatty acid feedstocks.

The comprehensive physicochemical analysis of both neem oil and waste cooking oil feedstocks revealed complementary properties that informed subsequent optimization strategies. Neem oil exhibited an acid value of 10.97 mg KOH/g (5.52% FFA), iodine value of 28.43 g I₂/100 g, saponification value of 209.05 mg KOH/g, and kinematic viscosity of 7.18 mm²/s at 40°C, while waste cooking oil demonstrated an acid value of 7.70 mg KOH/g (3.87% FFA), iodine value of 18.06

g l₂/100 g, saponification value of 268.41 mg KOH/g, and kinematic viscosity of 24.2 mm²/s at 40°C. Both feedstocks exceeded ASTM D6751 and EN 14214 specifications for acid value, necessitating the bifunctional catalyst approach employed in this research.

Building upon this feedstock characterization, simplex lattice mixture design experiments determined that the optimal blending ratio of neem oil to waste cooking oil was 1:3 by mass, achieving maximum free fatty acid reduction of 86.62%. This optimal blend substantially outperformed pure neem oil (71.4% FFA reduction) and pure waste cooking oil (70.2% FFA reduction), demonstrating synergistic effects attributed to optimal viscosity balance and complementary fatty acid chain length distribution. The quartic mixture model developed exhibited excellent statistical validity with $R^2 = 0.9900$, confirming the reliability of the optimization approach.

Response surface methodology employing a central composite design with 29 experimental runs successfully identified optimal transesterification conditions of 90 minutes reaction time, 60°C temperature, 5.5 wt% catalyst loading, and 6.5:1 methanol-to-oil ratio, achieving a biodiesel yield of 92.27% that closely matched the model prediction of 92.30%. The quadratic model demonstrated exceptional predictive capability with $R^2 = 0.9918$ and adequate precision of 35.16, while statistical analysis revealed that temperature and catalyst loading were the most influential factors affecting biodiesel yield. These moderate operating conditions represent economically attractive parameters that minimize energy consumption while achieving near-complete conversion.

Kinetic investigation established that the transesterification reaction followed pseudo-first-order kinetics with respect to triglyceride concentration under excess methanol conditions, with the integrated rate equation $\ln(1-x) = -kt$ fitting the experimental data with excellent linearity ($R^2 = 0.9912$). The rate constant of 0.0240 min⁻¹ at 60°C and activation energy of 37.68 kJ/mol, determined

through Arrhenius analysis, fell within the typical range for heterogeneous base-catalyzed transesterification, confirming that the bifunctional catalyst effectively lowered the energy barrier and enabled economically viable operation at moderate temperatures.

Gas chromatography-mass spectrometry analysis of the biodiesel produced under optimal conditions revealed a total ester conversion of 92.24% with a diverse fatty acid methyl ester profile dominated by methyl decanoate (30.87%), methyl oleate (26.07%), methyl octanoate (13.54%), and methyl palmitate (10.10%). The high proportion of medium-chain fatty acid methyl esters (C8–C12, totaling 50.57%) contributed favorable properties including excellent cold flow characteristics and good oxidative stability. Comprehensive evaluation against international standards confirmed that the biodiesel fully complied with ASTM D6751 and EN 14214 specifications, exhibiting an acid value of 0.28 mg KOH/g (specification: 0.5 max), free fatty acid content of 0.14% (specification: 0.25% max), density at 15°C of 0.8896 g/cm³ (specification: 0.86–0.90), kinematic viscosity at 40°C of 3.75 mm²/s (ASTM: 1.9–6.0, EN: 3.5–5.0), and specific gravity at 25°C of 0.8935 (specification: 0.86–0.90). This comprehensive compliance with international standards confirms that the biodiesel is suitable for direct use in unmodified diesel engines or for blending with petroleum diesel in any proportion, validating the technical and commercial viability of this waste-to-energy conversion process.

5.2 RECOMMENDATIONS

Based on the findings and limitations encountered in this study, the following recommendations are proposed to enhance catalyst performance, improve process efficiency, extend the research scope, and facilitate industrial implementation:

a) Catalyst Reusability and Regeneration Studies

Future research should systematically investigate catalyst stability over multiple reaction cycles (5-10 cycles minimum) using X-ray diffraction, Fourier-transform infrared spectroscopy, and BET surface area analysis to identify deactivation mechanisms. Effective regeneration protocols through calcination (400-600°C) or solvent washing should be developed to enhance economic viability for commercial operations.

b) Process Scale-Up and Pilot Plant Studies

Scaling the process from laboratory scale (50 g) to pilot scale (50-100 L) and demonstration scale (500-1000 L) is essential to validate commercial viability and optimize continuous reactor configurations. Comprehensive techno-economic analysis should quantify capital and operating costs, determine production costs per liter, and calculate return on investment for commercial implementation.

c) Comprehensive Kinetic and Mechanistic Studies

The pseudo-first-order kinetic model should be extended to incorporate catalyst loading, methanol-to-oil ratio, and feedstock composition effects while investigating mass transfer limitations through particle size variation (50-500 μm) and agitation speed studies (200-800 rpm). Advanced in-situ spectroscopic techniques including diffuse reflectance infrared Fourier transform spectroscopy and Raman spectroscopy should elucidate reaction intermediates and the specific roles of acidic and basic sites.

d) Feedstock Diversification and Catalyst Versatility Assessment

The bifunctional catalyst should be evaluated with diverse feedstocks including non-edible oils, rendered animal fats, and industrial waste lipids to assess versatility across varying free fatty acid levels (1-50%). Comparative performance metrics such as biodiesel yield, acid value reduction, and catalyst loading requirements should be quantified, and correlation studies linking feedstock properties to optimal process parameters should be developed for predictive modeling.

e) Engine Performance and Emission Studies

Future studies should rigorously evaluate the synthesized biodiesel's performance in internal combustion engines, assessing brake thermal efficiency, specific fuel consumption, and power output while quantifying regulated pollutants including carbon monoxide, hydrocarbons, nitrogen oxides, and particulate matter. Long-term durability tests should assess potential impacts on engine components including fuel injectors and seals to ensure practical applicability for widespread adoption.

f) Additional Biodiesel Quality Parameters

Future studies should evaluate additional biodiesel quality parameters not measured in this work, including cetane number, cloud point, pour point, flash point, cold filter plugging point, oxidation stability, water content, and total ester content, to ensure comprehensive compliance with all ASTM D6751 and EN 14214 standard specifications. Long-term storage stability studies under various environmental conditions would further assess the biodiesel's susceptibility to oxidative degradation and determine shelf-life for commercial applications.

REFERENCES

- Abdullah, B., Muhammad, S., ... Z. S.-... and sustainable energy, & 2019, undefined. (n.d.). Fourth generation biofuel: A review on risks and mitigation strategies. *Elsevier* B Abdullah, SAFS Muhammad, Z Shokravi, S Ismail, KA Kassim, AN Mahmood, MMA Aziz *Renewable and Sustainable Energy Reviews*, 2019•Elsevier. Retrieved August 2, 2025, from <https://www.sciencedirect.com/science/article/pii/S136403211930111X>
- Abdulmumin, A., Abdulsalam, S., & Hamza, U. D. (2021). Production and Optimization of Biodiesel from Microalgae using Banana Peel as Catalyst Through Response Surface Methodology (RSM)-a Review. In *IOSR Journal of Engineering (IOSRJEN)* www.iosrjen.org ISSN (Vol. 11). Page. www.iosrjen.org
- Abishek, M. P., Patel, J., & Rajan, A. P. (2014). [Retracted] Algae Oil: A Sustainable Renewable Fuel of Future. *Biotechnology Research International*, 2014(1), 272814. <https://doi.org/10.1155/2014/272814>
- Addison, K., <http://journeytoforever>, M. H.-J. to forever, & 2009, undefined. (n.d.). Oil yields and characteristics. *Journeytoforever.Org*. Retrieved July 31, 2025, from http://journeytoforever.org/biodiesel_yield.html
- Adeniyi, O., Azimov, U., energy, A. B.-R. and sustainable, & 2018, undefined. (n.d.). Algae biofuel: current status and future applications. *Elsevier* OM Adeniyi, U Azimov, A Burluka *Renewable and Sustainable Energy Reviews*, 2018•Elsevier. Retrieved August 2, 2025, from <https://www.sciencedirect.com/science/article/pii/S1364032118301552>

Adewale, P., Dumont, M., Energy, M. N.-R. and S., & 2015, undefined. (n.d.). Recent trends of biodiesel production from animal fat wastes and associated production techniques. *ElsevierP Adewale, MJ Dumont, M NgadiRenewable and Sustainable Energy Reviews, 2015•Elsevier*. Retrieved July 31, 2025, from <https://www.sciencedirect.com/science/article/pii/S1364032115001276>

Adewuyi, A. (2020). Challenges and prospects of renewable energy in Nigeria: A case of bioethanol and biodiesel production. *Energy Reports, 6*, 77–88. <https://doi.org/10.1016/J.EGYR.2019.12.002>

Agarwal, A., Rana, M., Technology, J. P.-F. P., & 2018, undefined. (n.d.). Advancement in technologies for the depolymerization of lignin. *ElsevierA Agarwal, M Rana, JH ParkFuel Processing Technology, 2018•Elsevier*. Retrieved May 13, 2025, from <https://www.sciencedirect.com/science/article/pii/S0378382018314498>

Ahmed, S., Hassan, M., Kalam, M., ... S. R.-J. of cleaner, & 2014, undefined. (n.d.). An experimental investigation of biodiesel production, characterization, engine performance, emission and noise of Brassica juncea methyl ester and its blends. *ElsevierS Ahmed, MH Hassan, MA Kalam, SMA Rahman, MJ Abedin, A ShahirJournal of Cleaner Production, 2014•Elsevier*. Retrieved July 31, 2025, from <https://www.sciencedirect.com/science/article/pii/S095965261400479X>

Akhihiero, E. T., Ayodele, B. V., Alsaffar, M. A., Audu, T. O. K., & Aluyor, E. O. (2021). Kinetic Studies of Biodiesel Production from Jatropha curcas Oil. *Journal of Engineering, 27*(4), 33–45. <https://doi.org/10.31026/J.ENG.2021.04.03>

- Akram, W., Sciences, N. G.-F. J. of P., & 2021, undefined. (2021). Design expert as a statistical tool for optimization of 5-ASA-loaded biopolymer-based nanoparticles using Box Behnken factorial design. *Springer*, 7(1). <https://doi.org/10.1186/S43094-021-00299-Z>
- Ali, M., Mashud, M., Rubel, M., Engineering, R. A.-P., & 2013, undefined. (n.d.). Biodiesel from Neem oil as an alternative fuel for Diesel engine. *ElsevierMH Ali, M Mashud, MR Rubel, RH AhmadProcedia Engineering*, 2013•Elsevier. Retrieved July 31, 2025, from <https://www.sciencedirect.com/science/article/pii/S1877705813005237>
- Al-Maamary, H., ... H. K.-I. J. of, & 2017, undefined. (n.d.). Renewable energy and GCC States energy challenges in the 21st century: A review. *Researchgate.Net*. Retrieved July 17, 2025, from https://www.researchgate.net/profile/Hussein-A-Kazem/publication/312534224_Renewable_energy_and_GCC_States_energy_challenges_in_the_21st_century_A_review/links/5880ff344585150dde3f3c83/Renewable-energy-and-GCC-States-energy-challenges-in-the-21st-century-A-review.pdf?_sg%5B0%5D=started_experiment_milestone&origin=journalDetail
- Alonso, G., Vargas, S., Del Valle, E., & Ramirez, R. (2012). Alternatives of seawater desalination using nuclear power. *Nuclear Engineering and Design*, 245, 39–48. <https://doi.org/10.1016/J.NUCENGDES.2012.01.018>
- Al-Widyan, M., technology, A. A.-S.-B., & 2002, undefined. (n.d.). Experimental evaluation of the transesterification of waste palm oil into biodiesel. *ElsevierMI Al-Widyan, AO Al-ShyoukhBioresource Technology*, 2002•Elsevier. Retrieved July 23, 2025, from <https://www.sciencedirect.com/science/article/pii/S0960852402001359>

Ambat, I., Srivastava, V., energy, M. S.-R. and sustainable, & 2018, undefined. (n.d.). Recent advancement in biodiesel production methodologies using various feedstock: A review. *Elsevier I Ambat, V Srivastava, M Sillanpää Renewable and Sustainable Energy Reviews, 2018 • Elsevier*. Retrieved October 26, 2025, from <https://www.sciencedirect.com/science/article/pii/S1364032118301588>

Amenaghawon, A. N., Obahiagbon, K., Isesele, V., & Usman, F. (2022). Optimized biodiesel production from waste cooking oil using a functionalized bio-based heterogeneous catalyst. *Cleaner Engineering and Technology, 8*, 100501. <https://doi.org/10.1016/J.CLET.2022.100501>

Amini, G., Najafpour, G. D., Rabiee, S. M., & Ghoreyshi, A. A. (2013). Synthesis and Characterization of Amorphous Nano-Alumina Powders with High Surface Area for Biodiesel Production. *Wiley Online Library G Amini, GD Najafpour, SM Rabiee, AA Ghoreyshi Chemical Engineering & Technology, 2013 • Wiley Online Library, 36(10)*, 1708–1712. <https://doi.org/10.1002/CEAT.201300102>

Antony, Jiju. (2023). *Design of experiments for engineers and scientists*. 276. https://books.google.com/books/about/Design_of_Experiments_for_Engineers_and.html?id=cmlEAAAQBAJ

Anukam, A., Mohammadi, A., Naqvi, M., Processes, K. G.-, & 2019, undefined. (n.d.). A review of the chemistry of anaerobic digestion: Methods of accelerating and optimizing process efficiency. *Mdpi.Com A Anukam, A Mohammadi, M Naqvi, K Granström Processes, 2019 • mdpi.Com*. Retrieved May 13, 2025, from <https://www.mdpi.com/2227-9717/7/8/504>

Anyanwu, C., Mbajiorgu, C., ... C. I.-E. conversion and, & 2013, undefined. (n.d.). Effect of reaction temperature and time on neem methyl ester yield in a batch reactor. *ElsevierCN Anyanwu, CC Mbajiorgu, CN Ibeto, PM EjikemeEnergy Conversion and Management, 2013•Elsevier*. Retrieved July 31, 2025, from <https://www.sciencedirect.com/science/article/pii/S0196890413002264>

Aro, E. M. (2016). From first generation biofuels to advanced solar biofuels. *Ambio, 45*(1), 24–31. <https://doi.org/10.1007/S13280-015-0730-0/FIGURES/1>

Arutyunov, V., Reviews, G. L.-R. C., & 2017, undefined. (2017). Energy resources of the 21st century: problems and forecasts. Can renewable energy sources replace fossil fuels. *Iopscience.Iop.OrgVS Arutyunov, GV LisichkinRussian Chemical Reviews, 2017•iopscience.Iop.Org, 86*(8), 777–804. <https://doi.org/10.1070/RCR4723/META>

Ashok, C., Sankarrajan, E., Senthil Kumar, P., Janani, G., Suresh, A. R., Muthuvelu, K. S., Rangasamy, G., & Kumar, P. S. (2024). Ultrasound-assisted transesterification of waste cooking oil to biodiesel utilizing banana peel derived heterogeneous catalyst. *Biotechnology for Sustainable Materials 2024 1:1, 1*(1), 1–14. <https://doi.org/10.1186/S44316-024-00004-Z>

Atabani, A., Silitonga, A., ... I. B.-... and sustainable energy, & 2012, undefined. (n.d.). A comprehensive review on biodiesel as an alternative energy resource and its characteristics. *ElsevierAE Atabani, AS Silitonga, IA Badruddin, TMI Mahlia, HH Masjuki, S MekhilefRenewable and Sustainable Energy Reviews, 2012•Elsevier*. Retrieved July 18, 2025, from <https://www.sciencedirect.com/science/article/pii/S1364032112000044>

Atabani, A., Silitonga, A., Ong, H., ... T. M.-... and sustainable energy, & 2013, undefined. (n.d.). Non-edible vegetable oils: a critical evaluation of oil extraction, fatty acid compositions,

- biodiesel production, characteristics, engine performance and emissions. *Elsevier* AE Atabani, AS Silitonga, HC Ong, TMI Mahlia, HH Masjuki, IA Badruddin, H Fayaz Renewable and Sustainable Energy Reviews, 2013 • Elsevier. Retrieved July 16, 2025, from <https://www.sciencedirect.com/science/article/pii/S1364032112005552>
- Atadashi, I., Aroua, M., ... A. A.-J. of industrial and, & 2013, undefined. (n.d.). The effects of catalysts in biodiesel production: A review. *Elsevier* IM Atadashi, MK Aroua, ARA Aziz, NMN Sulaiman *Journal of Industrial and Engineering Chemistry*, 2013 • Elsevier. Retrieved October 24, 2025, from <https://www.sciencedirect.com/science/article/pii/S1226086X1200233X>
- Atadashi, I., Aroua, M., energy, A. A.-R. and sustainable, & 2010, undefined. (n.d.). High quality biodiesel and its diesel engine application: a review. *Elsevier* IM Atadashi, MK Aroua, AA Aziz *Renewable and Sustainable Energy Reviews*, 2010 • Elsevier. Retrieved July 18, 2025, from <https://www.sciencedirect.com/science/article/pii/S1364032110000754>
- Ba, D., & Boyaci, I. H. (2007). Modeling and optimization I: Usability of response surface methodology. *Journal of Food Engineering*, 78(3), 836–845. <https://doi.org/10.1016/J.JFOODENG.2005.11.024>
- Balajii, M., & Niju, S. (2020). Banana peduncle – A green and renewable heterogeneous base catalyst for biodiesel production from Ceiba pentandra oil. *Renewable Energy*, 146, 2255–2269. <https://doi.org/10.1016/J.RENENE.2019.08.062>
- Balat, M., & Balat, H. (2010). Progress in biodiesel processing. *Applied Energy*, 87(6), 1815–1835. <https://doi.org/10.1016/J.APENERGY.2010.01.012>

- Balat, M., management, H. B.-E. conversion and, & 2008, undefined. (n.d.). A critical review of bio-diesel as a vehicular fuel. *ElsevierM Balat, H BalatEnergy Conversion and Management, 2008•Elsevier*. Retrieved July 23, 2025, from <https://www.sciencedirect.com/science/article/pii/S0196890408001192>
- Banković–Ilić, I., ... M. M.-... and S. E., & 2017, undefined. (n.d.). Application of nano CaO–based catalysts in biodiesel synthesis. *ElsevierIB Banković–Ilić, MR Miladinović, OS Stamenković, VB VeljkovićRenewable and Sustainable Energy Reviews, 2017•Elsevier*. Retrieved July 17, 2025, from <https://www.sciencedirect.com/science/article/pii/S1364032117300862>
- Banković-Ilić, I. B., Stamenković, O. S., & Veljković, V. B. (2012). Biodiesel production from non-edible plant oils. *Renewable and Sustainable Energy Reviews, 16*(6), 3621–3647. <https://doi.org/10.1016/J.RSER.2012.03.002>
- Banković-Ilić, I. B., Stojković, I. J., Stamenković, O. S., Veljkovic, V. B., & Hung, Y. T. (2014). Waste animal fats as feedstocks for biodiesel production. *Renewable and Sustainable Energy Reviews, 32*, 238–254. <https://doi.org/10.1016/J.RSER.2014.01.038>
- Bartholomew, D. (1981). Viewpoint - Vegetable oil fuel. *Journal of the American Oil Chemists Society, 58*(4), 286A-288A. <https://doi.org/10.1007/BF02541575/METRICS>
- Baş, D., engineering, İ. B.-J. of food, & 2007, undefined. (n.d.). Modeling and optimization I: Usability of response surface methodology. *ElsevierD Baş, İH BoyacıJournal of Food Engineering, 2007•Elsevier*. Retrieved October 23, 2025, from <https://www.sciencedirect.com/science/article/pii/S0260877405007843>

- Bell, S. (2012). Landscape: Pattern, perception and process. *Landscape: Pattern Perception and Process*, 1–350. <https://doi.org/10.4324/9780203120088>
- Bernardes, O. L., Bevilaqua, J. V., Leal, M. C. M. R., Freire, D. M. G., & Langone, M. A. P. (2007). Biodiesel fuel production by the transesterification reaction of soybean oil using immobilized lipase. *SpringerOL Bernardes, JV Bevilaqua, MCMR Leal, DMG Freire, MAP LangoneApplied Biochemistry and Biotechnology*, 2007•Springer, 137–140(1–12), 105–114. <https://doi.org/10.1007/S12010-007-9043-5>
- Bertrand, E., & Dussap, C.-G. (2022). *First Generation Bioethanol: Fundamentals—Definition, History, Global Production, Evolution*. 1–12. https://doi.org/10.1007/978-3-031-01241-9_1
- Betiku, E., Omilakin, O., Ajala, S., Energy, A. O.-, & 2014, undefined. (n.d.). Mathematical modeling and process parameters optimization studies by artificial neural network and response surface methodology: A case of non-edible neem. *ElsevierE Betiku, OR Omilakin, SO Ajala, AA Okeleye, AE Taiwo, BO SolomonEnergy*, 2014•Elsevier. Retrieved October 26, 2025, from <https://www.sciencedirect.com/science/article/pii/S0360544214005829>
- Bezerra, M., Santelli, R., Oliveira, E., Talanta, L. V.-, & 2008, undefined. (n.d.). Response surface methodology (RSM) as a tool for optimization in analytical chemistry. *ElsevierMA Bezerra, RE Santelli, EP Oliveira, LS Villar, LA EscaleiraTalanta*, 2008•Elsevier. Retrieved October 23, 2025, from <https://www.sciencedirect.com/science/article/pii/S0039914008004050>
- Bharadwaj, S., Ram, S., Pancha, I., for, S. M.-M. cultivation, & 2020, undefined. (n.d.). Recent trends in strain improvement for production of biofuels from microalgae. *Elsevier*. Retrieved August 2, 2025, from <https://www.sciencedirect.com/science/article/pii/B978012817536100014X>

Bharti, R., Singh, B., & Oraon, R. (2023). Synthesis of Sn-CaO as a bifunctional catalyst and its application for biodiesel production from waste cooking oil. *Biofuels*, 14(6), 607–617.

<https://doi.org/10.1080/17597269.2022.2161128>

bioenergy, A. D.-B. and, & 2009, undefined. (n.d.). Production of biodiesel fuels from linseed oil using methanol and ethanol in non-catalytic SCF conditions. *ElsevierA DemirbasBiomass and Bioenergy*, 2009•Elsevier. Retrieved July 31, 2025, from

<https://www.sciencedirect.com/science/article/pii/S0961953408001141>

Bohlouli, A., & Mahdavian, L. (2021). Catalysts used in biodiesel production: a review. *Taylor & Francis*, 12(8), 885–898. <https://doi.org/10.1080/17597269.2018.1558836>

Bokhari, A., Chuah, L., Yusup, S., ... J. K.-B., & 2016, undefined. (n.d.). Optimisation on pretreatment of rubber seed (*Hevea brasiliensis*) oil via esterification reaction in a hydrodynamic cavitation reactor. *Elsevier*. Retrieved July 17, 2025, from

<https://www.sciencedirect.com/science/article/pii/S0960852415011177>

Borges, M., Reviews, L. D.-R. and S. E., & 2012, undefined. (n.d.). Recent developments on heterogeneous catalysts for biodiesel production by oil esterification and transesterification reactions: A review. *ElsevierME Borges, L DíazRenewable and Sustainable Energy Reviews*, 2012•Elsevier. Retrieved October 24, 2025, from

<https://www.sciencedirect.com/science/article/pii/S1364032112000834>

Box, G., & Draper, N. (1987). *Empirical model-building and response surfaces*.

<https://psycnet.apa.org/record/1987-97236-000>

- Brask, J., Damstrup, M. L., Nielsen, P. M., Holm, H. C., Maes, J., & De Greyt, W. (2011). Combining enzymatic esterification with conventional alkaline transesterification in an integrated biodiesel process. *Springer J Brask, ML Damstrup, PM Nielsen, HC Holm, J Maes, W De Greyt Applied Biochemistry and Biotechnology, 2011•Springer, 163(7), 918–927.*
<https://doi.org/10.1007/S12010-010-9095-9>
- Brito, G., Chicon, M., Coelho, E., ... D. F.-J. of R., & 2020, undefined. (n.d.). Eco-green biodiesel production from domestic waste cooking oil by transesterification using LiOH into basic catalysts mixtures. *Pubs.Aip.Org*. Retrieved July 16, 2025, from
<https://pubs.aip.org/aip/jrse/article/12/4/043101/284946>
- Budhwani, A. A. A., Maqbool, A., Hussain, T., & Syed, M. N. (2019). Production of biodiesel by enzymatic transesterification of non-edible *Salvadora persica* (Pilu) oil and crude coconut oil in a solvent-free system. *Bioresources and Bioprocessing, 6(1), 1–9.*
<https://doi.org/10.1186/S40643-019-0275-3/TABLES/2>
- Canakci, M., ASAE, J. V. G.-T. of the, & 2003, undefined. (n.d.). A pilot plant to produce biodiesel from high free fatty acid feedstocks. *Elibrary.Asabe.Org M Canakci, J Van Gerpen Transactions of the ASAE, 2003•elibrary.Asabe.Org*. Retrieved July 23, 2025, from
<https://elibrary.asabe.org/abstract.asp?aid=13949>
- Canesin, E., Oliveira, C. de, ... M. M.-E. J. of, & 2014, undefined. (n.d.). Characterization of residual oils for biodiesel production. *Elsevier EA Canesin, CC de Oliveira, M Matsushita, LF Dias, MR Pedrao, NE de Souza Electronic Journal of Biotechnology, 2014•Elsevier*. Retrieved October 25, 2025, from
<https://www.sciencedirect.com/science/article/pii/S0717345813000080>

Chaemchuen, S., Zhou, K., & Verpoort, F. (2016). From Biogas to Biofuel: Materials Used for Biogas Cleaning to Biomethane. *ChemBioEng Reviews*, 3(6), 250–265.

<https://doi.org/10.1002/CBEN.201600016>

Chan, C., Yusoff, R., physicochemical, G. N.-I. extraction by, & 2017, undefined. (n.d.). An energy-based approach to scale up microwave-assisted extraction of plant bioactives. *Elsevier*.

Retrieved October 23, 2025, from

<https://www.sciencedirect.com/science/article/pii/B9780128115213000156>

Changmai, B., Van Lal Chhandama, M., Vanlalveni, C., Wheatley, A. E. H., & Rokhum, S. L.

(2022). Advances in Bifunctional Solid Catalysts for Biodiesel Production. *Biodiesel Production: Feedstocks, Catalysts, and Technologies*, 209–227.

<https://doi.org/10.1002/9781119771364.CH11>

Chaturvedi, S., Dave, P., Society, N. S.-J. of S. C., & 2012, undefined. (n.d.). Applications of nano-catalyst in new era. *ElsevierS Chaturvedi, PN Dave, NK ShahJournal of Saudi Chemical Society*, 2012•Elsevier.

Retrieved October 24, 2025, from

<https://www.sciencedirect.com/science/article/pii/S1319610311000305>

chemistry, A. G.-O. & biomolecular, & 2003, undefined. (n.d.). The utility of cyclodextrins in lipase-catalyzed transesterification in organic solvents: enhanced reaction rate and

enantioselectivity. *Pubs.Rsc.OrgA GhanemOrganic & Biomolecular Chemistry*,

2003•pubs.Rsc.Org. Retrieved July 23, 2025, from

<https://pubs.rsc.org/en/content/articlehtml/2003/ob/b301086d>

Chen, K., Wang, J., Dai, Y., Wang, P., ... C. L.-J. of the T., & 2013, undefined. (n.d.). Rice husk ash as a catalyst precursor for biodiesel production. *ElsevierKT Chen, JX Wang, YM Dai, PH*

- Wang, CY Liou, CW Nien, JS Wu, CC Chen *Journal of the Taiwan Institute of Chemical Engineers*, 2013 • Elsevier. Retrieved October 24, 2025, from <https://www.sciencedirect.com/science/article/pii/S1876107013000126>
- Chen, W. H., Lee, K. T., & Ong, H. C. (2019). Biofuel and Bioenergy Technology. *Energies* 2019, Vol. 12, Page 290, 12(2), 290. <https://doi.org/10.3390/EN12020290>
- Chisti, Y. (2007). Biodiesel from microalgae. *Biotechnology Advances*, 25(3), 294–306. <https://doi.org/10.1016/J.BIOTECHADV.2007.02.001>
- Choi, G., Um, H., Kim, M., Kim, Y., ... H. K.-... of microbiology and, & 2010, undefined. (n.d.). Isolation and characterization of ethanol-producing *Schizosaccharomyces pombe* CHFY0201. *Europepmc.Org* GW Choi, HJ Um, M Kim, Y Kim, HW Kang, BW Chung, YH Kim *Journal of Microbiology and Biotechnology*, 2010 • europepmc.Org. Retrieved May 13, 2025, from <https://europepmc.org/article/med/20467261>
- Christopher, L., Kumar, H., Energy, V. Z.-A., & 2014, undefined. (n.d.). Enzymatic biodiesel: Challenges and opportunities. *ElsevierLP Christopher, H Kumar, VP Zambare Applied Energy*, 2014 • Elsevier. Retrieved October 24, 2025, from <https://www.sciencedirect.com/science/article/pii/S0306261914000361>
- Chuah, L., Amin, M., Yusup, S., ... N. R.-J. of C., & 2016, undefined. (n.d.). Influence of green catalyst on transesterification process using ultrasonic-assisted. *ElsevierLF Chuah, MM Amin, S Yusup, NA Raman, A Bokhari, JJ Klemeš, MS Alnarabiji Journal of Cleaner Production*, 2016 • Elsevier. Retrieved July 15, 2025, from <https://www.sciencedirect.com/science/article/pii/S0959652616304589>

- Chuah, L., Klemeš, J., Yusup, S., ... A. B.-J. of cleaner, & 2017, undefined. (n.d.). A review of cleaner intensification technologies in biodiesel production. *Elsevier* LF Chuah, JJ Klemeš, S Yusup, A Bokhari, MM Akbar *Journal of Cleaner Production*, 2017•Elsevier. Retrieved July 15, 2025, from <https://www.sciencedirect.com/science/article/pii/S0959652616304723>
- Crabbe, E., Nolasco-Hipolito, C., ... G. K.-P., & 2001, undefined. (n.d.). Biodiesel production from crude palm oil and evaluation of butanol extraction and fuel properties. *Elsevier*. Retrieved July 31, 2025, from <https://www.sciencedirect.com/science/article/pii/S0032959201001789>
- da Silva, K. R. N., Corazza, M. Z., & Raposo, J. L. (2018). Renewable Energy Sources: A Sustainable Strategy for Biodiesel Productions. *Green Energy and Technology*, 0(9783319735511), 1–31. https://doi.org/10.1007/978-3-319-73552-8_1
- Dalvand, P., & Mahdavian, L. (2018). Calculation of the properties of biodiesel produced from castor seed by eggshell catalyst. *Taylor & Francis* P Dalvand, L Mahdavian *Biofuels*, 2018•Taylor & Francis, 9(6), 705–710. <https://doi.org/10.1080/17597269.2017.1302668>
- De Boer, K. (2010). *Optimised small scale reactor technology, a new approach for the Australian biodiesel industry*. <https://researchportal.murdoch.edu.au/esploro/outputs/doctoral/Optimised-small-scale-reactor-technology-a/991005543885107891>
- Demirbaş, A. (2002). Biodiesel from vegetable oils via transesterification in supercritical methanol. *Energy Conversion and Management*, 43(17), 2349–2356. [https://doi.org/10.1016/S0196-8904\(01\)00170-4](https://doi.org/10.1016/S0196-8904(01)00170-4)

- Demirbas, A. (2006). Biodiesel production via non-catalytic SCF method and biodiesel fuel characteristics. *Energy Conversion and Management*, 47(15–16), 2271–2282.
<https://doi.org/10.1016/J.ENCONMAN.2005.11.019>
- Demirbas, A., Sources, S. K.-E., A, P., & 2007, undefined. (2007). Biodiesel production facilities from vegetable oils and animal fats. *Taylor & Francis A Demirbas, S Karlioglu Energy Sources, Part A, 2007*•Taylor & Francis, 29(2), 133–141.
<https://doi.org/10.1080/009083190951320>
- Elkady, M. F., Zaatout, A., & Balbaa, O. (2015). Production of biodiesel from waste vegetable oil via KM micromixer. *Wiley Online Library MF Elkady, A Zaatout, O Balbaa Journal of Chemistry, 2015*•Wiley Online Library, 2015. <https://doi.org/10.1155/2015/630168>
- engineering, S. K.-R. surface methodology in, & 2021, undefined. (n.d.). Application of response surface methodology in food process modeling and optimization. *Intechopen.Com SW Kidane Response Surface Methodology in Engineering Science, 2021*•intechopen.Com. Retrieved October 23, 2025, from <https://www.intechopen.com/chapters/78667>
- Enguilo Gonzaga, V., Romero, R., Gómez-Espinosa, R. M., Romero, A., Martínez, S. L., & Natividad, R. (2021). Biodiesel Production from Waste Cooking Oil Catalyzed by a Bifunctional Catalyst. *ACS Omega*, 6(37), 24092–24105.
<https://doi.org/10.1021/ACSOMEGA.1C03586>
- Etim, A. O., Musonge, P., & Eloka-Eboka, A. C. (2020). Effectiveness of biogenic waste-derived heterogeneous catalysts and feedstock hybridization techniques in biodiesel production. *Wiley Online Library AO Etim, P Musonge, AC Eloka-Eboka Biofuels, Bioproducts and Biorefining, 2020*•Wiley Online Library, 14(3), 620–649. <https://doi.org/10.1002/BBB.2094>

- Farooq, M. A., Nóvoa, H., Araújo, A., & Tavares, S. M. O. (2016). An innovative approach for planning and execution of pre-experimental runs for Design of Experiments. *European Research on Management and Business Economics*, 22(3), 155–161.
<https://doi.org/10.1016/J.IEDEE.2014.12.003>
- Feuge, R., Society, A. G.-J. of the A. O. C., & 1949, undefined. (1949). Modification of vegetable oils. VII. Alkali catalyzed interesterification of peanut oil with ethanol. *SpringerRO Feuge, AT GrosJournal of the American Oil Chemists' Society, 1949•Springer*, 26(3), 97–102.
<https://doi.org/10.1007/BF02665167>
- Fitriana, N., Husin, H., Yanti, D., Pontas, K., Alam, P. N., & Ridho, M. (2018). Synthesis of K₂O/Zeolite catalysts by KOH impregnation for biodiesel production from waste frying oil. *Iopscience.Iop.OrgN Fitriana, H Husin, D Yanti, K Pontas, PN Alam, M RidhoIOP Conference Series: Materials Science and Engineering, 2018•iopscience.Iop.Org*.
<https://doi.org/10.1088/1757-899X/334/1/012011/META>
- Fraile, J., García, N., Mayoral, J., ... E. P.-A. C. A., & 2009, undefined. (n.d.). The influence of alkaline metals on the strong basicity of Mg–Al mixed oxides: the case of transesterification reactions. *ElsevierJM Fraile, N García, JA Mayoral, E Pires, L RoldánApplied Catalysis A: General, 2009•Elsevier*. Retrieved October 24, 2025, from
<https://www.sciencedirect.com/science/article/pii/S0926860X09003755>
- Fukuda, H., Kondo, A., & Noda, H. (2001). Biodiesel fuel production by transesterification of oils. *Journal of Bioscience and Bioengineering*, 92(5), 405–416. [https://doi.org/10.1016/S1389-1723\(01\)80288-7](https://doi.org/10.1016/S1389-1723(01)80288-7)

- Galadima, A. A., & Muraza, O. O. (2014). *Biodiesel production from algae by using heterogeneous catalysts: a critical review*. <https://doi.org/10.5555/20153065690>
- Goff, M. J., Bauer, N. S., Lopes, S., Sutterlin, W. R., & Suppes, G. J. (2004). Acid-catalyzed alcoholysis of soybean oil. *Wiley Online Library* MJ Goff, NS Bauer, S Lopes, WR Sutterlin, GJ Suppes. *Journal of the American Oil Chemists' Society*, 2004•*Wiley Online Library*, 81(4), 415–420. <https://doi.org/10.1007/S11746-004-0915-6>
- Guldhe, A., Moura, C., Singh, P., Rawat, I., Energy, E. M.-R., & 2017, undefined. (n.d.). Conversion of microalgal lipids to biodiesel using chromium-aluminum mixed oxide as a heterogeneous solid acid catalyst. *Elsevier* A Guldhe, CVR Moura, P Singh, I Rawat, EM Moura, Y Sharma, F Bux. *Renewable Energy*, 2017•*Elsevier*. Retrieved October 24, 2025, from <https://www.sciencedirect.com/science/article/pii/S0960148116311107>
- Hannon, M., Gimpel, J., Tran, M., Rasala, B., & Mayfield, S. (2010). Biofuels from algae: challenges and potential. *Taylor & Francis* M Hannon, J Gimpel, M Tran, B Rasala, S Mayfield. *Biofuels*, 2010•*Taylor & Francis*, 1(5), 763–784. <https://doi.org/10.4155/BFS.10.44>
- Hassani, M., Najafpour, G., Sci, M. M.-J. M. E., & 2016, undefined. (n.d.). Transesterification of waste cooking oil to biodiesel using γ -alumina coated on zeolite pellets. *Researchgate.Net* M Hassani, GD Najafpour, M Mohammadi. *J Mater Environ Sci*, 2016•*researchgate.Net*. Retrieved October 24, 2025, from https://www.researchgate.net/profile/Ghasem-Najafpour/publication/297704437_Transesterification_of_Waste_Cooking_Oil_to_Biodiesel_using_g-alumina_Coated_on_Zeolite_Pellets/links/56e0758d08ae9b93f79c320b/Transesterification-of-Waste-Cooking-Oil-to-Biodiesel-using-g-alumina-Coated-on-Zeolite-Pellets.pdf

Hazniza, A., Osman, A., SCIENCE, H. G.-... A. F., & 2006, undefined. (n.d.). Optimisation of formulation in development of candied musk lime peel using response surface methodology (RSM). *Researchgate.Net* A Hazniza, A Osman, HM Ghazali, RA Rahman, S Yusof *JOURNAL OF TROPICAL AGRICULTURE AND FOOD SCIENCE*, 2006•*researchgate.Net*. Retrieved October 23, 2025, from https://www.researchgate.net/profile/Hazniza_Adnan/publication/277802791_Optimisation_of_Enzyme_Aided_Peeling_of_Musk_Lime_Citrus_Mitis_B_and_Development_of_Its_Candied_Peel/links/59dec417aca27247d7946300/Optimisation-of-Enzyme-Aided-Peeling-of-Musk-Lime-Citrus-Mitis-B-and-Development-of-Its-Candied-Peel.pdf

Helwani, Z., Othman, M., Aziz, N., ... J. K.-A. C. A., & 2009, undefined. (n.d.). Solid heterogeneous catalysts for transesterification of triglycerides with methanol: a review. *Elsevier* Z Helwani, MR Othman, N Aziz, J Kim, WJN Fernando *Applied Catalysis A: General*, 2009•*Elsevier*. Retrieved October 24, 2025, from <https://www.sciencedirect.com/science/article/pii/S0926860X09003652>

Higman, E. B., Higman, H. C., Chortyk, O. T., & Schmeltz, I. (1973). Studies on the Thermal Degradation of Naturally Occurring Materials. II. Products from the Pyrolysis of Triglycerides at 400°. *Journal of Agricultural and Food Chemistry*, 21(2), 202–204. https://doi.org/10.1021/JF60186A030/ASSET/JF60186A030.FP.PNG_V03

Inambao, Freddie. (2021). *Bioethanol Technologies*.

https://books.google.com/books/about/Bioethanol_Technologies.html?id=AztbEAAAQBAJ

Issariyakul, T., Reviews, A. D.-R. and S. E., & 2014, undefined. (n.d.). Biodiesel from vegetable oils. *Elsevier* T Issariyakul, AK Dalai *Renewable and Sustainable Energy Reviews*,

2014•Elsevier. Retrieved October 24, 2025, from

<https://www.sciencedirect.com/science/article/pii/S1364032113007508>

Jankovic, A., Chaudhary, G., & Goia, F. (2021). Designing the design of experiments (DOE) – An investigation on the influence of different factorial designs on the characterization of complex systems. *Energy and Buildings*, 250, 111298.

<https://doi.org/10.1016/J.ENBUILD.2021.111298>

Jitjamnong, J., Thunyaratchatanon, C., Luengnaruemitchai, A., Kongrit, N., Kasetsomboon, N., Sopajarn, A., Chuaykarn, N., & Khantikulanon, N. (2021). Response surface optimization of biodiesel synthesis over a novel biochar-based heterogeneous catalyst from cultivated (*Musa sapientum*) banana peels. *Biomass Conversion and Biorefinery*, 11(6), 2795–2811.

<https://doi.org/10.1007/S13399-020-00655-8/METRICS>

Joshi, S., Hadiya, P., Shah, M., and, A. S.-B. E., & 2019, undefined. (2019). Techno-economical and experimental analysis of biodiesel production from used cooking oil. *SpringerS Joshi, P Hadiya, M Shah, A SircarBiophysical Economics and Resource Quality*, 2019•Springer, 4(1).

<https://doi.org/10.1007/S41247-018-0050-7>

Jürgensen, L., Ehimen, E. A., Born, J., & Holm-Nielsen, J. B. (n.d.). *A combination anaerobic digestion scheme for biogas production from dairy effluentdCSTR and ABR, and biogas upgrading*. <https://doi.org/10.1016/j.biombioe.2017.04.007>

Karmakar, A., Karmakar, S., technology, S. M.-B., & 2010, undefined. (n.d.). Properties of various plants and animals feedstocks for biodiesel production. *ElsevierA Karmakar, S Karmakar, S MukherjeeBioresource Technology*, 2010•Elsevier. Retrieved July 21, 2025, from

<https://www.sciencedirect.com/science/article/pii/S0960852410007650>

Kaur, B., & Kaur, R. (2013). Application of Response Surface Methodology for Optimizing

Arginine Deiminase Production Medium for *Enterococcus faecium* sp. GR7. *Wiley Online*

Library B Kaur, R Kaur *The Scientific World Journal*, 2013 • *Wiley Online Library*, 2013.

<https://doi.org/10.1155/2013/892587>

Khan, H., Iqbal, T., Yasin, S., Ali, C., Catalysts, M. A.-, & 2021, undefined. (n.d.). Application of

agricultural waste as heterogeneous catalysts for biodiesel production. *Mdpi.Com* HM Khan, T

Iqbal, S Yasin, CH Ali, MM Abbas, MA Jamil, A Hussain, ME M. Soudagar *Catalysts*,

2021 • *mdpi.Com*. Retrieved July 16, 2025, from <https://www.mdpi.com/2073-4344/11/10/1215>

Khan, M. A. H., Bonifacio, S., Clowes, J., Foulds, A., Holland, R., Matthews, J. C., Percival, C. J.,

& Shallcross, D. E. (2021). Investigation of Biofuel as a Potential Renewable Energy Source.

Atmosphere 2021, Vol. 12, Page 1289, 12(10), 1289.

<https://doi.org/10.3390/ATMOS12101289>

Khuri, A., reviews, S. M.-W. interdisciplinary, & 2010, undefined. (2010). Response surface

methodology. *Wiley Online Library* AI Khuri, S Mukhopadhyay *Wiley Interdisciplinary*

Reviews: Computational Statistics, 2010 • *Wiley Online Library*, 2(2), 128–149.

<https://doi.org/10.1002/WICS.73>

Knothe, G., technology, K. S.-B., & 2009, undefined. (n.d.). A comparison of used cooking oils: a

very heterogeneous feedstock for biodiesel. *Elsevier* G Knothe, KR Steidley *Bioresource*

Technology, 2009 • *Elsevier*. Retrieved August 1, 2025, from

<https://www.sciencedirect.com/science/article/pii/S0960852409006981>

Kulkarni, M., chemistry, A. D.-I. & engineering, & 2006, undefined. (2006). Waste cooking oil an

economical source for biodiesel: a review. *ACS Publications* MG Kulkarni, AK Dalai *Industrial*

& Engineering Chemistry Research, 2006•ACS Publications, 45(9), 2901–2913.

<https://doi.org/10.1021/IE0510526>

Kumar, A., Kumar, K., Kaushik, N., Sharma, S., & Mishra, S. (2010). Renewable energy in India: Current status and future potentials. *Renewable and Sustainable Energy Reviews, 14(8), 2434–2442.* <https://doi.org/10.1016/J.RSER.2010.04.003>

Kumar, D., Kumar, G., Sonochemistry, C. S.-U., & 2010, undefined. (n.d.). Fast, easy ethanolysis of coconut oil for biodiesel production assisted by ultrasonication. *ElsevierD Kumar, G Kumar, CP SinghUltrasonics Sonochemistry, 2010•Elsevier.* Retrieved July 31, 2025, from <https://www.sciencedirect.com/science/article/pii/S1350417709001825>

Kumar, D., Singh, B., Banerjee, A., production, S. C.-J. of cleaner, & 2018, undefined. (n.d.). Cement wastes as transesterification catalysts for the production of biodiesel from Karanja oil. *Elsevier.* Retrieved October 24, 2025, from <https://www.sciencedirect.com/science/article/pii/S0959652618304347>

Lapuerta, M., ... O. A.-P. in energy and, & 2008, undefined. (n.d.). Effect of biodiesel fuels on diesel engine emissions. *Elsevier.* Retrieved July 21, 2025, from <https://www.sciencedirect.com/science/article/pii/S0360128507000421>

Lapuerta, M., Armas, O., & Rodríguez-Fernández, J. (2008). Effect of biodiesel fuels on diesel engine emissions. *Progress in Energy and Combustion Science, 34(2), 198–223.* <https://doi.org/10.1016/J.PECS.2007.07.001>

Lee, C.-H. (2012). Renewable and Sustainable Energy Reviews. *Coastal and Ocean, 5(2), 62–70.*

- Lee, S. L., Wong, Y. C., Tan, Y. P., & Yew, S. Y. (2015). Transesterification of palm oil to biodiesel by using waste obtuse horn shell-derived CaO catalyst. *Energy Conversion and Management*, 93, 282–288. <https://doi.org/10.1016/J.ENCONMAN.2014.12.067>
- Li, Y., Horsman, M., Wu, N., Lan, C. Q., & Dubois-Calero, N. (2012). Biofuels from microalgae. *Microalgae for Biofuel Production and CO*, 24(4), 65–86. <https://doi.org/10.1021/BP070371K;WGROU:STRING:PUBLICATION>
- Li, Y., & Khanal, S. (2016). *Bioenergy: principles and applications*. https://books.google.com/books?hl=en&lr=&id=hZRZDgAAQBAJ&oi=fnd&pg=PR19&ots=O8MYQiP8lk&sig=yphVoL_h2tHhanPvLBgexOScCjM
- Likozar, B., energy, J. L.-A., & 2014, undefined. (n.d.). Transesterification of canola, palm, peanut, soybean and sunflower oil with methanol, ethanol, isopropanol, butanol and tert-butanol to biodiesel: Modelling of. *ElsevierB Likozar, J LevecApplied Energy, 2014•Elsevier*. Retrieved July 23, 2025, from <https://www.sciencedirect.com/science/article/pii/S0306261914001901>
- LiPing, Z. Z., BoYang, S. S., & Zhong, X. X. (2010). *Kinetics of transesterification of palm oil and dimethyl carbonate for biodiesel production at the catalysis of heterogeneous base catalyst*. <https://doi.org/10.5555/20103263420>
- Liu, Y., Lotero, E., Chemical, J. G. J.-J. of M. C. A., & 2006, undefined. (n.d.). Effect of water on sulfuric acid catalyzed esterification. *ElsevierY Liu, E Lotero, JG Goodwin JrJournal of Molecular Catalysis A: Chemical, 2006•Elsevier*. Retrieved July 23, 2025, from <https://www.sciencedirect.com/science/article/pii/S1381116905007004>

- Lotti, M., Pleiss, J., Valero, F., & Ferrer, P. (2018). Enzymatic production of biodiesel: strategies to overcome methanol inactivation. *Wiley Online Library* M Lotti, J Pleiss, F Valero, P Ferrer *Biotechnology Journal*, 2018 • *Wiley Online Library*, 13(5).
<https://doi.org/10.1002/BIOT.201700155>
- Ma, F., & Hanna, M. A. (1999a). Biodiesel production: a review. *Bioresource Technology*, 70(1), 1–15. [https://doi.org/10.1016/S0960-8524\(99\)00025-5](https://doi.org/10.1016/S0960-8524(99)00025-5)
- Ma, F., & Hanna, M. A. (1999b). Biodiesel production: a review. *Bioresource Technology*, 70(1), 1–15. [https://doi.org/10.1016/S0960-8524\(99\)00025-5](https://doi.org/10.1016/S0960-8524(99)00025-5)
- MacEiras, R., Cancela, A., ... M. V.-C. E., & 2010, undefined. (n.d.). Enzymatic alholysis for biodiesel production from waste cooking oil. *Hero.Epa.Gov*. Retrieved October 24, 2025, from https://hero.epa.gov/hero/index.cfm/reference/details/reference_id/1116511
- Maceiras, R., Rodri, M., Cancela, A., Urréjola, S., energy, A. S.-A., & 2011, undefined. (n.d.). Macroalgae: raw material for biodiesel production. *Elsevier* R Maceiras, M Rodri, A Cancela, S Urréjola, A Sánchez *Applied Energy*, 2011 • *Elsevier*. Retrieved July 21, 2025, from <https://www.sciencedirect.com/science/article/pii/S0306261910004903>
- Mahdavi, M., Abedini, E., Advances, A. hosein D.-R., & 2015, undefined. (n.d.). Biodiesel synthesis from oleic acid by nano-catalyst (ZrO 2/Al 2 O 3) under high voltage conditions. *Pubs.Rsc.Org*. Retrieved July 31, 2025, from <https://pubs.rsc.org/en/content/articlehtml/2015/ra/c5ra07081c>
- Maheshwari, P., Haider, M. B., Yusuf, M., Klemeš, J. J., Bokhari, A., Beg, M., Al-Othman, A., Kumar, R., & Jaiswal, A. K. (2022). A review on latest trends in cleaner biodiesel production:

Role of feedstock, production methods, and catalysts. *Journal of Cleaner Production*, 355, 131588. <https://doi.org/10.1016/J.JCLEPRO.2022.131588>

Mahfud, M., Suryanto, A., Qadariyah, L., Suprpto, S., & Kusuma, H. S. (2018). Production of methyl ester from coconut oil using microwave: Kinetic of transesterification reaction using heterogeneous CaO catalyst. *Korean Chemical Engineering Research*, 56(2), 275–280. <https://doi.org/10.9713/KCER.2018.56.2.275>

Management, A. D.-E. conversion and, & 2009, undefined. (2008). Progress and recent trends in biodiesel fuels. *ElsevierA DemirbasEnergy Conversion and Management*, 2009•Elsevier. <https://doi.org/10.1016/j.enconman.2008.09.001>

Management, M. B.-E. conversion and, & 2011, undefined. (2011). Potential alternatives to edible oils for biodiesel production—A review of current work. *ElsevierM BalatEnergy Conversion and Management*, 2011•Elsevier, 52, 1479–1492. <https://doi.org/10.1016/j.enconman.2010.10.011>

Mardhiah, H., Ong, H., Masjuki, H., ... S. L.-... and sustainable energy, & 2017, undefined. (n.d.). A review on latest developments and future prospects of heterogeneous catalyst in biodiesel production from non-edible oils. *ElsevierHH Mardhiah, HC Ong, HH Masjuki, S Lim, HV LeeRenewable and Sustainable Energy Reviews*, 2017•Elsevier. Retrieved October 24, 2025, from <https://www.sciencedirect.com/science/article/pii/S1364032116305329>

Mat Aron, N. S., Khoo, K. S., Chew, K. W., Show, P. L., Chen, W. H., & Nguyen, T. H. P. (2020). Sustainability of the four generations of biofuels – A review. *International Journal of Energy Research*, 44(12), 9266–9282. <https://doi.org/10.1002/ER.5557;WGROU:STRING:PUBLICATION>

- Matemilola, S., Fadeyi, O., & Sijuade, T. (2023). Paris Agreement. *Encyclopedia of Sustainable Management*, 2555–2559. https://doi.org/10.1007/978-3-031-25984-5_516
- Mazerolles, G., Mathieu, D., A, A. S.-J. of C., & 1989, undefined. (n.d.). Computer-assisted optimization with nemrod software. *ElsevierG Mazerolles, D Mathieu, AM SiouffiJournal of Chromatography A, 1989•Elsevier*. Retrieved October 23, 2025, from <https://www.sciencedirect.com/science/article/pii/S0021967301891548>
- Meher, L. C., Vidya Sagar, D., & Naik, S. N. (2006). Technical aspects of biodiesel production by transesterification—a review. *Renewable and Sustainable Energy Reviews*, 10(3), 248–268. <https://doi.org/10.1016/J.RSER.2004.09.002>
- Meher, L., Churamani, C., Arif, M., ... Z. A.-... and S. E., & 2013, undefined. (n.d.). Jatropha curcas as a renewable source for bio-fuels—A review. *ElsevierLC Meher, CP Churamani, MD Arif, Z Ahmed, SN NaikRenewable and Sustainable Energy Reviews, 2013•Elsevier*. Retrieved October 24, 2025, from <https://www.sciencedirect.com/science/article/pii/S1364032113003687>
- Meher, L., Sagar, D., energy, S. N.-R. and sustainable, & 2006, undefined. (n.d.). Technical aspects of biodiesel production by transesterification—a review. *ElsevierLC Meher, DV Sagar, SN NaikRenewable and Sustainable Energy Reviews, 2006•Elsevier*. Retrieved July 23, 2025, from <https://www.sciencedirect.com/science/article/pii/S1364032104001236>
- Meriatna, Husin, H., Riza, M., Faisal, M., Ahmadi, & Sulastri. (2023). Biodiesel production using waste banana peel as renewable base catalyst. *Materials Today: Proceedings*, 87, 214–217. <https://doi.org/10.1016/J.MATPR.2023.02.400>

- Metsoviti, M., Papapolymerou, G., Plants, I. K.-, & 2019, undefined. (n.d.). Comparison of growth rate and nutrient content of five microalgae species cultivated in greenhouses. *Mdpi.ComMN Metsoviti, G Papapolymerou, IT Karapanagiotidis, N KatsoulasPlants, 2019•mdpi.Com*. Retrieved July 31, 2025, from <https://www.mdpi.com/2223-7747/8/8/279>
- Mhetras, N., & Gokhale, D. (2025). Sustainable biodiesel production: importance of feedstock resources and production methods. *RSC Advances, 15*(33), 26739. <https://doi.org/10.1039/D5RA03084F>
- Ming, L., Ghazali, H., Chemistry, C. L.-F., & 1999, undefined. (n.d.). Use of enzymatic transesterified palm stearin-sunflower oil blends in the preparation of table margarine formulation. *ElsevierLO Ming, HM Ghazali, CC LetFood Chemistry, 1999•Elsevier*. Retrieved July 23, 2025, from <https://www.sciencedirect.com/science/article/pii/S0308814698000831>
- Mishra, V. K., & Goswami, R. (2018). A review of production, properties and advantages of biodiesel. *Biofuels, 9*(2), 273–289. <https://doi.org/10.1080/17597269.2017.1336350>
- Mohandass, R., Ashok, K., Selvaraju, A., & Rajagopan, S. (n.d.). *Homogeneous Catalysts used in Biodiesel Production: A Review*. Retrieved July 16, 2025, from <http://www.ijert.org>
- Mojib Zahraee, S., Hatami, M., Yusof, N. M., Rohani, J. M., & Ziaei, F. (2013). Combined use of design of experiment and computer simulation for resources level determination in concrete pouring process. *Journals.Utm.MySM Zahraee, M Hatami, NM Yusof, JM Rohani, F ZiaeiJurnal Teknologi (Sciences & Engineering), 2013•journals.Utm.My, 64, 2180–3722*. <https://journals.utm.my/jurnalteknologi/article/view/1315>

- Moravvej, Z., Makarem, M., feedstocks, M. R. generation of, & 2019, undefined. (n.d.). The fourth generation of biofuel. *Elsevier*. Retrieved August 1, 2025, from <https://www.sciencedirect.com/science/article/pii/B9780128151624000203>
- Murugesan, A., Umarani, C., ... T. C.-... and S. E., & 2009, undefined. (n.d.). Production and analysis of bio-diesel from non-edible oils—a review. *Elsevier* A Murugesan, C Umarani, TR Chinnusamy, M Krishnan, R Subramanian, N Neduzchezhain *Renewable and Sustainable Energy Reviews*, 2009 • Elsevier. Retrieved July 23, 2025, from <https://www.sciencedirect.com/science/article/pii/S1364032108000294>
- Myers, R. H. (1999). Response Surface Methodology—Current Status and Future Directions. *Journal of Quality Technology*, 31(1), 30–44. <https://doi.org/10.1080/00224065.1999.11979891>
- Naveenkumar, R., Technology, G. B.-B., & 2020, undefined. (n.d.). Optimization and techno-economic analysis of biodiesel production from *Calophyllum inophyllum* oil using heterogeneous nanocatalyst. *Elsevier* R Naveenkumar, G Baskar *Bioresource Technology*, 2020 • Elsevier. Retrieved October 26, 2025, from <https://www.sciencedirect.com/science/article/pii/S096085242031124X>
- Niphadkar, S., Bagade, P., & Ahmed, S. (2018). Bioethanol production: insight into past, present and future perspectives. *Biofuels*, 9(2), 229–238. <https://doi.org/10.1080/17597269.2017.1334338>;CSUBTYPE:STRING:SPECIAL;PAGE:STRING:ARTICLE/CHAPTER
- Noureddini, H., Harkey, D., & Medikonduru, V. (1998). A continuous process for the conversion of vegetable oils into methyl esters of fatty acids. *Springer* H Noureddini, D Harkey, V

Medikonduru *Journal of the American Oil Chemists' Society*, 1998 • *Springer*, 75(12), 1775–1783. <https://doi.org/10.1007/S11746-998-0331-1>

Ong, H., Tiong, Y., Goh, B., ... Y. G.-E. C. and, & 2021, undefined. (n.d.). Recent advances in biodiesel production from agricultural products and microalgae using ionic liquids: Opportunities and challenges. *Elsevier* HC Ong, YW Tiong, BHH Goh, YY Gan, M Mofijur, IMR Fattah, CT Chong, MA Alam, HV Lee *Energy Conversion and Management*, 2021 • *Elsevier*. Retrieved July 17, 2025, from <https://www.sciencedirect.com/science/article/pii/S0196890420311742>

Owunna, T., Rev., E. O.-J. E. Res., & 2022, undefined. (n.d.). Overview of the Benefits and Drawbacks of Renewable Energy in Nigeria. *Academia.Edu* TA Owunna, EI Obeagu *J. Energy Res. Rev.*, 2022 • *academia.Edu*. Retrieved May 12, 2025, from https://www.academia.edu/download/108616493/sciencedomain_2C_Obeagu1232022JENRR92294.pdf_filename_UTF-8sciencedomain_2C_Obeagu1232022JENRR92294.pdf

Owusu, P. A., & Asumadu-Sarkodie, S. (2016). A review of renewable energy sources, sustainability issues and climate change mitigation. *Taylor & Francis* PA Owusu, S Asumadu-Sarkodie *Cogent Engineering*, 2016 • *Taylor & Francis*, 3(1). <https://doi.org/10.1080/23311916.2016.1167990>

Oyedepo, S. O. (2012). Energy and sustainable development in Nigeria: The way forward. *Energy, Sustainability and Society*, 2(1), 1–17. <https://doi.org/10.1186/2192-0567-2-15/TABLES/9>

Pais, M. S., Peretta, I. S., Yamanaka, K., & Pinto, E. R. (2014). Factorial design analysis applied to the performance of parallel evolutionary algorithms. *Springer* MS Pais, IS Peretta, K

Yamanaka, ER Pinto *Journal of the Brazilian Computer Society*, 2014•Springer, 20(1), 1–17.

<https://doi.org/10.1186/1678-4804-20-6>

Perea-Moreno, A.-J., & Kalak, T. (2023). Potential Use of Industrial Biomass Waste as a Sustainable Energy Source in the Future. *Energies* 2023, Vol. 16, Page 1783, 16(4), 1783.

<https://doi.org/10.3390/EN16041783>

Petro Chem Eng, P. J. (2023). *Petroleum & Petrochemical Engineering Journal Committed to Create Value for Researchers Recent Advances in Biowaste-Derived Bifunctional Catalysts in Biodiesel Production: A Mini-Review Recent Advances in Biowaste-Derived Bifunctional Catalysts in Biodiesel Production: A Mini-Review*. <https://doi.org/10.23880/ppej-16000352>

Pienkos, P., Biofuels, A. D.-, Biorefining, B. and, & 2009, undefined. (2009). The promise and challenges of microalgal-derived biofuels. *Wiley Online Library* PT Pienkos, AL Darzins *Biofuels, Bioproducts and Biorefining: Innovation for a*, 2009•Wiley Online Library, 3(4), 431–440. <https://doi.org/10.1002/BBB.159>

Pikula, K., Zakharenko, A., Stratidakis, A., Razgonova, M., Nosyrev, A., Mezhuev, Y., Tsatsakis, A., & Golokhvast, K. (2020a). The advances and limitations in biodiesel production: feedstocks, oil extraction methods, production, and environmental life cycle assessment. *Green Chemistry Letters and Reviews*, 13(4), 11–30.

<https://doi.org/10.1080/17518253.2020.1829099>;JOURNAL:JOURNAL:TGCL20;REQUEST EDJOURNAL:JOURNAL:TGCL20;PAGE:STRING:ARTICLE/CHAPTER

Pikula, K., Zakharenko, A., Stratidakis, A., Razgonova, M., Nosyrev, A., Mezhuev, Y., Tsatsakis, A., & Golokhvast, K. (2020b). The advances and limitations in biodiesel production: feedstocks, oil extraction methods, production, and environmental life cycle assessment. *Green*

Chemistry Letters and Reviews, 13(4), 11–30.

<https://doi.org/10.1080/17518253.2020.1829099>;JOURNAL:JOURNAL:TGCL20;REQUESTEDJOURNAL:JOURNAL:TGCL20;PAGE:STRING:ARTICLE/CHAPTER

Polburee, P., Yongmanitchai, W., biology, N. L.-F., & 2015, undefined. (n.d.). Characterization of oleaginous yeasts accumulating high levels of lipid when cultivated in glycerol and their potential for lipid production from biodiesel-derived crude. *Elsevier*. Retrieved May 13, 2025, from <https://www.sciencedirect.com/science/article/pii/S1878614615001683>

Pooja, S., Anbarasan, B., Ponnusami, V., Energy, A. A.-R., & 2021, undefined. (n.d.). Efficient production and optimization of biodiesel from kapok (*Ceiba pentandra*) oil by lipase transesterification process: Addressing positive environmental impact. *ElsevierS Pooja, B Anbarasan, V Ponnusami, A ArumugamRenewable Energy, 2021•Elsevier*. Retrieved July 15, 2025, from <https://www.sciencedirect.com/science/article/pii/S0960148120317961>

Prasad, S., Dhanya, M., Gupta, N., Arch, A. K.-B. C., & 2012, undefined. (n.d.). Biofuels from biomass: a sustainable alternative to energy and environment. *Researchgate.NetS Prasad, MS Dhanya, N Gupta, A KumarBiochem Cell Arch, 2012•researchgate.Net*. Retrieved May 13, 2025, from https://www.researchgate.net/profile/Shiv-Prasad-3/publication/255792266_Biofuels_from_biomass_A_sustainable_alternative_to_energy_and_environment/data/5b94e75492851c78c402761a/Biofuels-from-biomass-a-sustainable-alternative-to-energy-and-environment.pdf

Qin, S., Sun, Y., Meng, X., & Zhang, S. (2010). Production and Analysis of Biodiesel from Non-Edible Seed Oil of *Pistacia Chinensis*. *Journals.Sagepub.Com*, 28(1), 37–46.

<https://doi.org/10.1260/0144-5987.28.1.37>

Raissi, S., science, R. F.-W. academy of, Engineering, undefined, & 2009, undefined. (n.d.).

Statistical process optimization through multi-response surface methodology.

Researchgate.Net S Raissi, RE Farsani World Academy of Science, Engineering and

Technology, 2009•*researchgate.Net*. Retrieved October 23, 2025, from

<https://www.researchgate.net/profile/Sadigh->

Raissi/publication/289199318_Statistical_process_optimization_Through_multi-

response_surface_methodology/links/5989c7a6aca27266adae00ca/Statistical-process-

optimization-Through-multi-response-surface-methodology.pdf

Reji, M., Res, R. K.-I. J. Microbiol., & 2022, undefined. (n.d.). Response surface methodology

(RSM): An overview to analyze multivariate data. *Academia.Edu* M Reji, R Kumar Indian J.

Microbiol. Res, 2022•*academia.Edu*. Retrieved October 23, 2025, from

<https://www.academia.edu/download/101381601/18202.pdf>

Reksowardojo, I. K., Lubis, I. H., Manggala, W., Brodjonegoro, T. P., Soerawidjaja, T. H.,

Arismunandar, W., Dung, N. N., & Ogawa, H. (2007). Performance and Exhaust Gas

Emissions of Using Biodiesel Fuel from Physic Nut (*Jatropha Curcas L.*) Oil on a Direct

Injection Diesel Engine (DI). *SAE Technical Papers*. <https://doi.org/10.4271/2007-01-2025>

Reviews, E. M.-C. S., & 2013, undefined. (n.d.). Immobilisation of enzymes on mesoporous silicate

materials. *Pubs.Rsc.Org E Magner Chemical Society Reviews*, 2013•*pubs.Rsc.Org*. Retrieved

October 24, 2025, from <https://pubs.rsc.org/en/content/articlehtml/2013/cs/c2cs35450k>

Rizwanul Fattah, I. M., Ong, H. C., Mahlia, T. M. I., Mofijur, M., Silitonga, A. S., Ashrafur

Rahman, S. M., & Ahmad, A. (2020). State of the Art of Catalysts for Biodiesel Production.

Frontiers in Energy Research, 8, 546060. <https://doi.org/10.3389/FENRG.2020.00101/XML>

Rodionova, M., Poudyal, R., ... I. T.-I. J. of, & 2017, undefined. (n.d.). Biofuel production:

Challenges and opportunities. *Elsevier* MV Rodionova, RS Poudyal, I Tiwari, RA Voloshin, SK Zharmukhamedov, HG Nam *International Journal of Hydrogen Energy*, 2017 • Elsevier.

Retrieved July 15, 2025, from

<https://www.sciencedirect.com/science/article/pii/S0360319916334139>

Rostamiyan, Y., Fereidoon, A., Design, M. R.-M. &, & 2015, undefined. (n.d.). Experimental and

optimizing flexural strength of epoxy-based nanocomposite: Effect of using nano silica and nano clay by using response surface design. *Elsevier* Y Rostamiyan, A Fereidoon, M

Rezaeiashtiyani, AH Mashhadzadeh, A Salmankhani *Materials & Design*, 2015 • Elsevier.

Retrieved October 23, 2025, from

<https://www.sciencedirect.com/science/article/pii/S026130691401005X>

Roy, T., Sahani, S., Production, Y. S.-J. of C., & 2020, undefined. (n.d.). Study on kinetics-

thermodynamics and environmental parameter of biodiesel production from waste cooking oil and castor oil using potassium modified ceria oxide. *Elsevier* T Roy, S Sahani, YC

Sharma *Journal of Cleaner Production*, 2020 • Elsevier. Retrieved July 15, 2025, from

<https://www.sciencedirect.com/science/article/pii/S0959652619340363>

Royon, D., Daz, M., Ellenrieder, G., technology, S. L.-B., & 2007, undefined. (2007). Enzymatic

production of biodiesel from cotton seed oil using t-butanol as a solvent. *Elsevier* D Royon, M Daz, G Ellenrieder, S Locatelli *Bioresource Technology*, 2007 • Elsevier, 98, 648–653.

<https://doi.org/10.1016/j.biortech.2006.02.021>

Sahar, Sadaf, S., Iqbal, J., Ullah, I., Bhatti, H. N., Nouren, S., Habib-ur-Rehman, Nisar, J., & Iqbal,

M. (2018). Biodiesel production from waste cooking oil: An efficient technique to convert

waste into biodiesel. *Sustainable Cities and Society*, 41, 220–226.

<https://doi.org/10.1016/J.SCS.2018.05.037>

Sahoo, P., engineering, T. B.-M. and manufacturing, & 2012, undefined. (n.d.). ANN modelling of fractal dimension in machining. *Elsevier*. Retrieved October 23, 2025, from

<https://www.sciencedirect.com/science/article/pii/B9780857091505500054>

Sai, B. A. V. S. L., Subramaniapillai, N., Khadhar Mohamed, M. S. B., & Narayanan, A. (2020).

Optimization of continuous biodiesel production from rubber seed oil (RSO) using calcined eggshells as heterogeneous catalyst. *Journal of Environmental Chemical Engineering*, 8(1),

103603. <https://doi.org/10.1016/J.JECE.2019.103603>

Salvi, B., reviews, N. P.-R. and sustainable energy, & 2012, undefined. (n.d.). Biodiesel resources and production technologies—A review. *ElsevierBL Salvi, NL PanwarRenewable and*

Sustainable Energy Reviews, 2012•Elsevier. Retrieved July 18, 2025, from

<https://www.sciencedirect.com/science/article/pii/S136403211200233X>

Schuchardt, U., Sercheli, R., Brazilian, R. V.-J. of the, & 1998, undefined. (1998).

Transesterification of vegetable oils: a review. *SciELO BrasilU Schuchardt, R Sercheli, RM VargasJournal of the Brazilian Chemical Society*, 1998•SciELO Brasil.

<https://www.scielo.br/j/jbchs/a/NFpfXWp4jyZq9WPMZ8N8pWm/?lang=en>

Schwab, A., Bagby, M., Fuel, B. F.-, & 1987, undefined. (n.d.). Preparation and properties of diesel fuels from vegetable oils. *ElsevierAW Schwab, MO Bagby, B FreedmanFuel*, 1987•Elsevier.

Retrieved July 23, 2025, from

<https://www.sciencedirect.com/science/article/pii/0016236187901840>

- Schwab, A. W., Dykstra, G. J., Selke, E., Sorenson, S. C., & Pryde, E. H. (1988). Diesel fuel from thermal decomposition of soybean oil. *Wiley Online Library*AW Schwab, GJ Dykstra, E Selke, SC Sorenson, EH Pryde*Journal of the American Oil Chemists' Society*, 1988•*Wiley Online Library*, 65(11), 1781–1786. <https://doi.org/10.1007/BF02542382>
- Shafinaz, A. I., & Embong, N. N. H. (2019). *A review for key challenges of the development of biodiesel industry*. <https://doi.org/10.5555/20193165263>
- Shah, S., Raja, I., Mahmood, Q., Technology, A. P.-B., & 2016, undefined. (n.d.). Improvement in lipids extraction processes for biodiesel production from wet microalgal pellets grown on diammonium phosphate and sodium bicarbonate. *Elsevier*SH Shah, IA Raja, Q Mahmood, A Pervez*Bioresource Technology*, 2016•*Elsevier*. Retrieved July 31, 2025, from <https://www.sciencedirect.com/science/article/pii/S0960852416305235>
- Shah, S., Raja, I., Rizwan, M., ... N. R.-... and S. E., & 2018, undefined. (n.d.). Potential of microalgal biodiesel production and its sustainability perspectives in Pakistan. *Elsevier*SH Shah, IA Raja, M Rizwan, N Rashid, Q Mahmood, FA Shah, A Pervez*Renewable and Sustainable Energy Reviews*, 2018•*Elsevier*. Retrieved July 31, 2025, from <https://www.sciencedirect.com/science/article/pii/S1364032117311139>
- Sharma, Y., reviews, B. S.-R. and sustainable energy, & 2009, undefined. (n.d.). Development of biodiesel: current scenario. *Elsevier*YC Sharma, B Singh*Renewable and Sustainable Energy Reviews*, 2009•*Elsevier*. Retrieved October 24, 2025, from <https://www.sciencedirect.com/science/article/pii/S1364032108001111>
- ShirReen, C. C., & HwaiChyuan, O. O. (2018). *Sustainable approaches for algae utilisation in bioenergy production*. <https://doi.org/10.5555/20193272296>

- Sikarwar, V., Zhao, M., Fennell, P., ... N. S.-P. in E. and, & 2017, undefined. (n.d.). Progress in biofuel production from gasification. *ElsevierVS Sikarwar, M Zhao, PS Fennell, N Shah, EJ AnthonyProgress in Energy and Combustion Science, 2017•Elsevier*. Retrieved July 15, 2025, from <https://www.sciencedirect.com/science/article/pii/S036012851630106X>
- Silitonga, A. S., Mahlia, T. M. I., Kusumo, F., Dharma, S., Sebayang, A. H., Sembiring, R. W., & Shamsuddin, A. H. (2019). Intensification of Reutealis trisperma biodiesel production using infrared radiation: Simulation, optimisation and validation. *Renewable Energy, 133*, 520–527. <https://doi.org/10.1016/J.RENENE.2018.10.023>
- Singh, A. R., Singh, S. K., & Jain, S. (2022). A review on bioenergy and biofuel production. *Materials Today: Proceedings, 49*, 510–516. <https://doi.org/10.1016/J.MATPR.2021.03.212>
- Singh, D., Sharma, D., Soni, S. L., Sharma, S., Kumar Sharma, P., & Jhalani, A. (2020). A review on feedstocks, production processes, and yield for different generations of biodiesel. *Fuel, 262*, 116553. <https://doi.org/10.1016/J.FUEL.2019.116553>
- Singh, D., Sharma, D., Soni, S., Sharma, S., Fuel, P. S.-, & 2020, undefined. (n.d.). A review on feedstocks, production processes, and yield for different generations of biodiesel. *ElsevierD Singh, D Sharma, SL Soni, S Sharma, PK Sharma, A JhalaniFuel, 2020•Elsevier*. Retrieved July 15, 2025, from <https://www.sciencedirect.com/science/article/pii/S0016236119319076>
- Singh, S., reviews, D. S.-R. and sustainable energy, & 2010, undefined. (n.d.). Biodiesel production through the use of different sources and characterization of oils and their esters as the substitute of diesel: a review. *ElsevierSP Singh, D SinghRenewable and Sustainable Energy Reviews, 2010•Elsevier*. Retrieved July 23, 2025, from <https://www.sciencedirect.com/science/article/pii/S1364032109001695>

- Slade, R., bioenergy, A. B.-B. and, & 2013, undefined. (n.d.). Micro-algae cultivation for biofuels: cost, energy balance, environmental impacts and future prospects. *Elsevier R Slade, A Bauen Biomass and Bioenergy, 2013*•Elsevier. Retrieved July 17, 2025, from <https://www.sciencedirect.com/science/article/pii/S096195341200517X>
- Soltani, S., Rashid, U., Yunus, R., & Taufiq-Yap, Y. H. (2015a). Synthesis of biodiesel through catalytic transesterification of various feedstocks using fast solvothermal technology: a critical review. *Taylor & Francis S Soltani, U Rashid, R Yunus, YH Taufiq-Yap Catalysis Reviews, 2015*•Taylor & Francis, 57(4), 407–435. <https://doi.org/10.1080/01614940.2015.1066640>
- Soltani, S., Rashid, U., Yunus, R., & Taufiq-Yap, Y. H. (2015b). Synthesis of biodiesel through catalytic transesterification of various feedstocks using fast solvothermal technology: a critical review. *Taylor & Francis S Soltani, U Rashid, R Yunus, YH Taufiq-Yap Catalysis Reviews, 2015*•Taylor & Francis, 57(4), 407–435. <https://doi.org/10.1080/01614940.2015.1066640>
- Srivastava, A., & Prasad, R. (2000). Triglycerides-based diesel fuels. *Renewable and Sustainable Energy Reviews, 4*(2), 111–133. [https://doi.org/10.1016/S1364-0321\(99\)00013-1](https://doi.org/10.1016/S1364-0321(99)00013-1)
- Srivastava, N., Kharwar, R., in, P. M.-N. and future developments, & 2019, undefined. (n.d.). Cost economy analysis of biomass-based biofuel production. *Elsevier*. Retrieved July 31, 2025, from <https://www.sciencedirect.com/science/article/pii/B9780444642233000011>
- Su, Y., Song, K., Zhang, P., Su, Y., Cheng, J., & Chen, X. (2017). Progress of microalgae biofuel's commercialization. *Renewable and Sustainable Energy Reviews, 74*, 402–411. <https://doi.org/10.1016/J.RSER.2016.12.078>

- Suresh, A., Technology, K. M.-B., & 2024, undefined. (n.d.). Investigation of pre-treatment techniques on spent substrate of *Pleurotus ostreatus* for enhanced biobutanol production using *Clostridium acetobutylicum* MTCC. *ElsevierAR Suresh, KS MuthuveluBioresource Technology, 2024•Elsevier*. Retrieved July 16, 2025, from <https://www.sciencedirect.com/science/article/pii/S0960852423016565>
- Tang, D., Khoo, K., Chew, K., Tao, Y., ... S. H.-B., & 2020, undefined. (n.d.). Potential utilization of bioproducts from microalgae for the quality enhancement of natural products. *ElsevierDYY Tang, KS Khoo, KW Chew, Y Tao, SH Ho, PL ShowBioresource Technology, 2020•Elsevier*. Retrieved July 31, 2025, from <https://www.sciencedirect.com/science/article/pii/S0960852420302662>
- Tariq, M., Ali, S., Reviews, N. K.-R. and S. E., & 2012, undefined. (n.d.). Activity of homogeneous and heterogeneous catalysts, spectroscopic and chromatographic characterization of biodiesel: A review. *ElsevierM Tariq, S Ali, N KhalidRenewable and Sustainable Energy Reviews, 2012•Elsevier*. Retrieved October 24, 2025, from <https://www.sciencedirect.com/science/article/pii/S1364032112004467>
- Thangaraj, B., Solomon, P. R., Muniyandi, B., Ranganathan, S., & Lin, L. (2019). Catalysis in biodiesel production—a review. *Clean Energy, 3*(1), 2–23. <https://doi.org/10.1093/CE/ZKY020>
- Thanigaivel, S., Vickram, S., Manikandan, S., Deena, S. R., Subbaiya, R., Karmegam, N., Govarthan, M., & Kim, W. (2022). Sustainability and carbon neutralization trends in microalgae bioenergy production from wastewater treatment: A review. *Bioresource Technology, 364*, 128057. <https://doi.org/10.1016/J.BIORTECH.2022.128057>

Today, M. V. H.-C., & 2006, undefined. (n.d.). From surface science to nanotechnology.

ElsevierMA Van HoveCatalysis Today, 2006•Elsevier. Retrieved October 24, 2025, from <https://www.sciencedirect.com/science/article/pii/S0920586105008783>

Torres-Jimenez, E., Jerman, M., Gregorc, A., Fuel, I. L.-, & 2011, undefined. (n.d.). Physical and chemical properties of ethanol–diesel fuel blends. *ElsevierE Torres-Jimenez, MS Jerman, A Gregorc, I Lisec, MP Dorado, B KeglFuel, 2011•Elsevier*. Retrieved July 21, 2025, from <https://www.sciencedirect.com/science/article/pii/S0016236110005168>

Ullah, F., Dong, L., Bano, A., Peng, Q., & Huang, J. (2016). Current advances in catalysis toward sustainable biodiesel production. *Journal of the Energy Institute, 89*(2), 282–292. <https://doi.org/10.1016/J.JOEI.2015.01.018>

Vassilev, S., Fuel, C. V.-, & 2016, undefined. (2016). Composition, properties and challenges of algae biomass for biofuel application: An overview. *ElsevierSV Vassilev, CG VassilevaFuel, 2016•Elsevier*. <https://doi.org/10.1016/j.fuel.2016.04.106>

Verma, P., & Sharma, M. P. (2016). Review of process parameters for biodiesel production from different feedstocks. *Renewable and Sustainable Energy Reviews, 62*, 1063–1071. <https://doi.org/10.1016/J.RSER.2016.04.054>

Vicente, G., Martinez, M., technology, J. A.-B., & 2004, undefined. (n.d.). Integrated biodiesel production: a comparison of different homogeneous catalysts systems. *ElsevierG Vicente, M Martinez, J AracilBioresource Technology, 2004•Elsevier*. Retrieved July 23, 2025, from <https://www.sciencedirect.com/science/article/pii/S096085240300230X>

- Wang, Y., Ho, S. H., Cheng, C. L., Guo, W. Q., Nagarajan, D., Ren, N. Q., Lee, D. J., & Chang, J. S. (2016). Perspectives on the feasibility of using microalgae for industrial wastewater treatment. *Bioresource Technology*, 222, 485–497.
<https://doi.org/10.1016/J.BIORTECH.2016.09.106>
- Wang, Y., Ou, S., Liu, P., Xue, F., A, S. T.-J. of molecular catalysis, & 2006, undefined. (n.d.). Comparison of two different processes to synthesize biodiesel by waste cooking oil. *ElsevierY Wang, S Ou, P Liu, F Xue, S TangJournal of Molecular Catalysis A: Chemical, 2006•Elsevier*. Retrieved October 24, 2025, from
<https://www.sciencedirect.com/science/article/pii/S1381116906005772>
- Xue, J., Grift, T. E., & Hansen, A. C. (2011). Effect of biodiesel on engine performances and emissions. *Renewable and Sustainable Energy Reviews*, 15(2), 1098–1116.
<https://doi.org/10.1016/J.RSER.2010.11.016>
- Xue, S. J., Chi, Z., Zhang, Y., Li, Y. F., Liu, G. L., Jiang, H., Hu, Z., & Chi, Z. M. (2018). Fatty acids from oleaginous yeasts and yeast-like fungi and their potential applications. *Taylor & FrancisSJ Xue, Z Chi, Y Zhang, YF Li, GL Liu, H Jiang, Z Hu, ZM ChiCritical Reviews in Biotechnology, 2018•Taylor & Francis, 38(7), 1049–1060*.
<https://doi.org/10.1080/07388551.2018.1428167>
- YieHua, T. T., & Abdullah, M. M. O. (2015). *Waste ostrich-and chicken-eggshells as heterogeneous base catalyst for biodiesel production from used cooking oil: catalyst characterization and biodiesel yield*. <https://doi.org/10.5555/20163010402>
- YuenMay, C. C. (2004). *Transesterification of palm oil: effect of reaction parameters*.
<https://doi.org/10.5555/20053079709>

- Yusoff, M. N. A. M., Zulkifli, N. W. M., Sukiman, N. L., Kalam, M. A., Masjuki, H. H., Syahir, A. Z., Awang, M. S. N., Mujtaba, M. A., Milano, J., & Shamsuddin, A. H. (2022). Microwave irradiation-assisted transesterification of ternary oil mixture of waste cooking oil – *Jatropha curcas* – Palm oil: Optimization and characterization. *Alexandria Engineering Journal*, *61*(12), 9569–9582. <https://doi.org/10.1016/J.AEJ.2022.03.040>
- Yusuf, M., Alnarabiji, M. S., & Abdullah, B. (2021). Clean Hydrogen Production Technologies. *Advances in Sustainable Energy: Policy, Materials and Devices*, 159–170. https://doi.org/10.1007/978-3-030-74406-9_5
- Zhang, X., Rong, Y., Morrill, S., Fang, J., Narayanasamy, G., Galhardo, E., Maraboyina, S., Croft, C., xia, F., & Penagaricano, J. (2018). Robust optimization in lung treatment plans accounting for geometric uncertainty. *Wiley Online Library*X Zhang, Y Rong, S Morrill, J Fang, G Narayanasamy, E Galhardo, S Maraboyina, C Croft *Journal of Applied Clinical Medical Physics*, 2018•Wiley Online Library, *19*(3), 19–26. <https://doi.org/10.1002/ACM2.12291>
- Zhang, Y., Dubé, M. A., McLean, D. D., & Kates, M. (2003). Biodiesel production from waste cooking oil: 1. Process design and technological assessment. *Bioresource Technology*, *89*(1), 1–16. [https://doi.org/10.1016/S0960-8524\(03\)00040-3](https://doi.org/10.1016/S0960-8524(03)00040-3)
- Zheng, L., Li, D., Jike, L., Xiaolei, G., ... Y. Z.-C. J. of, & 2010, undefined. (n.d.). Enzymatic synthesis of fatty acid methyl esters from crude rice bran oil with immobilized *Candida* sp. 99–125. *Elsevier*. Retrieved July 21, 2025, from <https://www.sciencedirect.com/science/article/pii/S1004954109601415>
- Živković, S., Veljković, M., ... I. B.-I.-... and S. E., & 2017, undefined. (n.d.). Technological, technical, economic, environmental, social, human health risk, toxicological and policy

considerations of biodiesel production and use. *Elsevier* SB Živković, MV Veljković, IB Banković-Ilić, IM Krstić, SS Konstantinović, SB Ilić *Renewable and Sustainable Energy Reviews*, 2017 • *Elsevier*. Retrieved July 15, 2025, from <https://www.sciencedirect.com/science/article/pii/S1364032117306846>

APPENDIX

Results of Response Surface Transesterification Optimization

Run	Factor 1 A: Time (mins)	Factor 2 B: Temperature (°C)	Factor 3 C: Catalyst (wt%)	Factor 4 D: Methanol (wt%)	Response 1: Biodiesel yield (wt%)	Acid value (AV)
1	150	60	5.5	10	81.6	0.85
2	90	60	1	10	71.05	0.28
3	150	60	1	6.5	66.33	1.13
4	30	60	5.5	10	56.38	0.28
5	90	40	5.5	3	46.06	0.28
6	150	80	5.5	6.5	89.73	0.55
7	150	60	5.5	3	57.71	0.28
8	90	60	5.5	6.5	88.27	0.29
9	90	80	5.5	10	79.02	0.28
10	90	40	1	6.5	40.35	0.86
11	150	60	10	6.5	84.81	0.28
12	90	60	10	10	71.63	0.28
13	90	80	5.5	3	65.77	0.28
14	90	60	5.5	6.5	92.27	0.29
15	90	60	5.5	6.5	92.27	0.29

16	90	60	1	3	42.83	0.55
17	30	60	1	6.5	51.07	0.28
18	90	60	5.5	6.5	92.27	0.28
19	30	80	5.5	6.5	67.34	0.54
20	30	60	10	6.5	77.76	0.85
21	90	40	10	6.5	82.49	0.57
22	90	80	1	6.5	82.79	2.43
23	90	40	5.5	10	59.41	0.28
24	30	60	5.5	3	62.27	0.29
25	30	40	5.5	6.5	62.54	0.80
26	90	80	10	6.5	82.35	0.57
27	90	60	5.5	6.5	92.27	0.28
28	90	60	10	3	79.86	0.78
29	150	40	5.5	6.5	53.32	0.55

Peak list:

FIND 427.73

PEAKS:

Position:

		Intensity:	0.0844
Position:	549.46	Intensity:	0.0492
Position:	872.40	Intensity:	0.351
Position:	1000.13	Intensity:	0.0509
Position:	1397.01	Intensity:	0.0326
Position:	1652.38	Intensity:	0.113
Position:	3484.07	Intensity:	-0.0106